AQUITARD CONTROL OF STREAM-AQUIFER INTERACTION AND FLOW TO A HORIZONTAL WELL IN COASTAL AQUIFERS

A Dissertation

by

DONGMIN SUN

Submitted to the Office of Graduate Studies of
Texas A&M University
in partial fulfillment of the requirements for the degree of

DOCTOR OF PHILOSOPHY

December 2005

Major Subject: Geology

AQUITARD CONTROL OF STREAM-AQUIFER INTERACTION AND FLOW TO A HORIZONTAL WELL IN COASTAL AQUIFERS

A Dissertation

by

DONGMIN SUN

Submitted to the Office of Graduate Studies of
Texas A&M University
in partial fulfillment of the requirements for the degree of

DOCTOR OF PHILOSOPHY

Approved by:

Chair of Committee,	Hongbin Zhan
Committee Members,	Mark. E. Everett
	Binayak P. Mohanty
	Clyde L. Munster
	Yalchin Efendiev
Head of Department,	Richard L. Carlson

December 2005

Major Subject: Geology

ABSTRACT

Aquitard Control of Stream-Aquifer Interaction and Flow to a Horizontal Well in Coastal Aquifers. (December 2005)

Dongmin Sun, B.S., Daqing Petroleum Institute, China;

M.S., Research Institute of Petroleum Exploration & Development, China

Chair of Advisory Committee: Dr. Hongbin Zhan

This dissertation is composed of three parts of major contributions:

In Chapter II, we developed a new conceptual model and derived a new semi-analytical model for flow to a horizontal well beneath a water reservoir. Instead of treating the leakage from aquitard as a source term inside the aquifer which is called Hantush's assumption (1964), we linked flows in aquitard and aquifer by the idea of continuity of flux and drawdown. The result in this chapter is compared with that of Zhan and Park in 2003 which Hantush's assumption is adopted at various hydraulic and well configurations. It shows that Hantush's assumption becomes inaccurate in regions where vertical velocity components are significant.

In Chapter III, we deal with the interaction of an aquifer with two parallel surface water bodies such as two streams or canals. In this chapter, new closed-form analytical and semi-analytical solutions are acquired for the pumping induced dynamic interaction between two streams and ground water for two different cases. In the first case, the sediment layers separating the streams from the aquifer ground water do not exist. In the second case, the two low permeable layers are considered. The effect of aquitard and

water right competition is addressed in this chapter. This model can be used for interpreting and deriving hydrologic parameters of aquitard and aquifer when pumping occurs between two channels. It can also be used to predict stream depletion which is essential for water management and ecology conservation.

In Chapter IV, we investigated the three dimensional upconing due to a finite-length of horizontal well and its critical conditions. The results are compared with those of vertical wells. The critical condition which includes the critical rise and the critical time at a certain pumping rate depends on the well length, the initial interface location, the well location, and the pumping rate. Our results show that horizontal well might be a better tool for coastal groundwater resources development. In real field applications, installing long wells as shallow as possible is always desirable for sustaining long periods of pumping with significant rates.

DEDICATION

To my beloved family

ACKNOWLEDGEMENTS

My dissertation committee deserves special thanks for their guidance in my graduate endeavor. I must first thank my primary research advisor, Dr. Hongbin Zhan. Dr. Zhan always encouraged me to pursue my ideas, offered innumerable creative insights, and guided me with outstanding wisdom and extreme patience. I could not have gotten to this stage without him.

I would like to thank Dr. Binayak Mohanty and Dr. Clyde Munster for providing me the opportunity to do an experiment which was a valuable experience for me. I really appreciate Dr. Mohanty's encouragement and comfort during my hard times. I give special thanks to Dr. Mark Everett and Dr.Yalchin Efendiev for their tremendous help during the past few years.

Special thanks goes to my good friend, Dr. Jianting Zhu, for comfort and support during my dark days in the past two years.

I wish to thank my grandparents and my parents for their constant support and encouragement throughout the years. I thank my husband Joe who has always been there for me during any circumstances. I really appreciate his unconditional love and care.

I also would like to thank anyone who had helped me during the past few years, including my colleagues in the hydrology group. Lastly, I appreciate the financial support from my department, Anadarko Petroleum, and ConocoPhilips Petroleum Company.

TABLE OF CONTENTS

Page

Page

LIST OF FIGURES

FIGURE Page

FIGURE Page

FIGURE Page

FIGURE Page

LIST OF TABLES

TABLE Page

CHAPTER I

INTRODUCTION

With the increase of population, the demand for water is steadily escalating. Surface water is easily accessible, yet often depleted, and furthermore, contaminated. Ground water resources are the most possible sources to meet the water demand. Despite its abundance, over extraction of groundwater and daily human activity can easily cause localized problems such as deterioration of water quality, land subsidence, reduced discharge to surface water, and sea water intrusion in coastal regions.

One critical issue is to develop good quality and greater quantity of groundwater resources to satisfy human being's needs both in coastal and inland regions. Hydrologists have been fighting for these by taking advantage of current technologies.

Aquifers sometimes are bounded by low permeable layers, so called aquitards from above and or/bottom. Flow and transport inside aquifer has been a very active research field among hydrologists and environmental scientists for several decades. However, the effect of aquitard is neglected and simplified in previous researches regarding flow and transport in aquifer and aquitard system even though aquitards have been proven to play important roles in many hydrological situations. First, the aquitards (low permeable sediment layers) often control the hydraulic connection between surface water and groundwater (e.g. Hunt, 1999, 2003; Butler et al., 2001).

This dissertation follows the style of Journal of Hydrology.

Aquitards control how much flux leaking from surface water to groundwater and the length of transient flow period, hence control the stream-depletion which is very important for surface water management and ecology conservation for wildlife. Second, aquitards could be very thick sometimes, such as 610 m in northwest of the Kansas state of Dakota aquifer. Aquitards are often less permeable, but have great porosity which enables them great capacity to store water and contaminants. When pumping starts inside the aquifer, the hydraulic gradient between aquifer and aquitard caused by pumping will drive water out of aquitard to aquifer, resulting in the dewatering of the aquitards. The loss of water and compaction of silty and clay materials which are composed of aquitards may cause subsidence. Land subsidence is one of the most challenging issues in many countries including Australia, China, India, Iran, Japan, Mexico, Poland, Sweden, Netherlands, UK, USA. It was reported that in 1995 there are more than 150 major cities in the world where subsidence were substantial (Barends et al., 1995). It will be critical to predict the degree of dewatering inside of aquitard which controls the degree of land subsidence.

Third, although water movement across the boundary of aquitard-aquifer is difficult, solute diffusion across the boundary is possible due to the concentration gradient across the boundary. Although field and laboratory results show that aquitard controls the retardation and tailing of the transport, effect of aquitard on solute transport is often ignored for the sake of mathematic simplification. It is of great importance to have a better understanding of the roles which aquitards play in solute transport in aquitard-aquifer system to provide guidance for field contaminant remediation.

In this study, we derived a series of conceptual, physical, and mathematical models which demonstrate the effects of aquitards in aquitard-aquifer system and stream-aquifer interaction system for both vertical and horizontal well scenarios. Different from previous studies which simplified aquitard effect, aquitards are treated as different flow systems and their influence on flow inside the aquifer and stream-aquifer interaction are thoroughly investigated by systematically analyzing the hydraulic parameters of aquitards. The degree of dewatering of aquitard is also acquired as well as the drawdown generated inside the aquifer, thus this study could be easily extended into subsidence prediction. In a similar way, this conceptual model could be easily modified for solute transport in aquitard-aquifer system. In Chapter II, flow to a horizontal well under a water reservoir is investigated. We have provided a new approach for solving drawdown and flux from aquitard to aquifer. In Chapter III, an analytical solution is obtained for a pumping induced interaction among two streams and groundwater. This study involves flows in aquifer and two low permeable layers which separate surface water from ground water. A fully penetrating well is positioned between two fully penetrating streams. This model could be used for the water management and water supply when pumping occurs between two channels of the same river, two different streams, or two canals.

In coastal zones, intensive extraction of groundwater will break the long established balance between fresh water and sea water, causing the so- called sea water intrusion problem. Coastal margins are one of the world's greatest natural resources and economics assets. To satisfy the escalating demand of water resources in coastal margins

due to the increasing human settlements and economic activities, it is critical to find better technologies to manage groundwater resources for coastal aquifers. The screen of a horizontal well is parallel to the horizontal directions. Because of their larger contact area with aquifers, horizontal wells have significant advantages over vertical wells in most well applications such as pumping and treat exercise, contaminant remediation, land stabilization, and many others. A horizontal well might generate much less drawdown than that of a vertical well because pumping strength is distributed along a longer screen, thus generates much less upconing of the fresh/sea water interface and has less chance to be invaded by the underneath saline water. Therefore, a horizontal well might be a better means for coastal aquifer development.

In Chapter IV, we proposed to use a horizontal well instead of vertical wells to pump near coastal aquifers. A three dimensional profile of sea-fresh water interface is investigated at various hydraulic conditions and well configurations. We also examine the critical conditions which include critical rise, critical time, and critical pumping rate. The result shows that horizontal well is a better tool in coastal aquifer water resources management.

CHAPTER II

FLOW TO A HORIZONTAL WELL IN AN AQUITARD-AQUIFER SYSTEM

A horizontal well is sometime installed in an aquifer beneath a water reservoir to get significant amount of groundwater with better quality. An aquitard often separates the surface water body from the underneath aquifer. Previous studies in vertical wells related to this subject treated leakage from the aquitard as a volumetric source term in the governing equation of flow in the main aquifer, a hypothesis termed "Hantush's assumption". In this study, flow in the aquitard and aquifer is treated as two systems which are linked through the continuity of flux and head at the aquitard-aquifer boundary. In particular, we treat leakage as a boundary at the aquitard-aquifer interface, not as a volumetric source. The leakage induced by the pumping horizontal well depends on several parameters such as the aquitard thickness, the vertical hydraulic conductivity of the aquitard, the aquitard specific storage, the well location, and the well length. In general, we find that the Hantush's assumption does not offer correct prediction of flux and drawdown during the transient flow condition, particularly at the early time. For steady-state flow, the Hantush's assumption works reasonably well under realistic conditions of aquitard thickness and hydraulic conductivity as long as the aquitard thickness is not too thin (aquitard-aquifer ratio less than 0.001). This assumption also works reasonably well under realistic horizontal well lengths and well locations as long as the well is not too close to the aquitard-aquifer boundary.

2.1 Introduction

Groundwater is commonly withdrawn near a surface water body such as a river, a stream, a lake, or a water reservoir because the quality is expected to be better than that of surface water. An aquitard often separates the surface water body from the underneath aquifer. Hydraulic connection between surface water and groundwater has long been recognized as a crucial factor in the management of water resources, ecologic conservation, irrigation and drainage, and many others subjects. Therefore, there are extensive studies about pumping induced stream-aquifer interaction (e.g. Theis, 1941; Glover and Balmer 1954; Hantush, 1965; Barlow and Moench, 1998; Hunt, 1999; Zlotnik and Huang, 1999; Barlow et al., 2000; Moench and Barlow, 2000; Butler et al., 2001; Lal, 2001; Chen et al., 2003; Kollet and Zlotnik, 2003). At present, most of these studies are focused on vertical wells.

Another way of withdrawing groundwater near a surface water body is to install a horizontal well whose axis is parallel to the horizontal directions. The advantages of using horizontal wells over the vertical wells have been addressed in an original work of Hantush and Papadopulos (1962), and in recent studies of Zhan (1999), Zhan et al. (2001), and Zhan and Zlotnik (2002). One of those advantages is that a horizontal well can have a great length of screen, thus can withdraw a significant amount of groundwater. In recent years, horizontal wells have gained increasing interests in the field of water resources management and environmental engineering, and a great deal of research can be found from Morgan (1992), Tarshish (1992), Cleveland (1994), Murdoch (1994), Falta (1995), Sawyer and Lieuallen-Dulam (1998), Zhan (1999), Zhan

and Cao (2000), Streward and Jin (2001), Zhan et al. (2001), Park and Zhan (2002, 2003), Zhan and Zlotnik (2002), Chen et al. (2003), Zhan and Park (2003), and others.

A horizontal well can be positioned in an aquifer underneath or along a surface water body. This study will focus on the former case. A different study will address the later case elsewhere. Between the surface water body and the underneath aquifer, there often exists a semi-permeable aquitard serving as a leakage layer. Therefore, study of flow to a horizontal well under a surface water body involves flow in an aquitard-aquifer system. Such a system is often called a leaky aquifer which has been extensively studied when vertical wells are used (Hantush, 1964; Neuman and Witherspoon, 1969a, b; Bear, 1979).

Hantush (1964) had proposed an important assumption in simplifying the problem of flow in a leaky aquifer. The essence of this assumption is to replace the leakage effect by a source term in the governing equation of flow in the aquifer. This is a necessary simplification to make the mathematical models amendable in many cases. As a result, this simplification is widely adopted in many studies related to leaky aquifers and stream-aquifer interaction (e.g. Jenkins, 1968; Hunt, 1999; Moench and Barlow, 2000; Butler et al., 2001; Lal, 2001). Zhan and Park (2003) have applied the Hantush's assumption to study flow to a horizontal well in a leaky aquifer. However, the aquitard leakage really should be a boundary effect that occurs at the aquitard-aquifer interface rather than a volumetric source term in the aquifer. Therefore, it is unclear how much derivation from the true solution will be resulted from the adoption of this assumption.

The purpose of this investigation is to study flow to a horizontal well in an aquitard-aquifer system based on the mass conservation law without using the Hantush's

assumption. In this study, flow in the aquitard and aquifer is treated as two systems which are linked through the continuity of flux and head at the aquitard-aquifer boundary. In particular, leakage is not treated as a volumetric source. We will investigate both steady-state and transient flow scenarios and compare the results with Zhan and Park (2003) to assess the validity of the Hantush's assumption for horizontal well cases. The physically based model developed in this study can be employed for water supply, contaminant remediation under a reservoir, and other applications.

2.2 Mathematical Model and Solutions

We first explain the conceptual model. A horizontal well is positioned under a water reservoir, which is treated as a constant-head boundary. An aquitard at the bottom of the water reservoir separates the water reservoir from the underneath aquifer. Both the aquitard and aquifer are horizontal with finite-thickness. The bottom of the aquifer is impermeable. The hydraulic conductivity of the aquitard is at least two orders of magnitude smaller than that of the aquifer, thus flow in the aquitard is nearly vertical. Horizontal well is treated as a line sink and flux distribution along the well axis is assumed uniform. The validity of this assumption has been carefully addressed by Zhan and Zlotnik (2002). The aquitard and aquifer are homogeneous, but anisotropic, and the lateral boundaries are infinitely far.

Figure 2.1 is a schematic diagram of the problem and the coordinate system setup. The x- and y- axes are in the horizontal directions and the z- axis is in the vertical direction. The origin is at the bottom of the aquifer. The well is positioned along the x-axis with its center at $(0,\ 0,\ z_w)$, where z_w is the distance from the well to the lower

impermeable boundary. Before solving flow to the horizontal well, we first solve the problem of flow to a point sink. After that, we integrate point source solutions along the horizontal well axis to get the horizontal well solutions.

2. 2.1 Transient flow solution

The governing equation and the associated initial and boundary conditions for the flow in the aquitard and the flow to a point sink in the aquifer are given as follows:

For flow in the aquitard:

$$K_z' \frac{\partial^2 h'}{\partial z^2} = S_s' \frac{\partial h'}{\partial t} \quad , \qquad B<z<B+B', \tag{2.1}$$

$$h'(x, y, z, 0) = h_0 , \tag{2.2}$$

$$h'(x = \pm\infty, y, z, t) = h'(x, y = \pm\infty, z, t) = h_0 \ , \tag{2.3}$$

$$h'(x, y, z = B + B', t) = h_0 , \tag{2.4}$$

$$h'(x, y, z = B, t) = h(x, y, z = B, t) , \tag{2.5}$$

$$K_z' \left.\frac{\partial h'}{\partial z}\right|_{z=B} = K_z \left.\frac{\partial h}{\partial z}\right|_{z=B} . \tag{2.6}$$

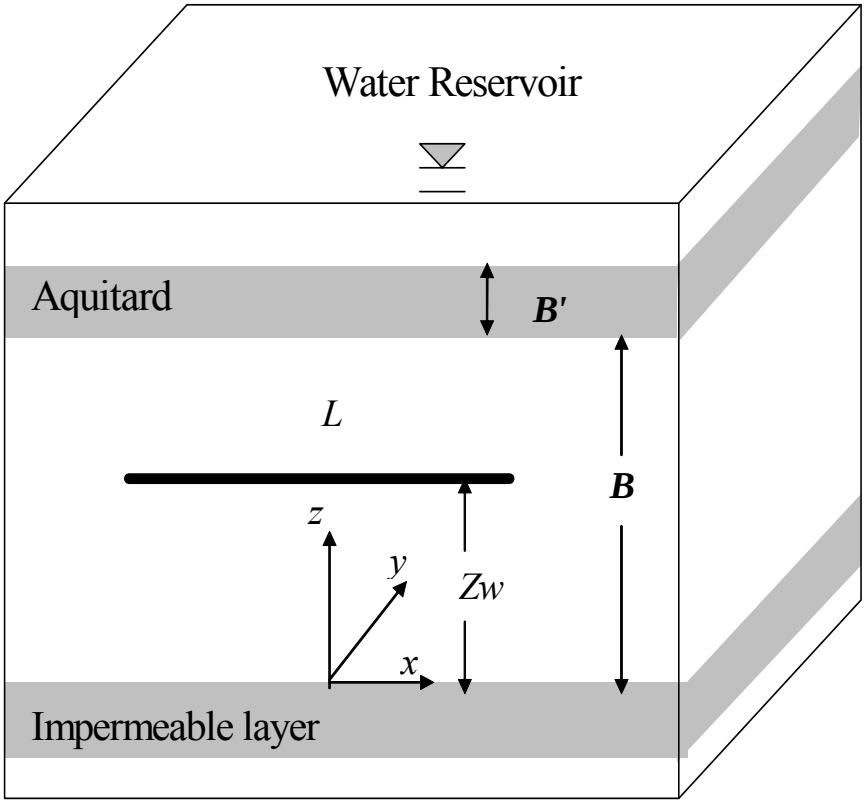

Figure 2.1 A schematic cross-sectional diagram of a finite-length pumping horizontal well beneath a water reservoir.

For flow to a point sink in the aquifer:

$$K_x \frac{\partial^2 h}{\partial x^2} + K_y \frac{\partial^2 h}{\partial y^2} + K_z \frac{\partial^2 h}{\partial z^2} = S_s \frac{\partial h}{\partial t} + Q\delta(x - x_0)\delta(y - y_0)\delta(z - z_0), \quad 0<z<B, \tag{2.7}$$

$$h(x, y, z, 0) = h_0, \tag{2.8}$$

$$h(x = \pm\infty, y, z, t) = h(x, y = \pm\infty, z, t) = h_0, \tag{2.9}$$

$$\frac{\partial h}{\partial z}\Big|_{z=0} = 0, \tag{2.10}$$

where h , h' are the hydraulic heads of the aquifer and aquitard respectively, h_0 is the initial hydraulic head in both the aquifer and the aquitard, K_z' and S_s' represent the vertical hydraulic conductivity and the aquitard specific storage, respectively, K_x, K_y, K_z are the principal hydraulic conductivities in the *x, y, z* axes respectively, S_s is the aquifer specific storage, B' and B are the thickness of the aquitard and aquifer respectively, Q is the pumping rate of the point sink, x_0, y_0, and z_0 are the coordinates of the point sink, and t is time.

Eq. (2.1) is the governing equation for vertical flow in the aquitard, Eq. (2.2) is the initial condition in the aquitard, Eq. (2.3) is the lateral boundary at infinity, Eq. (2.4) is the constant-head boundary condition at the surface water-aquitard boundary, and Eqs. (2.5) and (2.6) refer to the continuity of head and vertical flux at the aquitard-aquifer interface, respectively. Eq. (2.7) is the governing equation for three-dimensional flow to a point sink in the aquifer, Eq. (2.8) is the initial condition in the aquifer, Eqs. (2.9) and (2.10) are the lateral and bottom boundaries of the aquifer, respectively. Above equation

groups must be solved together to obtain the hydraulic heads at the aquitard and aquifer simultaneously. The procedure of problem-solving is illustrated as follows.

First, we change the hydraulic head to drawdown, thus the initial head h_0 can be removed and the initial and boundary conditions are simplified. After this, we transform all the terms into their dimensionless forms. This is not a required process; however, it could simplify the mathematical formats. In addition, it will reveal some lumped dimensionless parameters that otherwise will not appear in dimensional formats.

Second, we apply the Laplace transform to remove the t-dependent terms; this is a necessary step because of the difficulty of directly solving the problem in real-time domain.

Third, only vertical flow is considered in the aquitard, thus we first solve the governing equation of the aquitard considering the upper constant-head boundary and continuity of head at the lower aquitard-aquifer boundary. This step links the drawdown of the aquitard with the drawdown at the aquitard-aquifer boundary.

Fourth, a Fourier transform solution with a summation of a series of cosine functions is proposed for the aquifer considering the boundary conditions at z=0 and B. The frequency used in the cosine functions of the proposed solution is determined via the continuity of head and flux at the aquitard-aquifer boundary.

After that, the drawdowns in the aquifer and aquitard with a point-sink in the aquifer are derived in Laplace domain. Finally, integration of the point-sink solutions will yield the horizontal well solutions in Laplace domain, which will be subsequently inverted to yield the solutions in real time domain.

We define the following dimensionless parameters after changing hydraulic head h to drawdown $s=h_0-h$ and $s'=h_0-h'$:

$$x_D=\frac{x}{B}\sqrt{\frac{K_z}{K_x}}\quad,\quad y_D=\frac{y}{B}\sqrt{\frac{K_z}{K_y}}\quad,\quad z_D=\frac{z}{B}\quad,\quad z_{wD}=\frac{z_w}{B}\quad,\quad t_D=\frac{K_z}{B^2S_s}t\quad,\quad B_D=\frac{B'}{B}\quad,$$

$$L_D=\frac{L}{B}\sqrt{\frac{K_z}{K_x}},s_D=\frac{4\pi\sqrt{K_xK_y}B}{Q}s,s'_D=\frac{4\pi\sqrt{K_xK_y}B}{Q}s',$$

$$\alpha=\frac{(K_z/S_s)}{(K'_z/S'_s)},\ \beta=\frac{K_z}{K'_z}, \tag{2.11}$$

where L is the length of the horizontal well. Conducting Laplace transform to Eqs.(2.1)-(2.10) results in:

$$\frac{\partial^2\overline{s'_D}}{\partial z_D{}^2}=\alpha p\overline{s'_D}, \tag{2.12}$$

$$\overline{s'_D}(x_D=\pm\infty,y_D,z_D,p)=\overline{s'_D}(x_D,y_D=\pm\infty,z_D,p)=0, \tag{2.13}$$

$$\overline{s'_D}(x_D,y_D,z_D=1+B_D,p)=0, \tag{2.14}$$

$$\overline{s'_D}(x_D,y_D,z_D=1,p)=\overline{s_D}(x_D,y_D,z_D=1,p)=0, \tag{2.15}$$

$$\left.\frac{\partial\overline{s'_D}}{\partial z_D}\right|_{z_D=1}=\beta\left.\frac{\partial s_D}{\partial z_D}\right|_{z_D=1}, \tag{2.16}$$

$$\frac{\partial^2\overline{s_D}}{\partial x_D{}^2}+\frac{\partial^2\overline{s_D}}{\partial y_D{}^2}+\frac{\partial^2\overline{s_D}}{\partial z_D{}^2}=p\overline{s_D}+\frac{4\pi}{p}\delta(x_D-x_{0D})\delta(y_D-y_{0D})\delta(z_D-z_{0D}), \tag{2.17}$$

$$\overline{s_D}(x_D=\pm\infty,y_D,z_D,p)=\overline{s_D}(x_D,y_D=\pm\infty,z_D,p)=0, \tag{2.18}$$

$$\frac{\partial \overline{s_D}}{\partial z_D}\Big|_{z_D=0} = 0\,, \tag{2.19}$$

where overbar means the parameter in Laplace domain, and p is the Laplace transform parameter.

2. 2.1.1 Point-sink solution in Laplace domain

Following the similar procedures outlined by Zhan and Park (2003), the proposed solution of Eq. (2.17) in Laplace domain is a Fourier transform of cosine functions:

$$\overline{s_D} = \sum_{n=0}^{\infty} H_n(x_D, y_D, p)\cos(\omega_n z_D)\,, \tag{2.20}$$

where H_n is a function only depends on the horizontal coordinates and p, and ω_n is the frequency that will be determined via boundary condition. The details of solving Eqs. (2.12)-(2.19) are presented in Appendix A. The aquifer drawdown in Laplace domain for a point-sink is:

$$\overline{s_D} = \frac{4}{p}\sum_{n=0}^{\infty}\frac{\cos(\omega_n z_{wD})\cos(\omega_n z_D)}{f(\omega_n)} K_0(\sqrt{\omega_n^2 + p}\, r_D)\,, \tag{2.21}$$

where ω_n is determined by Eq. (A6), K_0 is the second-kind, zero-order, modified Bessel function, and

$$f(\omega_n) = 1 + \frac{\sin(2\omega_n)}{2\omega_n}\,,\ r_D = \left(x_D{}^2 + y_D{}^2\right)^{1/2}. \tag{2.22}$$

Substituting Eq. (2.21) into (A5) will result in the aquitard drawdown in Laplace domain for a point-sink as:

$$\overline{s'_D} = \frac{4}{p}\sum_{n=0}^{\infty}\frac{\cos(\omega_n z_{wD})\cos(\omega_n)}{f(\omega_n)} K_0(\sqrt{\omega_n^2 + p}\, r_D) \times \frac{\sinh(\sqrt{\alpha p}(1 + B_D - z_D))}{\sinh(\sqrt{\alpha p} B_D)}. \tag{2.23}$$

2.2.1.2 Horizontal well solution in Laplace domain

Integration of Eq. (2.21) along the horizontal well axis will yield the solution of a horizontal well in Laplace domain.

$$\overline{s_{DH}} = \frac{1}{L_D}\frac{4}{p}\sum_{n=0}^{\infty}\frac{\cos(\omega_n z_{wD})\cos(\omega_n z_D)}{f(\omega_n)} \int_{-L_D/2}^{L_D/2} K_0\left[\sqrt{\omega_n^2 + p}((x_D - x_{0D})^2 + {y_D}^2)^{1/2}\right] dx_{0D} \quad (2.24)$$

where $\overline{s_{DH}}$ is the aquifer drawdown in Laplace domain for a horizontal well. s_{DH} is defined in the same way as s_D in Eq. (2.11).

As a consequence, the aquitard drawdown in Laplace domain induced by a pumping horizontal well in the aquifer, $\overline{s'_{DH}}$, becomes:

$$\overline{s'_{DH}} = \frac{4}{pL_D} \times \frac{\sinh(\sqrt{\alpha p}(1 + B_D - z_D))}{\sinh(\sqrt{\alpha p} B_D)} \times \sum_{n=0}^{\infty}\frac{\cos(\omega_n z_{wD})\cos(\omega_n)}{f(\omega_n)} \int_{-L_D/2}^{L_D/2} K_0\left[\sqrt{\omega_n^2 + p}((x_D - x_{0D})^2 + {y_D}^2)^{1/2}\right] dx_{0D} \quad (2.25)$$

where s'_{DH} is defined in the same way as s_{DH}.

2.2.2 Steady-state flow solution

The transient flow discussed above might approach the steady-state condition rather rapidly if the thickness of the aquitard is relatively thin. Meanwhile, drawdowns in the aquitard-aquifer system after the long-term pumping could provide important information about water management. Therefore, it is worthwhile to discuss the steady-state solution. The steady-state solution can be obtained in two ways. One way is to directly solve the steady-state flow governing equations together with the boundary

conditions and continuity of head and flux at the aquitard-aquifer interface. Another way is to get the solution from the transient solution by letting $p \to 0$, which is equivalent to $t \to \infty$. We will proceed with the latter method.

When $p \to 0$, Eq. (A6) is simplified to

$$\beta\omega_n \tan(\omega_n) = 1/B_D . \tag{2.26}$$

This equation will determine the frequency ω_n. The point-sink solution in the aquifer in real-time domain can be obtained from Eq. (2.21) by allowing $p \to 0$ and noticing that $L^{-1}[1/p] = 1$, where L^{-1} denotes the inverse Laplace transform:

$$s_D = 4\sum_{n=0}^{\infty} \frac{\cos(\omega_n z_{wD})\cos(\omega_n z_D)}{f(\omega_n)} K_0(\omega_n r_D) \tag{2.27}$$

The steady-state point-sink solution in the aquitard can also been obtained from Eq. (2.23) as:

$$s'_D = 4\sum_{n=0}^{\infty} \frac{\cos(\omega_n z_{wD})\cos(\omega_n)}{f(\omega_n)} K_0(\omega_n r_D) \times \left[1 + \frac{1}{B_D} - \frac{z_D}{B_D}\right]. \tag{2.28}$$

The steady-state drawdowns in the aquifer and aquitard induced by a horizontal well can be accordingly obtained as:

$$s_{DH} = \frac{4}{L_D}\sum_{n=0}^{\infty} \frac{\cos(\omega_n z_{wD})\cos(\omega_n z_D)}{f(\omega_n)} \int_{-L_D/2}^{L_D/2} K_0\left[\omega_n((x_D - x_{0D})^2 + {y_D}^2)^{1/2}\right] dx_{0D} . \tag{2.29}$$

$$s'_{DH} = \frac{4}{L_D} \times \left[1 + \frac{1}{B_D} - \frac{z_D}{B_D}\right] \times \sum_{n=0}^{\infty} \frac{\cos(\omega_n z_{wD})\cos(\omega_n)}{f(\omega_n)} \cdot \int_{-L_D/2}^{L_D/2} K_0\left[\omega_n((x_D - x_{0D})^2 + {y_D}^2)^{1/2}\right] dx_{0D} \tag{2.30}$$

2.2.3 Numerical computation

Inverse Laplace transform is required to obtain the drawdowns in real-time for the transient flow problem. Integrations are needed to compute drawdowns for both transient and steady-state cases. It would be difficult to analytically invert the Laplace transform for this problem because ω_n is related to p. We propose to use Stehfest (1970) algorithm to numerically calculate the inverse Laplace transform based on a few considerations. First, Stehfest (1970) algorithm is a simple one that can be easily programmed. Second, this algorithm has been found quite robust and accurate in similar problems of studying flow to a horizontal well in previous studies (Zhan and Zlotnik, 2002). It is notable that Stehfest (1970) algorithm might not always converge for some problems, and alternative inverse Laplace transform algorithms might be needed (Talbot, 1979; de Hoog et al., 1982; Hollenbeck, 1998). However, our numerical experiments confirmed that the Stehfest (1970) algorithm is free of numerical oscillations or other problems at times of interests for this study.

The integrations are calculated using Gaussian Quadrature method (Abramowitz and Stegun, 1972, p.916; Press et al., 1989). ω_n is calculated using Newton-Raphson method (Press et al., 1989). The computer program is available from the authors free of charge upon request. The solutions of the mathematical models for both transient and steady-state flow will be employed to address a few key problems.

2.3. Analysis of Flux and Drawdown and Test of the Hantush's Assumption

2.3.1 A physical interpretation of the Hantush's assumption

Leakage from aquitard should be treated as a boundary condition at the aquitard-aquifer interface, an idea used in this study. However, it is traditionally treated as a source term in the governing equation of flow in the aquifer, namely the Hantush's assumption (Hantush, 1964). The essence of the Hantush's assumption is to replace the areal source at the aquitard-aquifer interface by a volumetric source inside the aquifer. The flux and drawdown calculated in this paper will be compared with those presented by Zhan and Park (2003) who adopted the Hantush's assumption. The difference might be related to well location, well length, thickness and hydraulic parameters of the aquitard. The dimensionless flux along the boundary is defined as $\Gamma = \frac{\partial s_D}{\partial z_D} = \frac{1}{\beta}\frac{\partial s'_D}{\partial z_D}$ at z_D=1.

From the definition of the dimensionless terms in Eq. (2.11), we can identify a few lumped parameters that control the dimensionless drawdown and flux. Those are aquitard-aquifer thickness ratio (B_D), aquifer-aquitard vertical diffusivity ratio (α), aquifer-aquitard vertical hydraulic conductivity ratio (β), dimensionless location of the well (z_{wD}), dimensionless length of the well (L_D), and dimensionless coordinates of the observation point x_D, y_D, z_D. These parameters can be classified into two categories: B_D, α, and β belong to the aquitard-aquifer properties, and z_{wD}, L_D, and x_D, y_D, z_D belong to the horizontal well configuration and observation parameters. Notice that $\alpha = \beta \times (S'_s / S_s)$, thus discussion of α can be separated as discussion of β and the

aquitard/aquifer specific storage ratio. We will first discuss the control of the aquitard/aquifer properties, followed by the discussion of the control of the horizontal well configuration and observation parameters.

The default parameters used in all the following figures are defined in Table 2.1.

2.3.2 Control of aquitard/aquifer properties on flux and drawdown

We will first discuss the results of the transient solution in which the aquitard storage has played an important role. After that, we will discuss the steady-state results where aquitard thickness and hydraulic conductivity appear to be the controlling factors. Notice that the key difference of this work and Zhan and Park (2003) is the treatment of flux at the aquitard-aquifer boundary. Therefore, we will focus on the characteristics of flux and drawdown along this boundary.

2.3.2.1 Aquitard-aquifer specific storage ratio (S_s'/S_s)

We like to see the transient characteristics of flux under different aquitard-aquifer specific storage ratios. To do so, we choose one representative observation point at x_D=0, y_D=0, and z_D=1. Figure 2.2 shows the flux at this point for three different specific storage ratios as functions of dimensionless time in a semi-log scale. Negative sign of flux means that flow is downward. Considering the fact that most aquitards are clayey materials that have much greater specific storages than those of the aquifers which are mostly sandy, we only concern the specific ratios that are greater than unity.

Table 2.1: The default values used in aquitard-aquifer system

Parameter	Default value
B	10m
B'	1m
K_x, K_y, K_z	1×10^{-4}m/s
K_z'	1×10^{-6}m/s
S_s	2×10^{-5}m^{-1}
L	100m
Z_w	5m
Q	0.001m^3/s
S_s'	1×10^{-3}m^{-1}

Note: When different aquitard/aquifer thickness ratios, specific storage ratios or hydraulic conductivity ratios are used, the properties of the aquifer are fixed and only the corresponding aquitard parameters are changed.

After the start of pumping, the hydraulic head in the aquifer will drop rapidly. However, the hydraulic head in the aquitard will not change immediately due to the relatively low permeability there. Such a head difference between the aquifer and the aquitard will drive water out of the aquitard slowly, a process called “dewatering”. Water leaked from the aquitard first comes from the storage, and one might see a continuous increase of flux across the aquitard-aquifer boundary, until reaching a maximal value. After that, the flux will gradually decrease to approach the steady-state where the leaked water comes entirely from the upper surface water reservoir. This argument has been exhibited in Figure 2.2 which shows an initial increase of flux to a maximum then a decrease of flux until reaching a common steady-state value (-0.162).

It is also interesting to see that an aquitard with a higher specific storage will generate a larger maximal flux due to the greater amount of water that can be dewatered. For example, the absolute values of dimensionless maximal flux for specific storage ratios of 500 and 50 are 0.25 and 0.47.

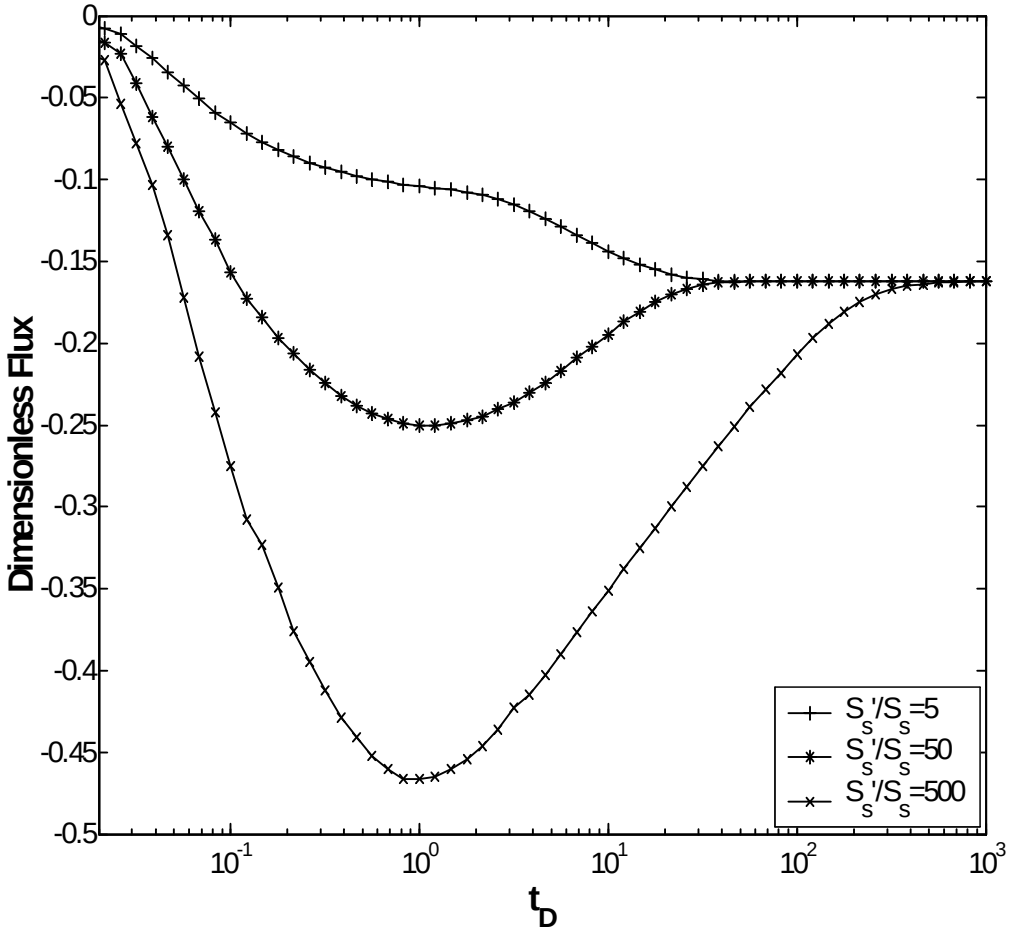

Figure 2.2 The effect of aquitard/aquifer specific storage ratio on the flux across the aquitard-aquifer boundary for a given aquitard/aquifer thickness ratio at point (x_D, y_D, z_D)=(0, 0, 1).

We also notice that when the thickness of the aquitard is too small, the aquitard storage effect will become negligible and one might only observe a monotonic increase of flux until reaching steady-state (see the case of $S_s'/S_s = 5$ in Figure 2.2).

If plotting the transient flux versus time in a semi-log scale for two specific storage ratios of 500 and 50 at two different aquitard thickness ratios of 0.1 and 0.01, one will observe some interesting finding in Figure 2.3.

First, for the same specific storage ratio but different aquitard thickness, the curves of flux are identical at early time, then separate at certain later times to approach different asymptotic steady-state values. For instance, the curves start to separate at dimensionless time 1 and 0.45 or dimensional time 20 seconds and 9 seconds for the specific ratios of 500, 50 respectively. Second, separation of the flux curves occurs earlier for a smaller specific storage. That is due to the shorter influence time of an aquitard with a smaller specific storage. As expected, a thinner aquitard will approach a greater steady-state flux, as shown in Figure 2.3.

Still using the representative point (x_D, y_D, z_D)=(0, 0, 1) as an example, if comparing the flux calculated from this article with that from Zhan and Park (2003) in a semi-log scale, one will observe some differences at the early time, reflected in Figure 2.4(A)-(B). In general, the method with the usage of the Hantush's assumption overestimates the flux at the early time. However, the difference becomes less obvious when time gets longer. In addition, the higher the specific storage of the aquitard, the greater difference between the flux obtained from this paper and that from Zhan and Park (2003) will be observed.

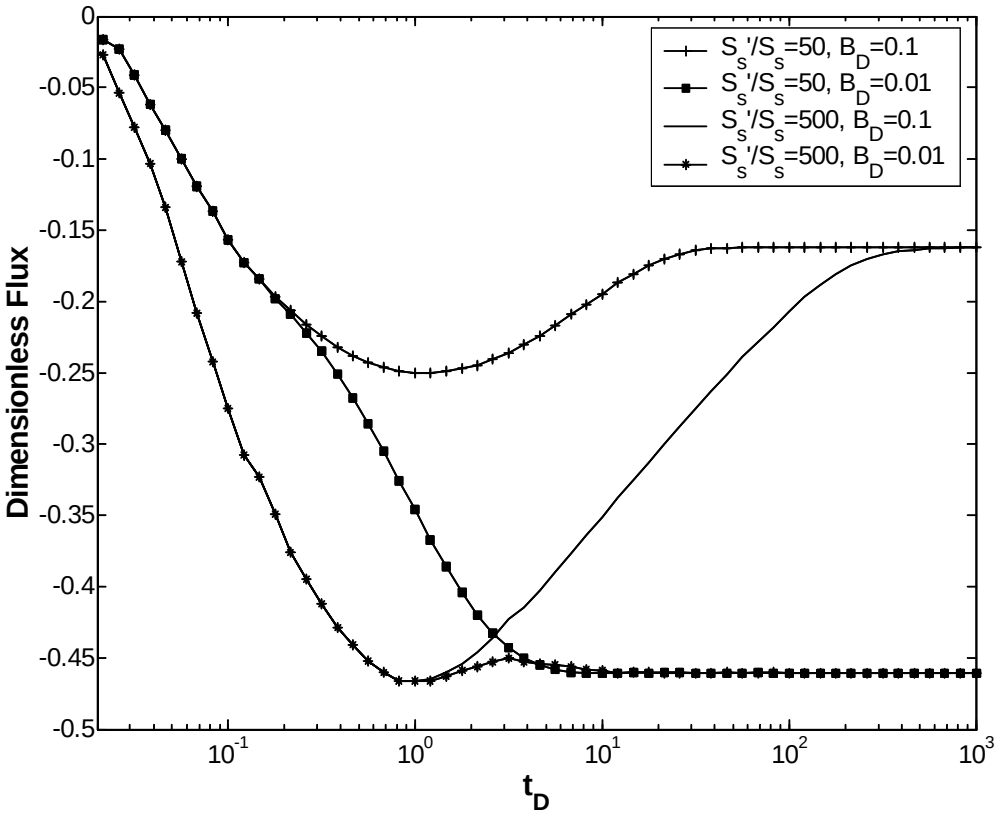

Figure 2.3 Comparison of the effect of aquitard/aquifer specific storage ratio on the flux across the aquitard-aquifer boundary for two different aquitard/aquifer thickness ratios at point (x_D, y_D, z_D)=(0, 0, 1).

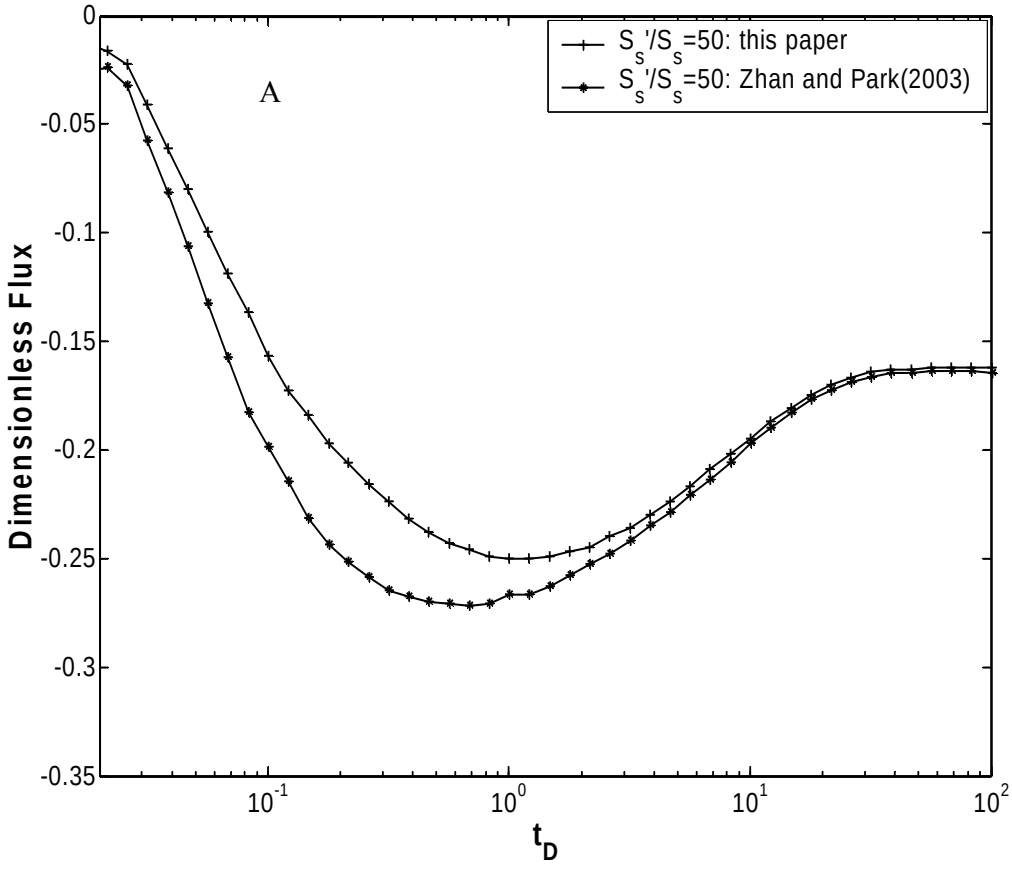

Figure 2.4 Comparison of the flux calculated in this paper and that in Zhan and Park (2003) with the Hantush's assumption at point (x_D, y_D, z_D)=(0, 0, 1) . (A) S_s'/S_s=50; (B) S_s'/S_s =500.

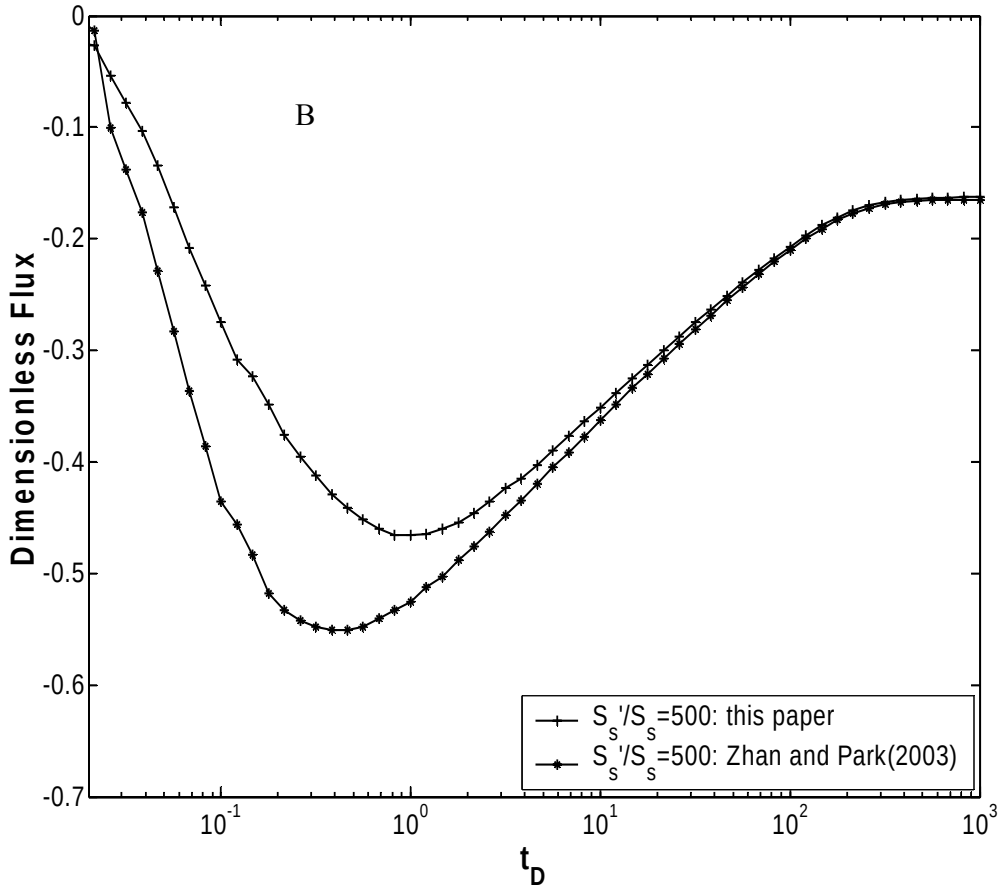

Figure 2.4 Continued

If observing the drawdowns at the point (x_D, y_D, z_D)=(0, 0, 1) with three different specific storage ratios 5, 50, and 500 for the same aquitard thickness, the one with a higher specific storage ratio will take a longer time to approach the steady-state condition, because of the larger amount of water that can be released from aquitard storage. This finding is shown in the semi-log scale diagram of Figure 2.5.

For example, it takes dimensionless time t_D about 1000, 100, and 46.42 or dimensional time t about 2.0×10^4 seconds, 2.0×10^3 seconds, and 928.4 seconds for the cases of specific storage ratio of 500, 50, and 5 to reach steady-state, respectively. Similar conclusion has been drawn by Zhan and Park (2003).

During the transient flow period, a higher flux across the aquitard-aquifer boundary will result in a less pumping stress imposed on the main aquifer, thus leads to a smaller drawdown in the aquifer. This point is noticed in Figure 2.5 which shows that the drawdown is smaller for a higher specific storage ratio, given the same time during the transient flow. Obviously, the steady-state drawdown will be independent of the specific storage of the aquitard, as seen in Figure 2.5.

The finding in this section suggests that the Hantush's assumption does not offer the correct flux and drawdown during the transient period of flow, particularly at the early time.

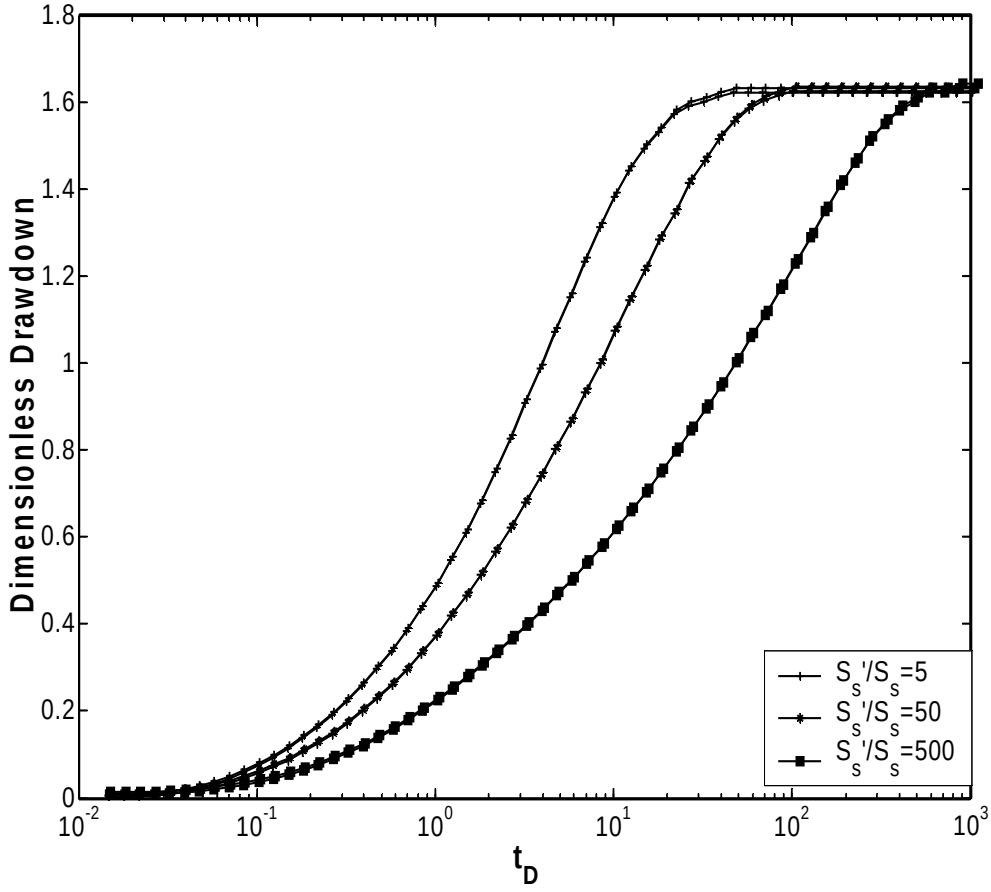

Figure 2.5 The effect of aquitard/aquifer specific storage ratio on drawdown at point (x_D, y_D, z_D)=(0, 0, 1).

In the following sections 2.3.2.2 and 2.3.2.3, we will discuss the influence of the aquitard-aquifer thickness ratio and the vertical hydraulic conductivity ratio. As an example, we select an observation line along the *y*-axis at the aquitard-aquifer boundary. Under steady-state condition, water pumped from the horizontal well comes entirely from the surface water leaked through the aquitard, and the flux at the aquitard-aquifer boundary is proportional to the hydraulic head difference across the aquitard according to Darcy's law. Because a constant-head is used at the upper boundary of the aquitard, a higher flux will result in a lower hydraulic head at the aquitard-aquifer boundary. We only discuss the flux in the following; the drawdown can be easily extracted from the flux using Darcy's law if needed.

2.3.2.2 Aquitard-aquifer thickness ratio (B_D)

At steady-state, the distribution of flux across the aquitard-aquifer boundary shows some special characteristics.

First, the flux is localized around a region right above the center of the well with the maximum flux at the point of x_D=0 and y_D=0. That is because the greatest drawdown generated by the pumping horizontal well along the aquitard-aquifer boundary is at that point.

Second, the distribution of flux and the maximum value of the flux are closely related to the thickness of the aquitard, as shown in Figure 2.6.

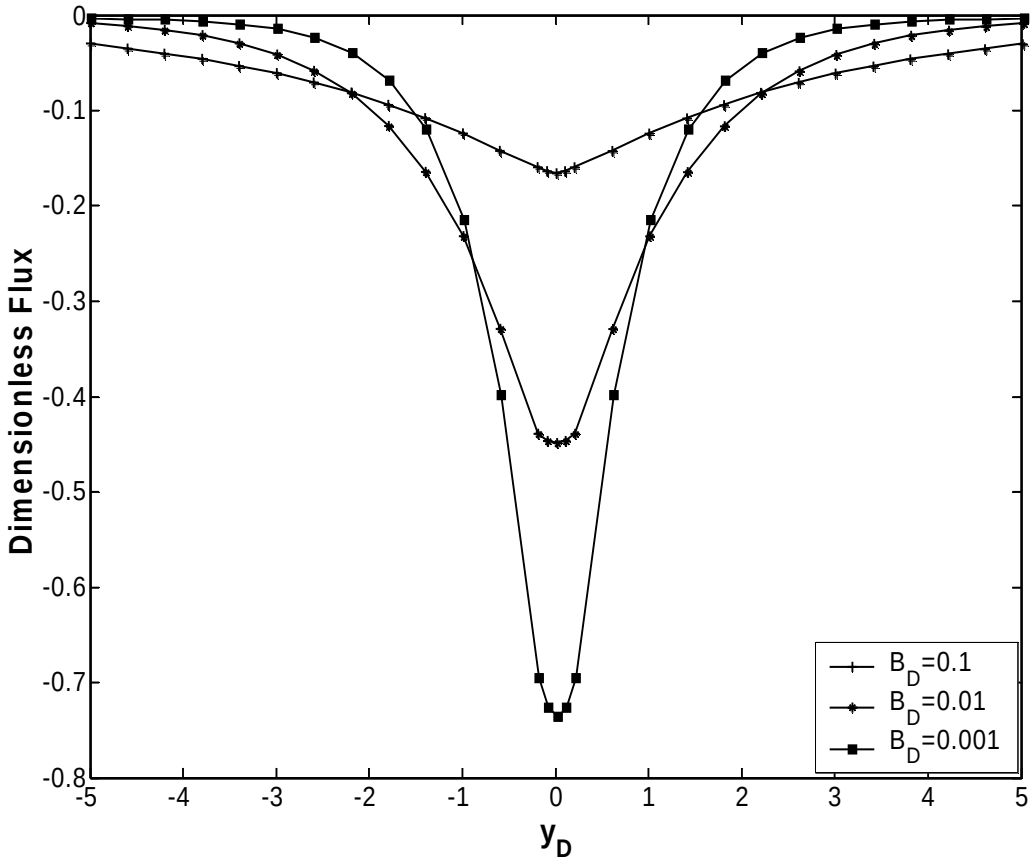

Figure 2.6 The effect of aquitard/aquifer thickness ratio along the line of y_{0D}=-5.0 to 5.0 with x_{0D}=0 and z_D=1 under steady-state condition.

The one with a thinner aquitard will have a higher maximum value of flux at the center because water is easier to flow across that aquitard. For instance, the absolute values of the dimensionless maximal fluxes are 0.162, 0.462, and 0.772 in Figure 2.6 for aquitard-aquifer thickness ratios of 0.1, 0.01, and 0.001, respectively. Notice that we only test the case where the thickness of the aquitard is less than that of the aquifer.

Third, it is interesting to see from Figure 2.6 that the thinner the aquitard, the degree of flux localization is higher. Considering the symmetry of flux, we consider the flux distribution along x_D=0, $0 \le y_D \le 5$, and z_D=1 for three different B_D of 0.1, 0.01, 0.001. We notice that the difference of result from this article and that from Zhan and Park (2003) is small when the aquitard-aquifer thickness ratio is relatively large (B_D = 0.1), as seen in Figure 2.7A. The only detectable difference for the case of B_D = 0.1 is near the point of x_D=0 and y_D=0. However, when the thickness is relatively thin, one can observe considerable difference, as shown in Figure 2.7B-2.7C..

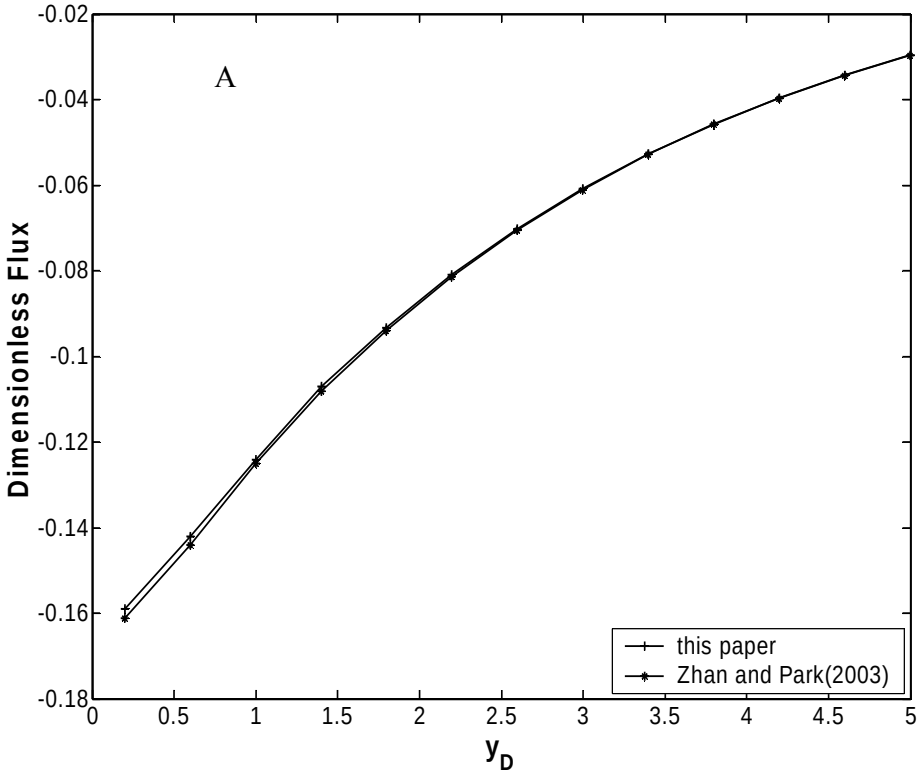

Figure 2.7 Comparison of the steady-state flux calculated in this paper and that in Zhan and Park (2003) with the Hantush's assumption along the line of y_{0D}=0 to 5.0 with x_{0D}=0 and z_D=1 for different aquitard/aquifer thickness ratios. (A) B_D=0.1; (B) B_D=0.01; (C) B_D=0.001.

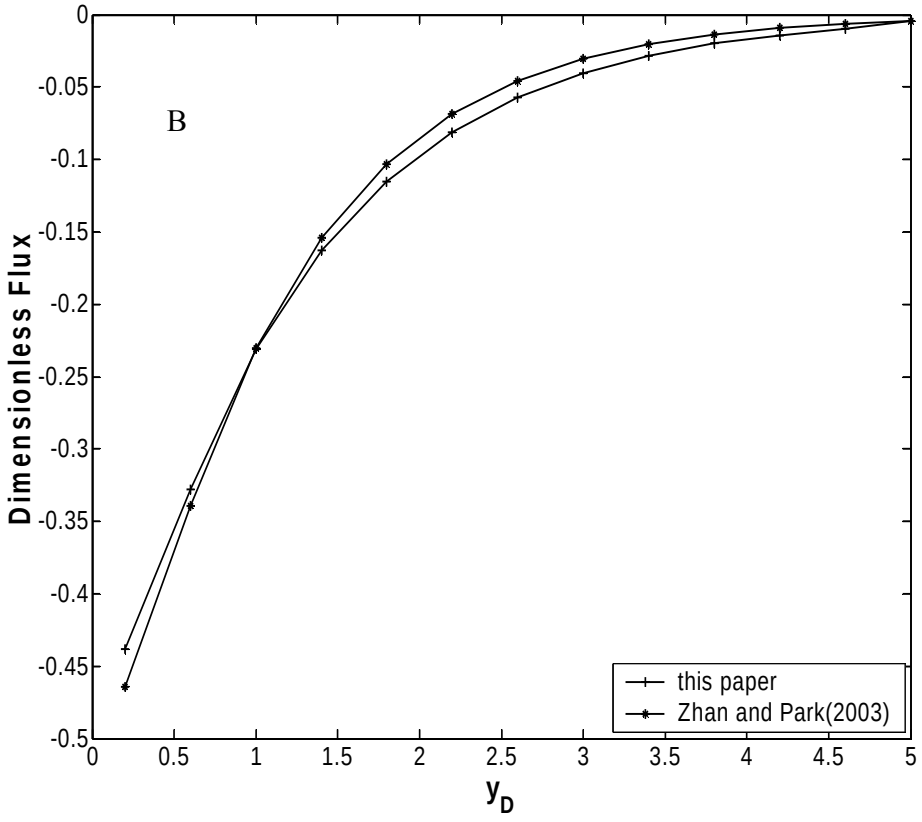

Figure 2.7 Continued

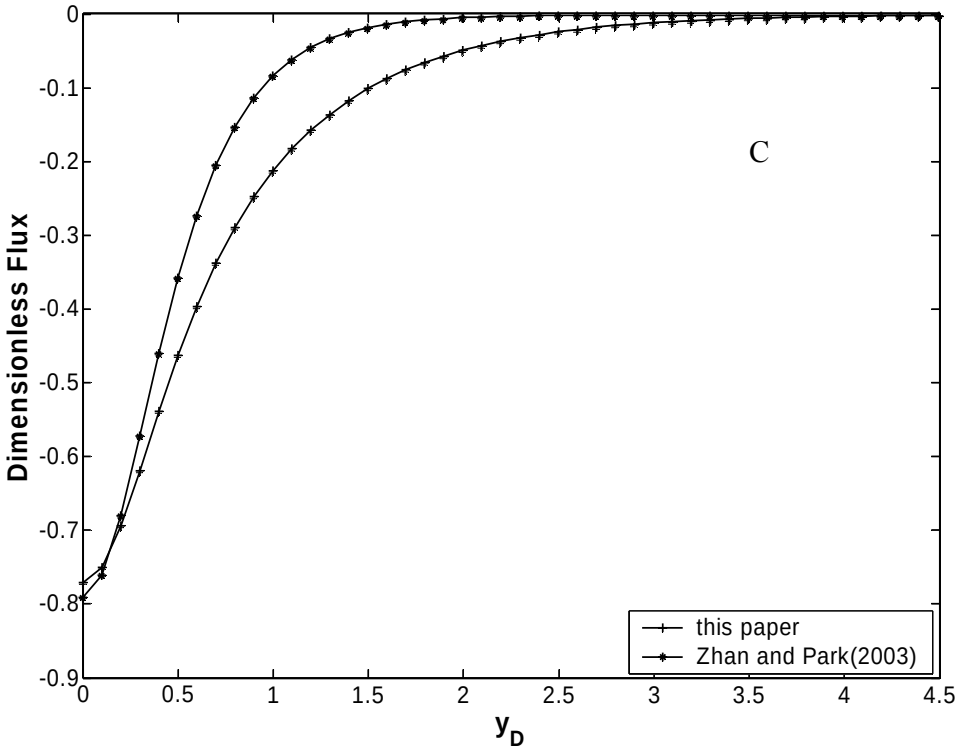

Figure 2.7 Continued

This suggests that the Hantush's assumption works reasonably well for a relatively thick aquitard under steady-state flow condition. When the aquitard is very thin, for instance, with an aquitard-aquifer thickness ratio of less than 0.001, the Hantush's assumption does not offer the correct value of flux.

2.3.2.3 Aquitard-aquifer vertical hydraulic conductivity ratio (β)

For an aquitard-aquifer thickness ratio of 0.1, we have tested the differences of flux derived by this paper and that by Zhan and Park (2003) for two different vertical hydraulic conductivity ratios of 0.001 and 0.01. Considering the fact that most aquitards have hydraulic conductivities that are a few orders of magnitude smaller than those of the aquifers, this choice of hydraulic conductivity ratios is reasonable. Except for the minor difference near the point of x_D=0 and y_D=0 for the case of 0.01, there is almost no distinguishable difference between the two solutions for the rest regions, as seen in Figures 2.8A-2.8B. This suggests that the Hantush's assumption works well for different ranges of aquitard-aquifer hydraulic conductivity ratios under steady-state flow condition.

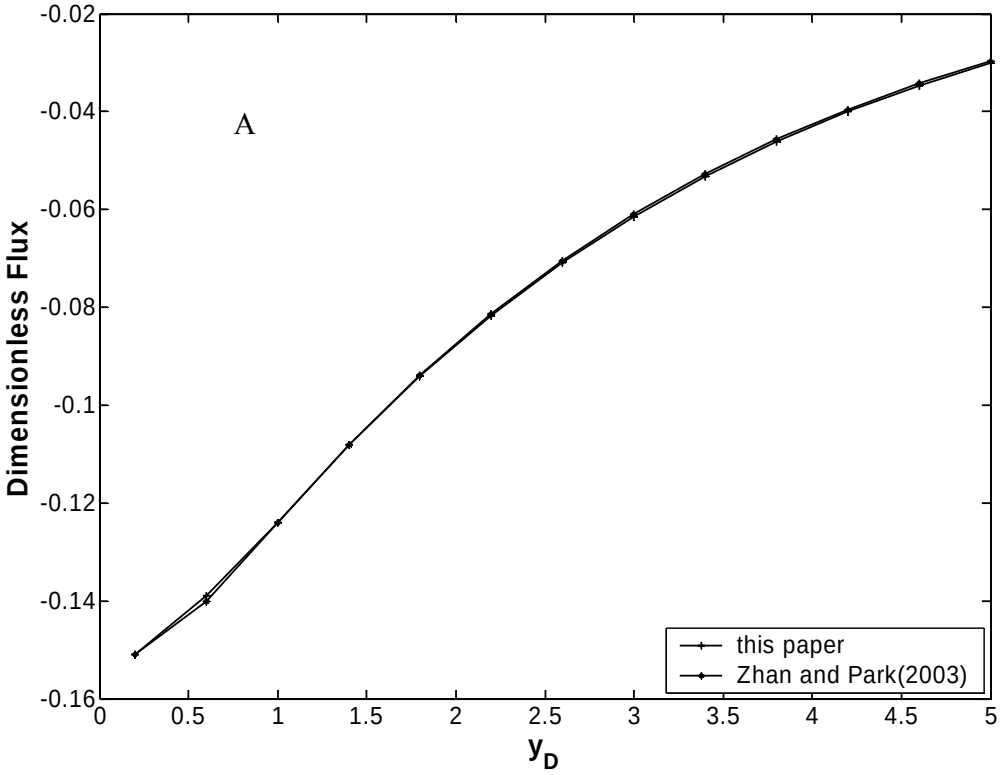

Figure 2.8 Comparison of the steady-state flux calculated in this paper and that in Zhan and Park (2003) with the Hantush's assumption along the line of y_{0D}=0 to 5.0 with x_{0D}=0 and z_D=1 for different aquitard/aquifer hydraulic conductivity ratios. (A) $K'/K_Z = 0.001$; (B) K'/K_Z=0.01.

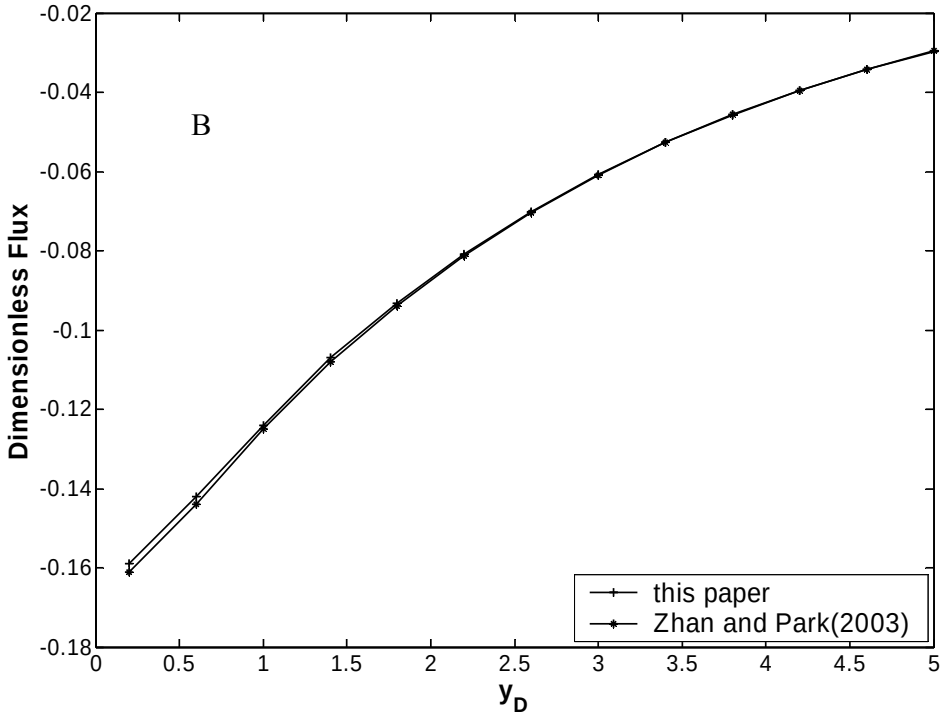

Figure 2.8 Continued

2.3.3 Control of horizontal well configuration on flux

2.3.3.1. Well location

We use two different well locations z_{wD}=0.2 (a lower well), and 0.9 (an upper well) to test the influence of well location on flux distribution under steady-state condition. As shown in Figure 2.9, a well closer to the upper aquitard-aquifer boundary will induce a larger flux around the point x_D=0 and y_D=0. For example, the absolute values of the dimensionless maximal flux are 0.15 and 0.19 for the cases of z_{wD}=0.2 and 0.9, respectively. But the influence in general is limited within a relatively small region around that point. If comparing the result of this article with that of Zhan and Park (2003) for a given well location, we do not observe noticeable difference for the case of a lower well (z_{wD}=0.2), as shown in Figure 2.10A. We do observe noticeably small difference for the upper well location in Figure 2.10B (z_{wD}= 0.9). This finding indicates that the Hantush's assumption works reasonably well when the location of the horizontal well is not too close to the aquitard-aquifer boundary under steady-state condition.

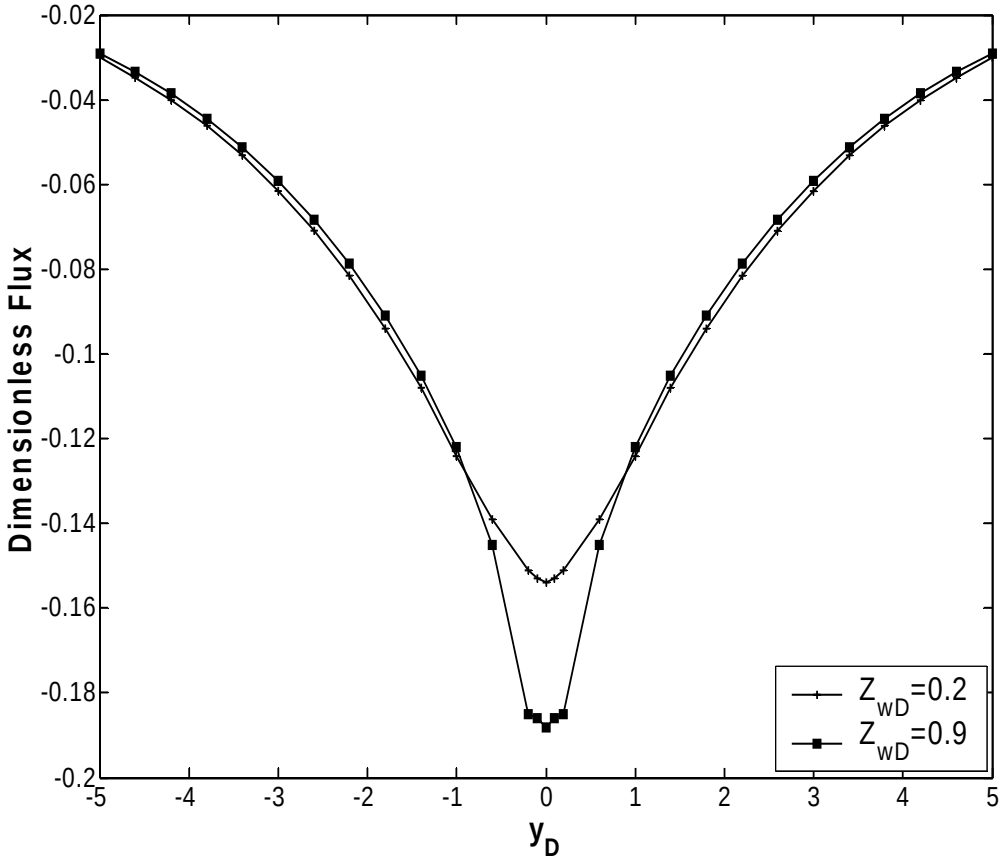

Figure 2.9 The effect of well location on the flux along the line of y_{0D}=0 to 5.0 with x_{0D}=0 and z_D=1.

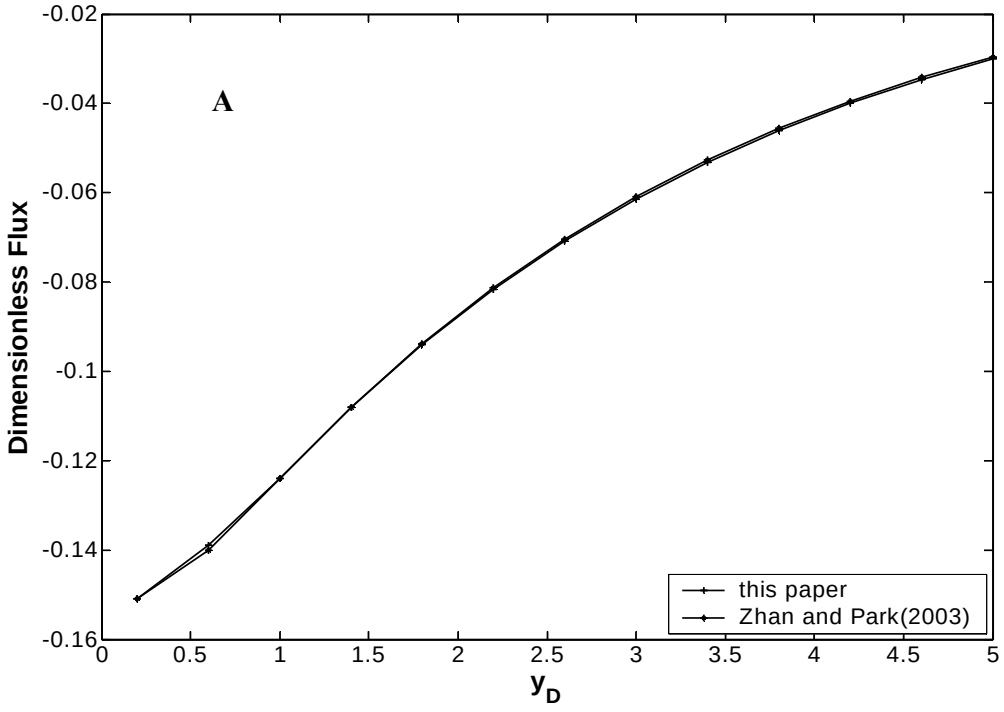

Figure 2.10 Comparison of the steady-state flux calculated in this paper and that in Zhan and Park (2003) with the Hantush's assumption along the line of y_{0D}=0 to 5.0 with x_{0D}=0 and z_D=1 for two different well locations. (A) z_{wD}=0.2;(B) z_{wD}=0.9.

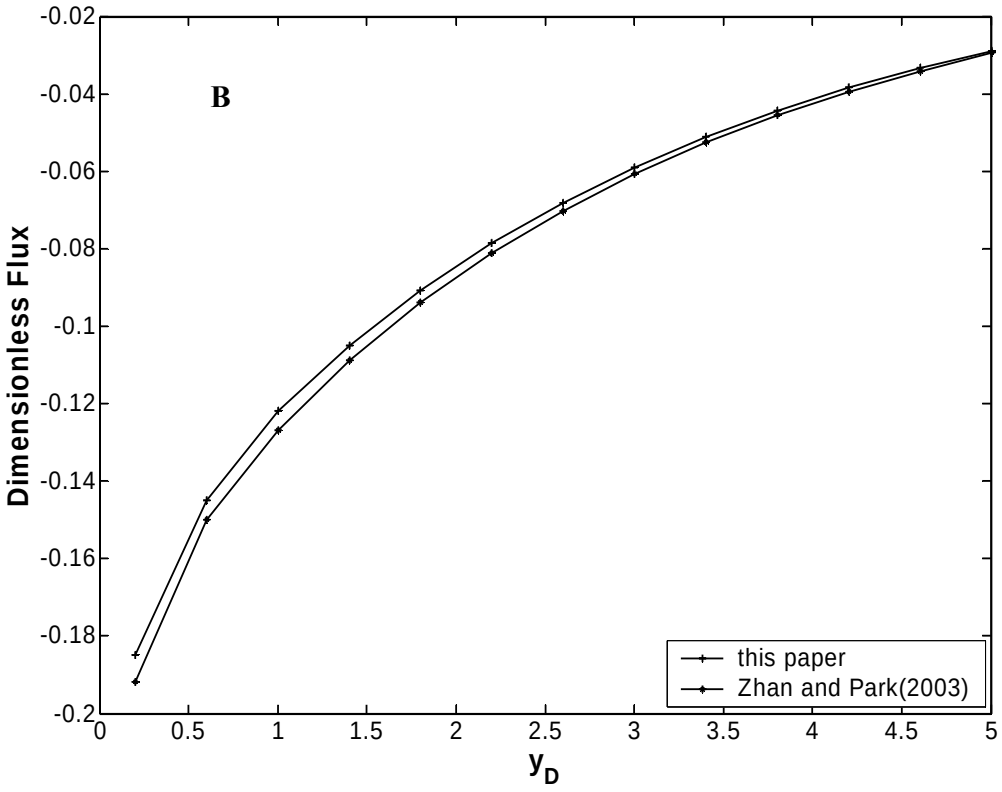

Figure 2.10 Continued

2.3.3.2 Well length

We use different well lengths L_D=0.5, 5, and 50 to observe the change of flux distribution under steady-state condition in Figure 2.11. The usage of the probably unrealistic case of L_D=0.5 is for the purpose of comparison. The cases of L_D=5 and 50 are probably more realistic for field applications. Given the same pumping rate, a shorter well means that the pumping strength is concentrated over a shorter distance, thus will induce higher flux around a small region right above the well. A longer well will distribute the pumping rate over a greater distance, thus will induce a broader flux distribution. For example, the values of dimensionless flux are -0.37, -0.23, and -0.034 for the cases of L_D=0.5, 5, and 50 respectively in Figure 2.11 at (x_D, y_D, z_D)=(0, 0, 1). If comparing the result of this article with that of Zhan and Park (2003), we only notice a small difference around the point of x_D=0 and y_D=0 for a very short, and probably unrealistic well length (L_D=0.5). For more realistic cases of L_D=5 and 50, there are no distinguishable differences. This supports the statement that the Hantush's assumption works reasonably well for typical lengths of horizontal wells used in the field.

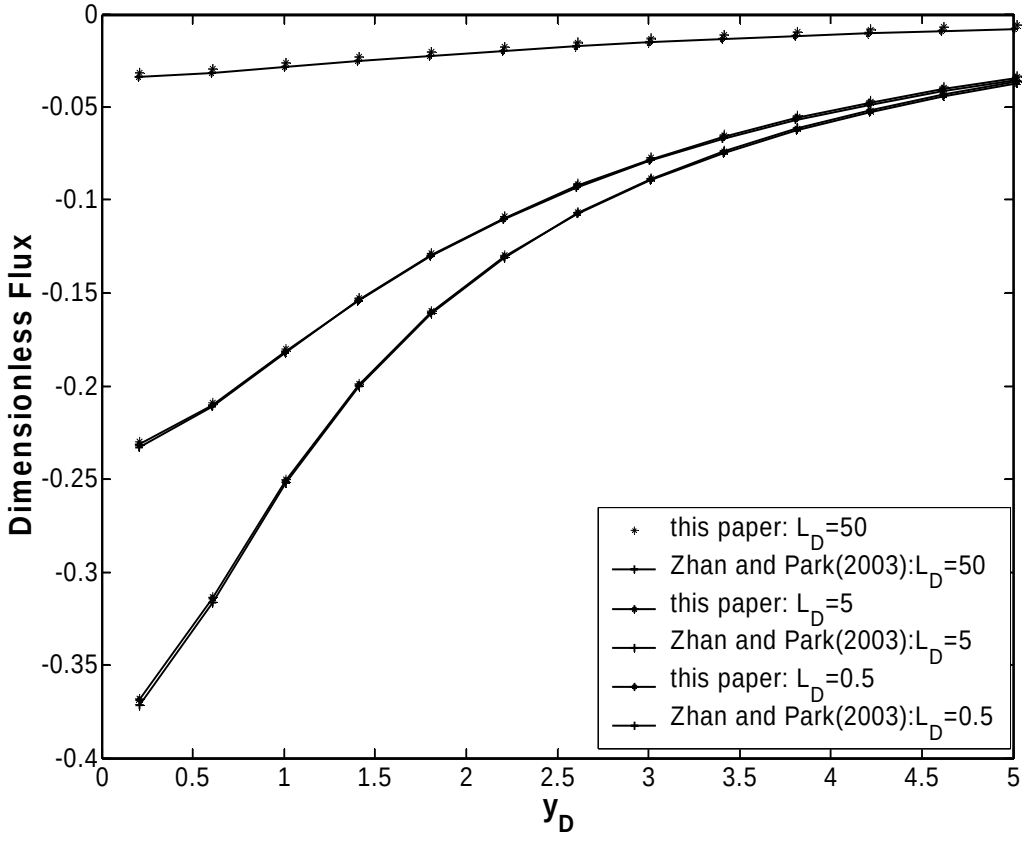

Figure 2.11 Comparison of the steady-state flux calculated in this paper and that in Zhan and Park (2003) with the Hantush's assumption along the line of y_{0D}=0 to 5.0 with x_{0D}=0 and z_D=1 for different well length.

2.4. Summary and Conclusions

We have provided new solutions of flow to a horizontal well in an aquitard-aquifer system based on the mass conservation law. Flow in the aquitard and aquifer is treated as two flow systems that are connected via the continuity of flux and head at the aquitard-aquifer boundary. We do not adopt the Hantush's assumption that was commonly used in previous studies, including Zhan and Park (2003). The leakage induced by the pumping horizontal well under different aquitard hydraulic conditions and a variety of well configurations is analyzed. The flux and the drawdown calculated in this paper are compared with that of Zhan and Park (2003) and the validity of the Hantush's assumption is tested for both transient and steady-state flow conditions. In particular, we draw the following conclusions from this study:

1. The leakage induced by the pumping horizontal well depends on several parameters such as the aquitard thickness, the vertical hydraulic conductivity of the aquitard, the aquitard storage, the well location, and the well length.
2. For transient flow, a continuous increase of flux will generally be observed across the aquitard-aquifer interface at early time until reaching a maximal value. After that, the flux will gradually decrease to approach the steady-state where the leaked water comes entirely from the upper surface water reservoir. The maximal value of the induced flux is a function of the aquitard specific storage. However, when the aquitard is relatively thin, one can only observe a monotonic increase of flux to approach the steady-state.

3. In general, we find that the Hantush's assumption does not offer correct prediction of flux and drawdown during the transient flow condition, particularly at the early time. For steady-state flow, the Hantush's assumption works reasonably well under realistic conditions of aquitard thickness and hydraulic conductivity as long as the aquitard thickness is not too thin (aquitard-aquifer ratio less than 0.001). This assumption also works reasonably well under realistic horizontal well lengths and well locations as long as the well is not too close to the aquitard-aquifer boundary.

CHAPTER III

PUMPING INDUCED INTERACTION AMONG GROUNDWATER AND TWO STREAMS

This study deals with the interaction of an aquifer with two parallel surface water bodies such as two streams or canals. Previous studies focus on one stream and aquifer system and treat leakage from the surface water body as a volumetric source term in the governing equation, a hypothesis termed "Hantush's assumption". In this paper, new closed-form analytical and semi-analytical solutions are acquired for the pumping induced dynamic interaction among two streams and ground water for two different cases. In the first case, the sediment layers separating the streams from the aquifer ground water do not exist. In the second case, the two low permeable layers are considered. We solve the problem based on rigorous mass conservation requirement by maintaining continuity of flux and head along the aquitard-aquifer boundaries. Aquitards properties control the competition of stream depletion when a pumping well is positioned between two streams. The aquitard hydraulic conductivity is the most important factor controlling the stream depletion, followed by the aquitard thickness which greatly influences the drawdown at observation points that are not too close to the pumping well. Aquitard storages do not play significant roles unless the two streams are very close to each other or the well is very close to either stream. When the two aquitards are identical, the so called "equal flux point" is located right at the center between the two aquitards. The equal flux point will move off the center when the aquitard thickness ratio and/or the aquitard hydraulic conductivity ratio are different than

unity. The results in this paper could provide guidance for well design and water management.

3.1 Introduction

Groundwater and stream interaction has become an active research area in hydrology because of the need of watershed management and water rights distribution (Bouwer and Maddock, 1997). There is a consensus among hydrologists that groundwater pumping near a stream will inevitably affect the stream flow, thus water rights related to groundwater and surface water must be considered together. Although sophisticated numerical models might be needed to deal with realistic situations, the requirement of many input parameters needed in those models might not always be available. Thus, analytical models are still commonly used by hydrologists and water managers to deal with stream-aquifer interaction (Hunt, 1999; Zlotnik and Huang, 1999; Butler et al., 2001). Theis (1941) was probably the first who analytically studied pumping induced groundwater-stream interaction for a fully penetrating stream perfectly connected with the adjacent aquifer. His work was later generalized by Glover and Balmer (1954) and Jenkins (1968), which have become standard tools for water management and water rights distribution, despite of serious limitations for many realistic problems (Zlotnik and Huang, 1999). Hantush (1965) considered pumping near a fully penetrating stream but considered a low-permeability streambed separating the stream from the aquifer.

In recent years, several investigators have considered pumping induced interaction of groundwater with partially penetrating streams. For instance, Hunt (1999) has developed a model for studying interaction between groundwater and a zero-penetrating, narrow

stream. Zlotnik and Huang (1999) developed a model that considered a finite-width of stream and their work is later extended by Butler et al. (2001) to consider the lateral boundaries. Moench and Barlow (2000) and Barlow et al. (2000) have considered interaction between a fully penetrating stream and groundwater but they did not consider any pumping wells there. Chen and Chen (2003a,b) and Kollet and Zlotnik (2003) have analyzed data of pumping tests conducted near streams to find out the parameters of the aquifers and stream-bed conductance.

Most of the research mentioned above only concerned interaction of groundwater with a single stream. As far as we know, there are still no researches that concern groundwater interaction with two streams which might be parallel to each other. This situation can occur when two channels or two tributaries are closely spaced. It can also occur in some engineered structures such as two closely spaced parallel water canals. For instance, as shown in Chen and Chen (2003b, Figure 7), in certain areas of the high plain of United States, two streams can be parallel and the distance between them could be as close as 270m. Therefore, pumping in an aquifer between these two streams will deplete flows from both streams. Competition of stream depletion from two streams could be an important issue in water rights adjudication. In fact, inadequately application of the single stream model to deal with the two streams might lead to significant errors (Kollet, 2005).

The purpose of this study is to develop an analytical model of interaction of groundwater with two parallels streams. We deal with two different kinds of stream-aquifer interfaces. One has a perfect hydraulic connection between the stream and the

aquifer. This condition commonly occurs in Northwest States of the United States such as Montana where streambed has the similar sediments as the adjacent aquifer (Wossner, 2000). The other has low-permeability streambed sediments separating the stream from the aquifer. Field evidences have shown that the values of streambed permeability could be much smaller than that of the aquifer in some situations (Larkin and Sharp, 1992; Conrad and Beljin, 1996). The thickness of the lower-permeability layer can vary between 0.5m-5m. The conceptual and mathematical models are presented in the following.

3.2 Conceptual and Mathematical Models

3. 2. 1 Conceptual model

A realistic stream-aquifer interaction system could be very complicated because of many issues such as meandering of stream channels, variation of water level in the streams, heterogeneity of streambed sediments and aquifer, partially penetrating streams, etc. It is necessary to make reasonable simplification to make the analytical models amenable. The primary simplifications used in this study, as well as in many previous analytical studies are listed below, followed by the justification. (1) The stream is straight and extends to a sufficiently long distance from the domain of interest; (2) the streams are fully penetrating; (3) the aquifer and the streambed are homogeneous but could be anisotropic; (4) the upper and lower boundaries of the aquifer are horizontal and extends to infinity; and (5) the pumping well is fully penetrating. The schematic diagrams of an aquifer bounded by two parallel streams are shown in Figure 3.1(A, B and C).

The first simplification is necessary to make the boundary condition simple enough to be handled analytically and is commonly used in previous analytical studies (Hunt, 1999; Zlotnik and Huang, 1999; Moench and Barlow, 2000; Butler et al., 2001). The second simplification is not required but will make the mathematical model easier. Partially penetrating two-stream systems will be discussed for a separate study. In fact, as shown in Butler et al. (2001, Figure 7), when the distance between the pumping well and the nearer bank of the river is greater than five times of the river width, the fully penetrating stream approach becomes a very good approximation of even a very shallow stream. Fully penetrating stream approach has also been used by Moench and Barlow (2000), Barlow et al. (2000), Chen (2003), etc. The third simplification will render the usage of deterministic model. If heterogeneity is considered, more sophisticated models such as geostatistic or stochastic models might be needed. The fourth simplification is not required but will make the upper and lower boundary condition easier to handle, thus is commonly used in many hydrological studies. The fifth simplification will ensure that vertical flow near the well will not become an issue. This simplification can be relaxed to a partially penetrating well as long as the distance between either streams or the observation point to the well is at least $1.5\sqrt{K_h / K_v}B$ to $2\sqrt{K_h / K_v}B$ where K_h, K_v, and B are the horizontal, vertical hydraulic conductivities, and saturated thickness of the aquifer (Hantush, 1964).

We deal with a confined aquifer first, but the model can be extended to an unconfined aquifer as long as the drawdown of the water table is much smaller than the saturated thickness of the aquifer and the vertical well is fully penetrating. If replacing S_s

by S_y/H, where S_s is the specific storage of the confined aquifer, and S_y and H are the specific yield and the initial saturated thickness of the unconfined aquifer, then the confined aquifer solutions are extended to the unconfined aquifer solution. For the simplicity of illustration, we assumed that there is no head difference between two streams. In fact, if a head difference exists between two streams, it can be simply superposed as a regional flow in the governing equation of the main aquifer. The hydrographs of the streams are not considered at present study. If time dependent stream stages are considered, time dependent boundary condition is needed. The solution will become a little bit more complex but the general methodology of the problem-solving will be similar to what presented below for steady stream stages. Influence of the stream hydrographs on the flow is out of the scope of this study and will be addressed elsewhere.

3.2.2 Flow to a fully penetrating vertical well in a perfectly connected stream-aquifer

Figure 3.1A is a schematic diagram of the problem and the coordinate system setup(planer view). The x- and y- axes are in the horizontal directions and the z- axis is in the vertical direction. The origin can be positioned anywhere along the interface of the aquifer and the first stream (Figure 3.1A). The center of the vertical well is at x=0 and $y= y_w$, where y_w is the distance from the well to the first stream. There are several different ways of solving this initial-boundary condition problem. For example, we can directly solving the two-dimensional horizontal flow equation in the main aquifer by treating the fully penetrating well as a vertical line source. The method that will be employed here is to first solve flow to a point sink in a vertically infinite domain, then

A.

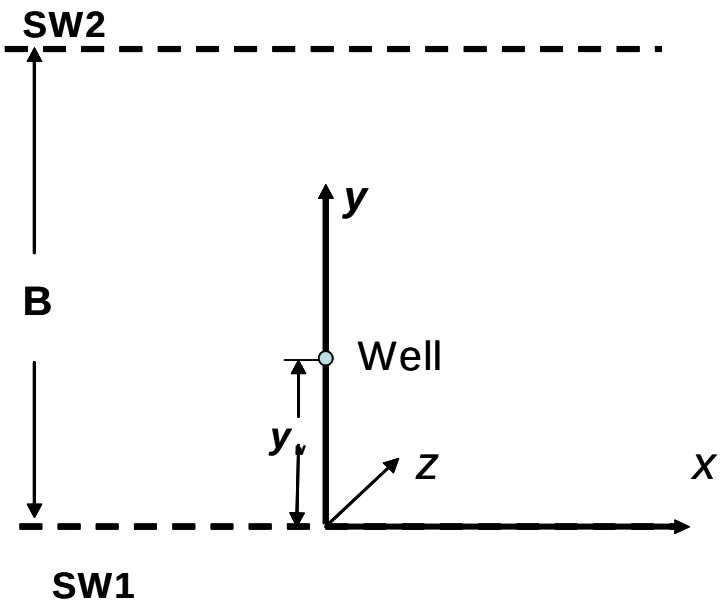

Figure 3.1 A Schematic diagram of pumping between two surface water bodies without sediment layers.

integrate the point sink solution from $-\infty$ to $+\infty$ along the vertical direction. This is equivalent to flow to a fully penetrating vertical well. This point sink method is quite general and has the advantage of dealing with any arbitrary well types in the future.

For flow to a point sink in the aquifer, one has

$$K_x \frac{\partial^2 h}{\partial x^2} + K_y \frac{\partial^2 h}{\partial y^2} + K_z \frac{\partial^2 h}{\partial z^2} = S_s \frac{\partial h}{\partial t} + Q\delta(x - x_0)\delta(y - y_0)\delta(z - z_0), \quad 0<y<B, \tag{3.1}$$

$$h(x, y, z, 0) = h_0, \tag{3.2}$$

$$h(x = \pm\infty, y, z, t) = h(x, y, z = \pm\infty, t) = h_0, \tag{3.3}$$

$$h(x, y = 0, z, t) = h(x, y = B, z, t) = h_0, \tag{3.4}$$

where h is the hydraulic head in the aquifer; h_0 is the initial hydraulic head; K_x, K_y, K_z are the three principal hydraulic conductivities in the x, y, z axes, respectively; S_s is the aquifer specific storage, Q is pumping rate of the point sink, (x_0, y_0, z_0) are the coordinates of the point sink, B is the distance between the two streams, and t is time. Eq. (3.1) is the governing equation in the aquifer, Eq. (3.2) is the initial condition in the aquifer, Eq. (3.3) is the lateral boundary at infinity, Eq. (3.4) is the constant-head boundary condition at the stream -aquifer boundary.

First, we would like to change the hydraulic head to drawdown, thus the initial head h_0 can be removed and the initial and boundary conditions are simplified. After this, we transform all the terms into their dimensionless forms. Second, we apply the Laplace transform to remove the t-dependent terms; a Fourier transform solution with a summation of a series of sine functions is proposed for the aquifer considering the boundary conditions at y=0 and B. The frequency used in the sine functions of the

proposed solution is determined via the constant head condition at the stream-aquifer boundary. After that, solutions of drawdown in the aquifer with a point-sink will be derived in Laplace domain. Finally, integration of the point-sink solution along the *z*-axis will yield the vertical well solution in Laplace domain, which will be subsequently inverted to yield the solution in real time domain.

We define drawdown $s=h_0-h$. The dimensionless parameters are defined Table 3.1.

Conducting Laplace transform to Eqs.(3.1)-(3.4) results in:

$$\frac{\partial^2 \overline{s_D}}{\partial {x_D}^2}+\frac{\partial^2 \overline{s_D}}{\partial {y_D}^2}+\frac{\partial^2 \overline{s_D}}{\partial {z_D}^2}=p\overline{s_D}+\frac{4\pi}{p}\delta(x_D-x_{0D})\delta(y_D-y_{0D})\delta(z_D-z_{0D}), \tag{3.5}$$

$$\overline{s_D}(x_D=\pm\infty, y_D, z_D, p)=\overline{s_D}(x_D, y_D, z_D=\pm\infty, p)=0, \tag{3.6}$$

$$\overline{s_D}(x_D, y_D=0, z_D, p)=\overline{s_D}(x_D, y_D=1, z_D, p)=0, \tag{3.7}$$

where overbar means the parameter in Laplace domain, and p is the Laplace transform parameter.

3.2.2.1 Point-sink solution in Laplace domain

Following the similar procedures outlined by Zhan and Park (2003), the proposed solution of Eq. (3.5) in Laplace domain is a Fourier transform of sine functions:

Table 3.1: Dimensionless variables

$x_D = \frac{x}{B}\sqrt{\frac{K_y}{K_x}}$, $z_D = \frac{y}{B}\sqrt{\frac{K_y}{K_z}}$,	$S_{D1} = \frac{4\pi\sqrt{K_x K_z}B}{Q} S_1$
$y_{wD} = \frac{y_w}{B}$	$S_{D2} = \frac{4\pi\sqrt{K_x K_z}B}{Q} S_2$
$s_D = \frac{4\pi\sqrt{K_x K_z}B}{Q} s$	$B_{D1} = \frac{B_1}{B}$, $B_{D2} = \frac{B_2}{B}$
$t_D = \frac{K_y}{B^2 S_s} t$	$\beta_1 = \frac{K_y}{K_{y1}}$, $\beta_2 = \frac{K_y}{K_{y2}}$
$y_D = \frac{y}{B}$,	$\alpha_1 = \frac{(K_y / S_s)}{(K_{y1} / S_{S1})}, \alpha_2 = \frac{(K_y / S_s)}{(K_{y2} / S_{S2})}$

$$\overline{s_D} = \sum_{n=0}^{\infty} H_n(x_D, y_D, p)\sin(\omega_n y_D) \tag{3.8}$$

where H_n is a function only depends on the horizontal coordinates and p, and ω_n is the frequency that will be determined via Eqs. (3.7) and (3.8). Substituting Eq. (3.8) into Eq. (3.7) results in $\sin(\omega_n) = 0$ when $y_D = 1$, thus

$$\omega_n = n\pi, \qquad n = 1,2,3,..... \tag{3.9}$$

The details of solving Eqs. (3.5)-(3.8) are shown in Zhan et al. (2001), Zhan and Zlotnik (2002) and Zhan and Park (2003). The aquifer drawdown in Laplace domain for a point-sink is:

$$\overline{s_{DP}} = \frac{4}{p}\sum_{n=0}^{\infty} \sin(n\pi y_D)\sin(n\pi y_{wD})K_0(\sqrt{(n\pi)^2 + p}\, r_D), \tag{3.10}$$

where K_0 is the second-kind, zero-order, modified Bessel function, and $r_D = \left(x_D{}^2 + z_D{}^2\right)^{1/2}$. Integration of Eq. (3.10) along the z-axis from $-\infty$ to $+\infty$ will yield the solution of flow to a fully penetrating vertical well in Laplace domain.

$$\overline{s_D}(p) = \frac{4\pi}{p}\sum_{n=1}^{\infty} \sin(n\pi y_D)\sin(n\pi y_{WD})\int_{-\infty}^{\infty} k_0\left(\sqrt{n^2\pi^2 + p}\left[(z_D - z_{0D})^2 + x_D^2\right]^{1/2}\right) dz_{0D} \tag{3.11}$$

The integration in Eq. (3.11) is easy to calculate and the final result is:

$$\overline{s_D}(p) = \frac{4\pi}{p}\sum_{n=1}^{\infty} \frac{\sin(n\pi y_D)\sin(n\pi y_{wD})}{\sqrt{(n\pi)^2 + p}}\exp\left(-\sqrt{(n\pi)^2 + p}\,|x_D|\right). \tag{3.12}$$

Inverse Laplace transform of Eq. (3.12) can be carried out analytically with more details given in Appendix B. The result in real time domain is:

$$\overline{s_D}(t_D) = 2\sum_{n=1}^{\infty} \frac{\sin(n\pi y_D)\sin(n\pi y_{wD})}{n} \times \left[e^{-n\pi|x_D|} erfc\left(\frac{|x_D|}{2\sqrt{t_D}} - n\pi\sqrt{t_D}\right) - e^{n\pi|x_D|} erfc\left(\frac{|x_D|}{2\sqrt{t_D}} + n\pi\sqrt{t_D}\right) \right] \tag{3.13}$$

where erfc( ) is the complementary error function.

The total flux along the boundaries of streams and aquifer can be calculated as,

$$Q(p) = \int_{-\infty}^{\infty} \frac{\partial s_D(p)}{\partial y} dx_D \tag{3.14}$$

Inserting Eq.(3.11) to (3.14) , one gets

$$Q(p) = \frac{8\pi}{p} \sum_{n=1}^{\infty} \frac{n\pi \sin(n\pi y_{WD})\cos(n\pi y_D)}{(n\pi)^2 + p} \tag{3.15}$$

The real time domain of Eq.(3.15) will be:

$$Q(t) = 8\sum_{n=1}^{\infty} \frac{\sin(n\pi y_{WD})\cos(n\pi y_D)}{n}(1 - e^{-(n\pi)^2 t_D}) \tag{3.16}$$

let $t_D \to \infty$, one will get

$$V = 8\sum_{n=1}^{\infty} \frac{\sin(n\pi y_{WD})\cos(n\pi y_D)}{n} \tag{3.17}$$

Where V is the total volume of water from stream to aquifer long time after pumping.

3.2.3 Flow to fully penetrating vertical well with separating layers

As shown in Figure 3.1B and Figure 3.1C, two low permeable layers, denoted as aquitard 1 and 2 separate the stream 1 and 2 from the aquifer, respectively. Different from section 3.2.2, the origin is at the boundary of the aquifer and aquitard 1. B now represents the length of aquifer in the y-direction between two aquitards. In this case, transient flow in two aquitards is also considered. Instead of using Hantush's

assumption (1964) where the leakage from stream was treated as a volumetric source inside the aquifer, flows in the aquitards and aquifer are linked together by the continuity of head and flux at the aquitard-aquifer interfaces. Similar to the procedure used in section 3.2.2, we first solve the problem of flow to a point sink, then integrating point source solution along the *z*-axis to get the solution of a vertical well.

The flow governing equation inside the aquifer is the same as in section 3.2.2. The flow equations in two aquitards and the associated initial and boundary conditions are listed below. The aquitards are often composed of clay or silty materials whose permeabilities are much at least two orders of magnitude lower than that of the aquifer, thus only the one-dimensional flow along the y-axis is considered in the aquitards.

Flow in aquitard 1:

$$K_{y1}\frac{\partial^2 h_1}{\partial y^2} = S_{s1}\frac{\partial h_1}{\partial t} \quad , \qquad -B_1 < y < 0 \tag{3.18}$$

$$h_1(x, y, z, 0) = h_0 \, , \tag{3.19}$$

$$h_1(x = \pm\infty, y, z, t) = h_1(x, y, z = \pm\infty, t) = h_0 \, , \tag{3.20}$$

$$h_1(x, y = -B_1, z, t) = h_0 \, , \tag{3.21}$$

$$h_1(x, y = 0, z, t) = h(x, y = 0, z, t) \, , \tag{3.22}$$

$$K_{y1}\frac{\partial h_1}{\partial y}\bigg|_{y=0} = K_y \frac{\partial h}{\partial y}\bigg|_{y=0} \, . \tag{3.23}$$

B.

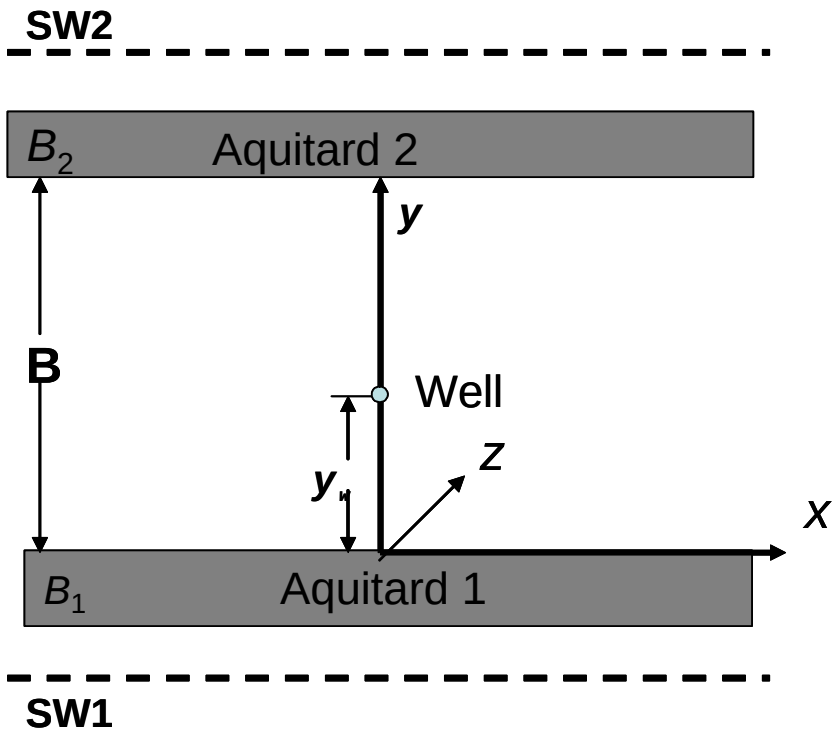

Figure 3.1.B Schematic diagram of pumping between two surface water bodies with sediment layers.

C.

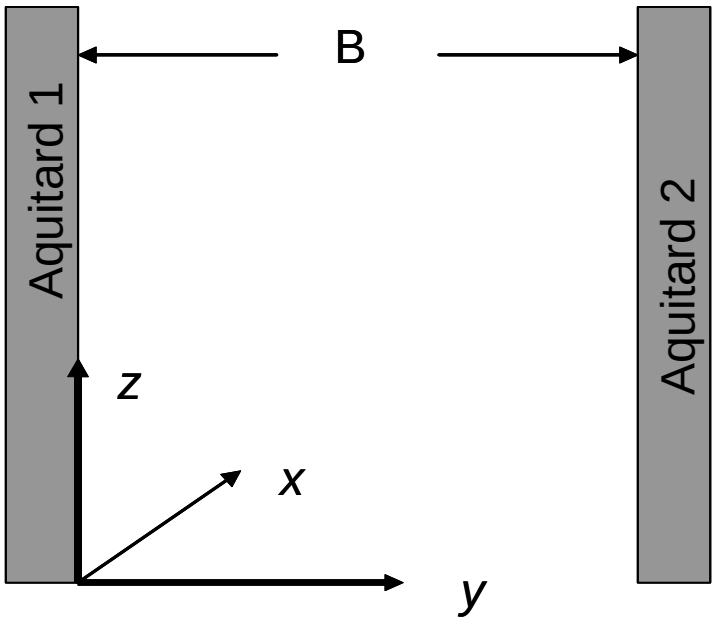

Figure 3.1.C Cross section of pumping between two surface water bodies with sediment layers.

Flow in aquitard 2:

$$K_{y2}\frac{\partial^2 h_2}{\partial y^2}=S_{s2}\frac{\partial h_2}{\partial t}\quad , \qquad B<y<B+B_2 \tag{3.24}$$

$$h_2(x,y,z,0)=h_0\,, \tag{3.25}$$

$$h_2(x=\pm\infty,y,z,t)=h_2(x,y,z=\pm\infty,t)=h_0\ , \tag{3.26}$$

$$h_2(x,y=B+B_2,z,t)=h_0\,, \tag{3.27}$$

$$h_2(x,y=B,z,t)=h(x,y=B,z,t)\,, \tag{3.28}$$

$$K_{y2}\left.\frac{\partial h_2}{\partial y}\right|_{y=B}=K_y\left.\frac{\partial h}{\partial y}\right|_{y=B}\,. \tag{3.29}$$

where h_1 and h_2 are the hydraulic heads in aquitards 1 and 2 respectively, h_0 is the initial hydraulic head, K_{y1} and K_{y2} represent the hydraulic conductivities in y axis of aquitards 1 and 2 respectively; S_{s1} and S_{s2} are the specific storages of aquitards 1 and 2, B_1 and B_2 are the thicknesses of aquitards 1 and 2, respectively.

Eqs. (3.18) and (3.24) are the governing equations for transient flow in *y*-direction in aquitards 1 and 2. Eqs. (3.19) and (3.25) are the initial conditions. Eqs. (3.20) and (3.26) are the lateral boundaries at infinity, Eqs. (3.21) and (3.27) are the constant-head boundaries condition at the stream-aquitard boundary, Eqs. (3.22) and (3.23) refer to the continuity of head and flux at aquitard 1-aquifer interface, and Eqs. (3.28) and (3.29) refer to the continuity of head and flux at aquitard 2- aquifer interface.

Transient flow in the aquitards might be needed if the thickness of the aquitard in respect to *B* is not too small, thus aquitard storage will affect the early stage of flow. If, however, the thickness of the aquitard in respect to *B* is very small, then the aquitard

storage can be neglected. This can be done by simply allowing S_{s1} and S_{s2} to be zeros in above equations. Nevertheless, only when a general transient flow model is available, can one quantitatively assess if the aquitard storage is negligible or not. That is one motive for us to present this general transient flow model here.

Additional dimensionless terms are defined and shown in Table 3.1. Conducting the Laplace transform to Eqs. (3.18)-(3.29) results in

$$\frac{\partial^2 \overline{s_{D1}}}{\partial {y_D}^2} = \alpha_1 p \overline{s_{D1}}, \tag{3.30}$$

$$\overline{s_{D1}}(x_D = \pm\infty, y_D, z_D, p) = \overline{s_{D1}}(x_D, y_D, z_D = \pm\infty, p) = 0, \tag{3.31}$$

$$\overline{s_{D1}}(x_D, y_D = -B_1, z_D, p) = 0, \tag{3.32}$$

$$\overline{s_{D1}}(x_D, y_D = 0, z_D, p) = \overline{s_D}(x_D, y_D = 0, z_D, p) = 0, \tag{3.33}$$

$$\left.\frac{\partial \overline{s_{D1}}}{\partial y_D}\right|_{y_D=0} = \beta_1 \left.\frac{\partial s_D}{\partial z_D}\right|_{y_D=0}, \tag{3.34}$$

$$\frac{\partial^2 \overline{s_{D2}}}{\partial {y_D}^2} = \alpha_2 p \overline{s_{D2}}, \tag{3.35}$$

$$\overline{s_{D2}}(x_D = \pm\infty, y_D, z_D, p) = \overline{s_{D2}}(x_D, y_D, z_D = \pm\infty, p) = 0, \tag{3.36}$$

$$\overline{s_{D2}}(x_D, y_D = 1 + B_2, z_D, p) = 0, \tag{3.37}$$

$$\overline{s_{D2}}(x_D, y_D = 1, z_D, p) = \overline{s_D}(x_D, y_D = 1, z_D, p) = 0, \tag{3.38}$$

$$\left.\frac{\partial \overline{s_{D2}}}{\partial y_D}\right|_{y_D=1} = \beta_2 \left.\frac{\partial s_D}{\partial z_D}\right|_{y_D=1}. \tag{3.39}$$

3.2.3.1 Point sink solution in Laplace domain

The proposed solution of Eq.(3.6) in Laplace domain is written as:

$$\overline{s_D} = \sum_{n=0}^{\infty} H_n(x_D, y_D, p)\cos(\omega_n y_D + \mu_n)\,. \tag{3.40}$$

Notice that a phase term μ_n is included in the cosine Fourier transformation. If there is no aquitards, $\mu_n = -\pi/2$ and the solution goes back to Eq. (3.8). Similar methodology has been applied by Zlotnik and Zhan (2005). The details of solving equations of these three flow systems are shown in Appendix C. The drawdown of a point sink is:

$$\overline{s_D} = \frac{4}{p}\sum_{n=0}^{\infty} \frac{\cos(\omega_n y_{wD} + \mu_n)\cos(\omega_n y_D + \mu_n)}{f(\omega_n)} K_0(\sqrt{\omega_n^2 + p}\, r_D)\,, \tag{3.41}$$

here

$$f(\omega_n, \mu_n) = 1 + \frac{1}{2\omega_n}\left[\sin(2\omega_n + 2\mu_n) - \sin(2\mu_n)\right], \tag{3.42}$$

Here ω_n and μ_n can be obtained via boundary conditions as shown in Appendix C.

Solution of flow to a fully penetrating well is:

$$\overline{s_D} = \frac{4}{p}\sum_{n=1}^{\infty} \frac{\cos(\omega_n y_{wD} + \mu_n)\cos(\omega_n y_D + \mu_n)}{f(\omega_n, \mu_n)} \frac{\pi}{\sqrt{\omega^2{}_n + p}} \exp(-\sqrt{\omega_n{}^2 + p}\,|x_D|)\,. \tag{3.43}$$

Total flux along the boundaries of aquitards and aquifer can be calculated as following:

$$Q(p) = -\frac{8\pi}{p}\sum_{n=1}^{\infty} \frac{\omega_n \sin(\omega_n y_D + \mu_n)\cos(\omega_n y_{WD} + \mu_n)}{f(\omega_n, \mu_n)(\omega_n^2 + p)} \tag{3.44}$$

3.2.4 Numerical computation

Inverse Laplace transform is required to obtain the drawdowns in real-time for the transient flow problem in section 3.2.3. It would be difficult to analytically invert the Laplace transform for this problem because ω_n and μ_n are related to p. In this article, Stehfest (1970) algorithm is used to numerically calculate the inverse Laplace transform.

Stehfest (1970) algorithm is a simple algorithm that can be easily programmed. It has been found quite robust and accurate in similar problems of studying flow to a horizontal well in previous studies (Zhan and Zlotnik, 2002). It is notable that Stehfest (1970) algorithm might not always converge for some problems, and alternative inverse Laplace transform algorithms might be needed (Talbot, 1979; de Hoog et al., 1982; Hollenbeck, 1998). However, our numerical experiments confirmed that the Stehfest (1970) algorithm is free of numerical oscillations or other problems at times of interests for this study.

ω_n and μ_n are calculated using Newton-Raphson method (Press et al., 1989). The computer program is available from the authors free of charge upon request. We have to point out that one needs to be very careful when calculating ω_n and μ_n using equation (C13) and (C12). The first root of ω_n, n=1, is probably the most important root in the ω_n series, and it is a negative number. Our numerical experiment shows that the negative ω_1 might not be found if the initial guess value of ω_1 is not adequate. We recommend trying several different initial ω_1 within the range of [$-\pi$, 0] and checking the solution of ω_n to ensure that ω_1 is a negative one.

There are six dimensionless parameters α_1, α_2, β_1, β_2, B_1, and B_2 that will affect the solutions.

3.3. Analysis of Drawdown and Flux

3.3.1 Effect of two identical aquitards

Previous studies indicated that aquitards play important roles in stream-aquifer interaction issue (e.g. Hunt, 1999; Kollet and Zlotnik, 2003; Hunt, 2003). In this section, the effect of aquitard is investigated. The solutions without aquitards will be compared with those that consider two identical aquitards. The default parameters used in this comparison are listed in Table 3.2. The flux along the boundary is defined here based on Eqs. (3.34) and (3.39) as $\Gamma_2 = \frac{\partial s_D}{\partial y_D} = \frac{K_{y_2}}{K_y}\frac{\partial s_{D2}}{\partial y_D}$ at y_D=1; $\Gamma_1 = \frac{\partial s_D}{\partial y_D} = \frac{K_{y_1}}{K_y}\frac{\partial s_{D1}}{\partial y_D}$ at y_D=0.

When the aquitards are not considered, the relative ratio of stream depletion only depends on the well location. When the aquitards exist, properties of the aquitards and aquifer in addition to the well location control the dynamic interaction of stream and aquifer. In this section, the control of the aquitard parameters on the interaction will be fully investigated. The pumping well is positioned at the center between two streams. Drawdown profile is plotted along the *y*-axis to demonstrate the effect of aquitards.

Table 3.2: The default values used in two river systems

Parameter	Default value
B	1000m
B_1	1m
B_2	1m
K_x, K_y	1×10^{-4}m/s
K_{y1}, K_{y2}	1×10^{-6}m/s
S_s	2×10^{-5}m^{-1}
y_w	500m
Q	0.001m^3/s
S_{s1}, S_{s2}	1×10^{-3}m^{-1}

Note: When different aquitards thickness ratios, specific storage ratios or hydraulic conductivity ratios are used, the properties of the aquitard 2 are fixed and only the corresponding aquitard 1 parameters are changed.

3.3.1.1 Thickness of the aquitard

Figure 3.2 shows the drawdown profile along the *y*-axis for two cases when $B_1=B_2$=1m and 0.1 m in comparison with the case without aquitard. The case without aquitards means that the stream is directly connected with groundwater system, and water in the stream will leak into the groundwater system freely right after pumping starts. As expected, there is no noticeable difference between the case of $B_1=B_2$=0.1m and the case of without aquitard. When the thickness of aquitard $B_1=B_2$=1m, there is considerable difference when the observation point is not too close to the well. The maximum drawdown difference is 0.54, at the observation point on the aquitard-aquifer boundary. Within the dimensionless distance 0.05 from the well, the aquitard thickness effect is indistinguishable in Figure 3.2, drawdown difference is only about 0.01 and 0.04 for the cases of $B_1=B_2$=0.1m and $B_1=B_2$=1m respectively.

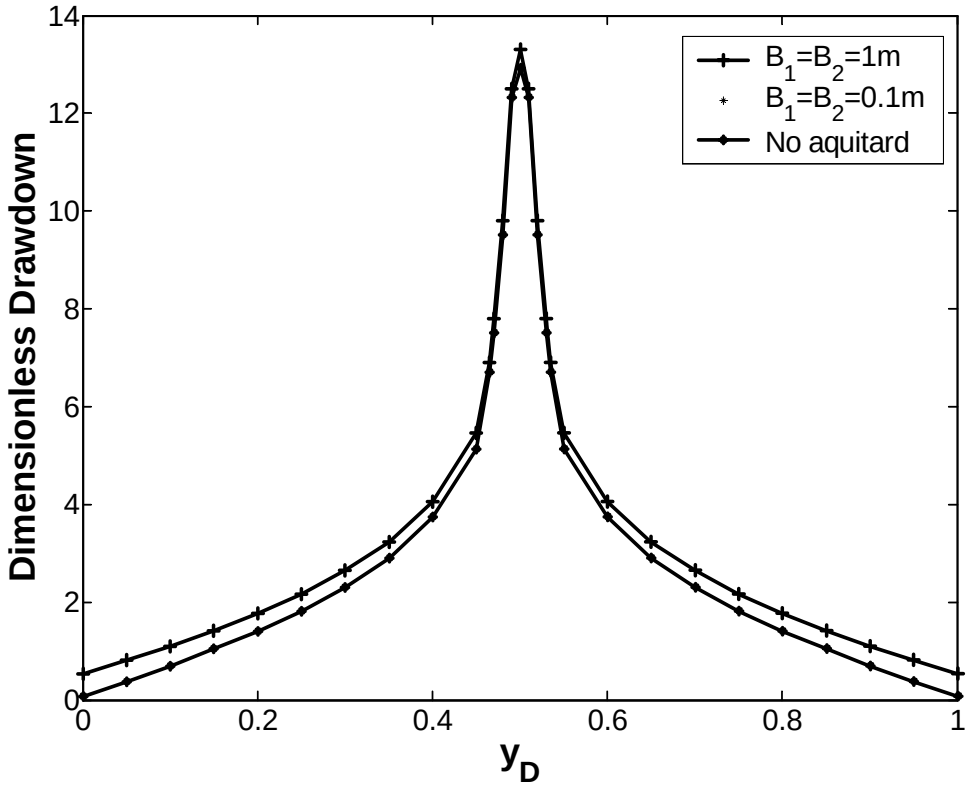

Figure 3.2 Effect of aquitard thickness.

3.3.1.2 Hydraulic conductivity of the aquitard

As shown in Figure 3.3, we have tested the effects of aquitard hydraulic conductivity on the drawdown profile along the *y*-axis for two different hydraulic conductivity ratios ($K_{y1}/K_y = K_{y2}/K_y$) of 0.001 and 0.01. When the aquitard is not considered, stream water is easy to leak into the main aquifer, thus less drawdown is generated in the main aquifer because of the surface water supply. There is almost no distinguishable difference between the cases with and without aquitards when $K_{y1}/K_y = K_{y2}/K_y$ equals 0.01. A considerable difference has been observed along the *y*-axis when $K_{y1}/K_y = K_{y2}/K_y$ equals 0.001. The smallest difference is 2.55 at the well location. The difference increases when the observation point moves away from the well. The maximum drawdown difference 3.18 is at the boundary of aquitard-aquifer.

3.3.1.3 Specific storage ratio

The specific storage of aquitard is often one or two orders of magnitude greater than that of aquifer. The effect of specific storage ratio is demonstrated by plotting the drawdown profile along the *y*-axis in Figure 3.4A at t_D=1 when the system is in transient flow state. There is no noticeable difference when the storage effect is considered when B equals 1000m and $S_{s1}/S_s = S_{s2}/S_{s2} = 500$. Figure 3.4B shows the effect of specific storage ratio on the drawdown in the aquifer when the two streams are relatively close (100m away) which is possible such as the two channels of the same river or two close canals as shown in the field site of Chen and Chen (2003b, Fig. 7).

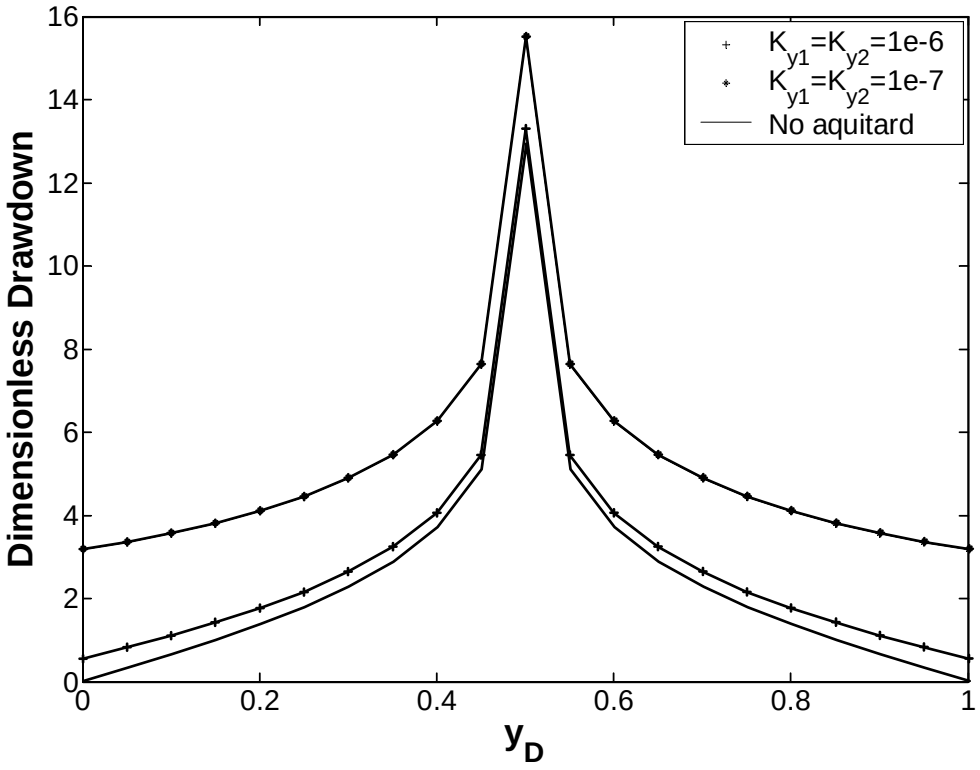

Figure 3.3 Effect of aquitard: hydraulic conductivity.

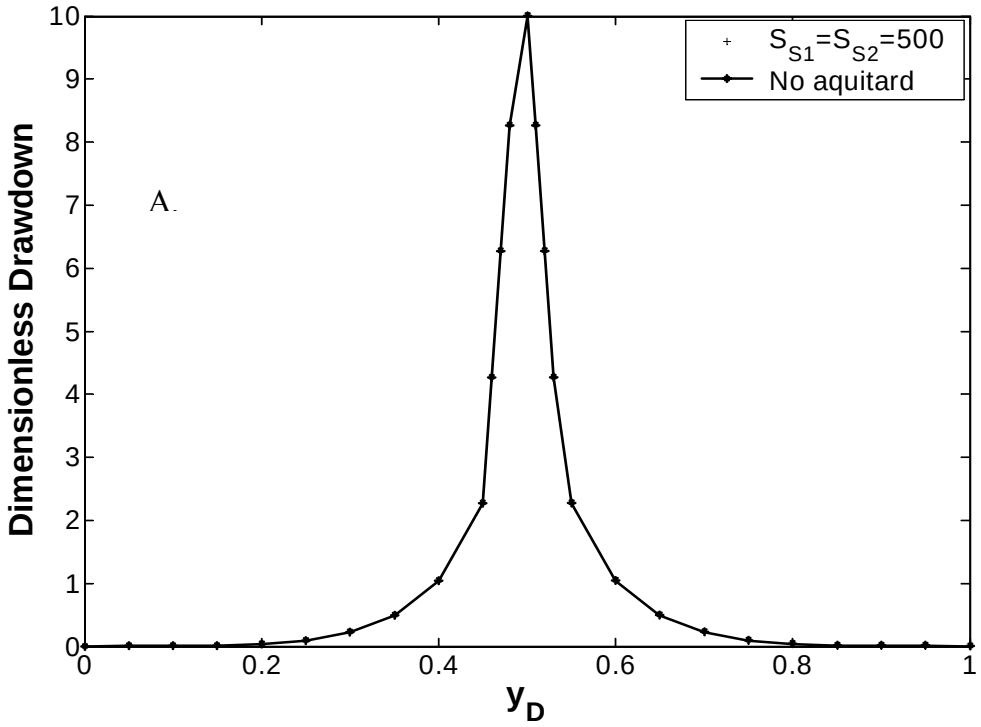

Figure 3.4 Effect of aquitard: specific storage. A: B=1000m; B: B=100m.

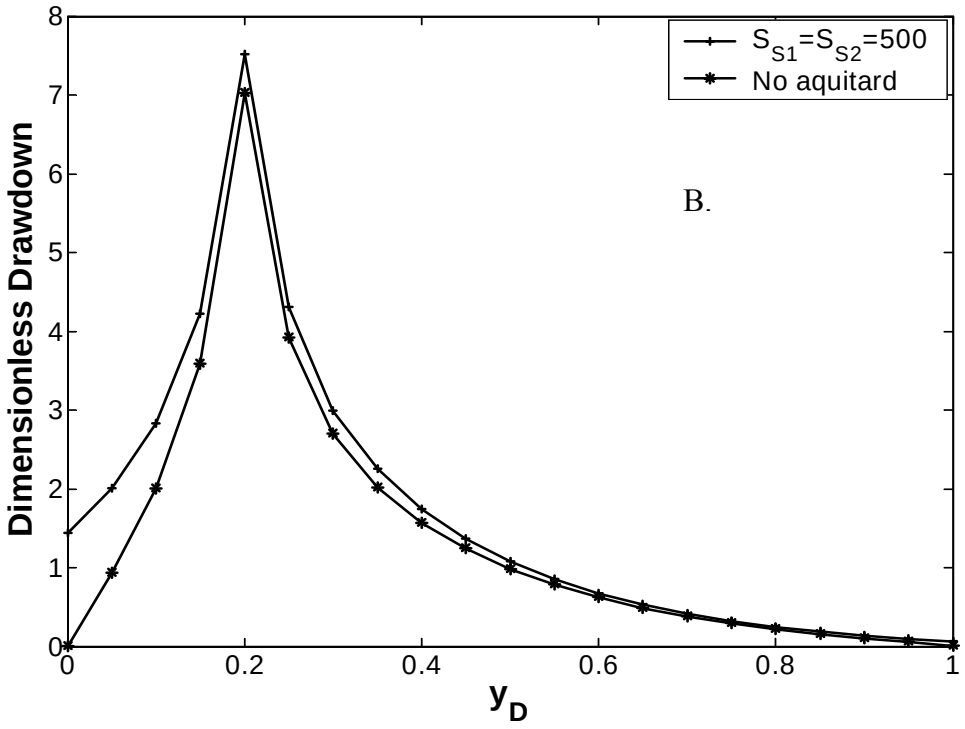

Figure 3.4 Continued

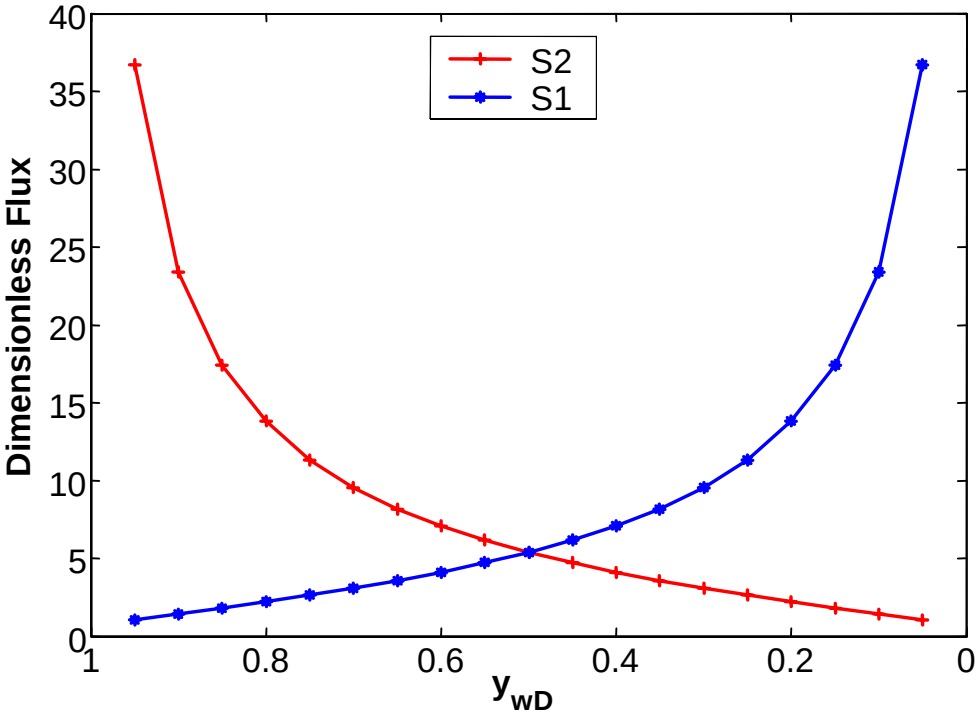

Figure 3.5 Fluxes at points (x_D, y_D) =(0, 0) and (0, 1) when two aquitards are identical.

Different from Figure 3.4A where the well is at the center of the aquifer, a fully penetrating well is positioned at 20m away from the stream 1 in Figure 3.4B. As shown in Figure 3.4B, there is noticeable difference around the boundary of aquitard and aquifer and the region close to the well. The maximal dimensionless drawdown difference is 1.5 on the boundary of aquitard1 and aquifer. Besides the observation points close to boundary, there is also considerable difference observed as shown in Figure 3.4B.

3.3.2 Competition of stream depletion between two streams

The sensitivity analysis in section 3.3.1 uses identical parameters for two aquitards. In reality, the two aquitards may have different physical parameters. Under this circumstance, stream depletion will greatly depend on the difference of two aquitard parameters in addition to the well location. Even for a central well, stream depletion is rarely identical from two streams because of the difference of aquitard parameters. In this section, the stream depletion or water competition issue is addressed by testing the sensitivity of aquitard properties on the fluxes across both aquitard-aquifer boundaries when the well is positioned at different locations along the y-axis. This study will be used to guide water management and water supply strategy. The default parameters are the same as that in section 3.3.1 listed in Table 3.2. When the well is positioned between two streams, we are always interested to know how much amount of water is depleted from one stream in respect to the other stream. The solution developed in this section provides an answer to this question.

In this section, we focus on discussing the maximal fluxes along the boundaries of streams and aquifer, which occur at points (x_D, y_D)=(0, 0) and (0, 1).

For the special case of two identical aquitards, the fluxes at (x_D, y_D)=(0, 0) and (0, 1) versus well location is symmetric about y_{wD}=0.5 (a central well), which is expected in Figure 3.5. S1 and S2 in Figures 3.5-3.8A refer to the observation points at (x_D, y_D)=(0, 0) and (0, 1), respectively. An equal flux point refers to the particular well location when fluxes at S1 and S2 are equal. As shown in Figure 3.5, the equal flux point is located at y_{wD}=0.5. In the following discussion, the properties of aquifer and aquitard 2 are fixed and that of aquitard 1 is varied to investigate change of the equal flux point under different hydraulic properties.

3.3.2.1 Specific storage ratio (S_{s1}/S_{s2})

Figures 3.6A and 3.6B show the fluxes generated from S1 and S2 at t_D=1 when S_{s1}/S_{s2} equals to 5 and 50 respectively. Compared with Figure 3.5, there is no noticeable difference for the equal flux point position from Figure 3.5. The equal flux location is at $y_{wD}=0.51$ in Figure 3.6A. This indicates that if the well is positioned at the center, $y_{wD}=0.5$, a slightly greater amount of water will come from S1 than that from S2. The shape of flux distributions for S1 and S2 is approximately symmetric about the center. The equal flux point moves to $y_{wD}=0.52$ when S_{s1}/S_{s2} equals 50 in Figure 3.6B.

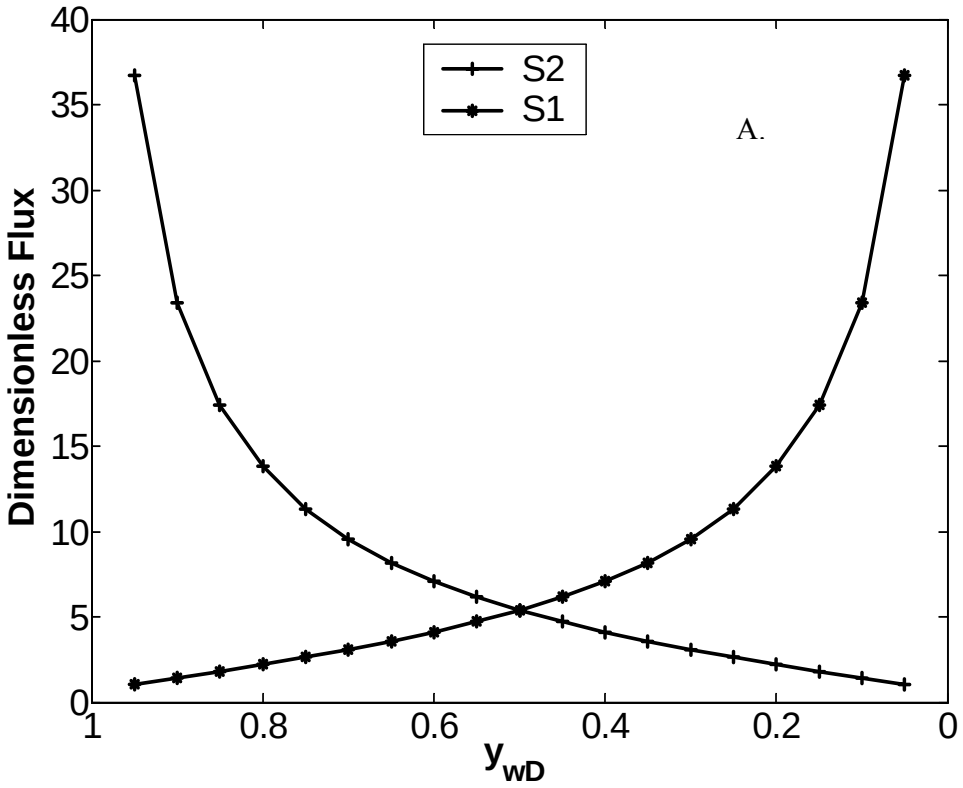

Figure 3.6 Specific storage control of water competition between two surface water bodies. A: S_{s1}/S_{s2}=5; B: S_{s1}/S_{s2}=50.

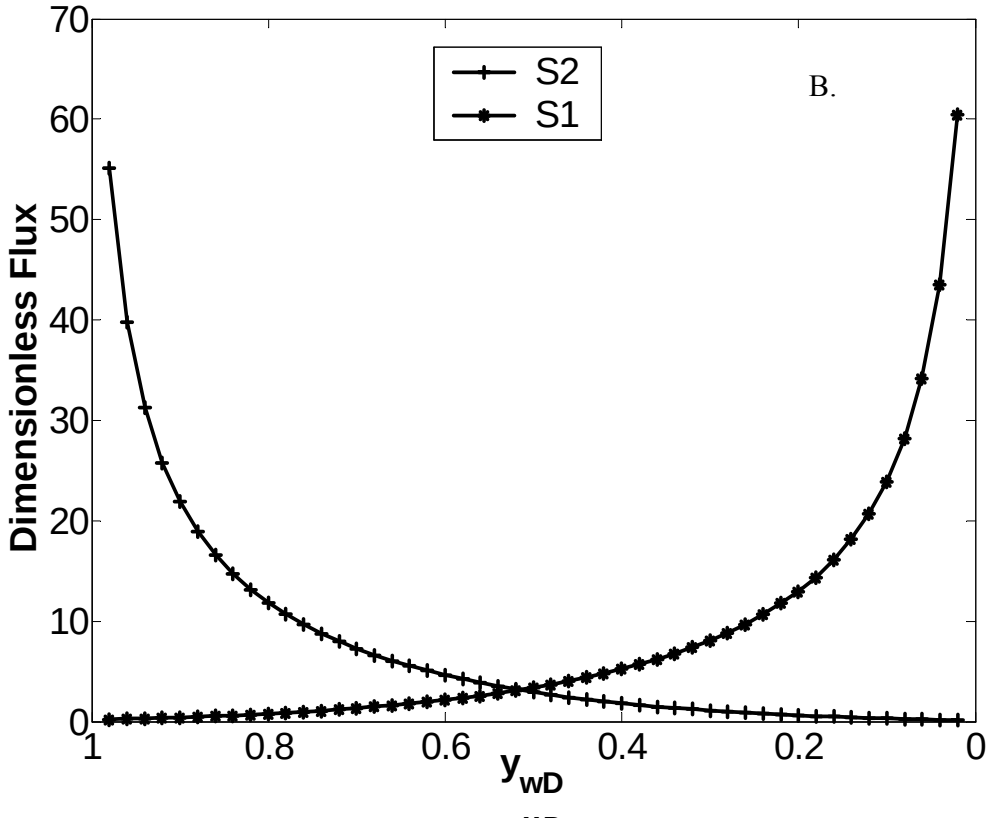

Figure 3.6 Continued

The shape of flux distributions for S1 and S2 shows some asymmetry about the center in Figure 3.6B. Given the same distance from the well to the aquitard, the flux generated from S1 is always greater than that from S2. For example, when the dimensionless distance between the well and the aquitard is 0.1, the fluxes from S1 and S2 are 61 and 55, respectively, with a ratio of 1.1. That is because an aquitard with a greater storage will released more water to the aquifer at a given time.

In general, the equal flux point is less sensitive to the aquitard storage, because the distance between two aquitards are far greater than the thickness of the aquitards themselves. When two streams get closer, one expects to see a greater aquitard storage effect upon the flow system.

3.3.2.2 Thickness ratio (B_1/B_2)

Figure 3.7A shows the fluxes at S1 and S2 for B_1/B_2 of 0.1. As expected, when the dimensionless distance between the well and the aquitard is 0.1, the fluxes from S1 and S2 are 68, and 37, respectively, with a ratio of 1.84. This ratio is greater than what has been observed in section 3.3.2.1. The equal flux point moves to $y_{wD} = 0.53$ in Figure 3.7A. This implies that when the well is positioned between 0 and 0.53, more water is withdrawn from stream 1 than that from stream 2. When B_1/B_2 decreases to 0.01, the equal flux point moves to $y_{wD} = 0.55$ in Figure 3.7B which shows equal flux point is not very strongly dependent on thickness ratio of aquitard.

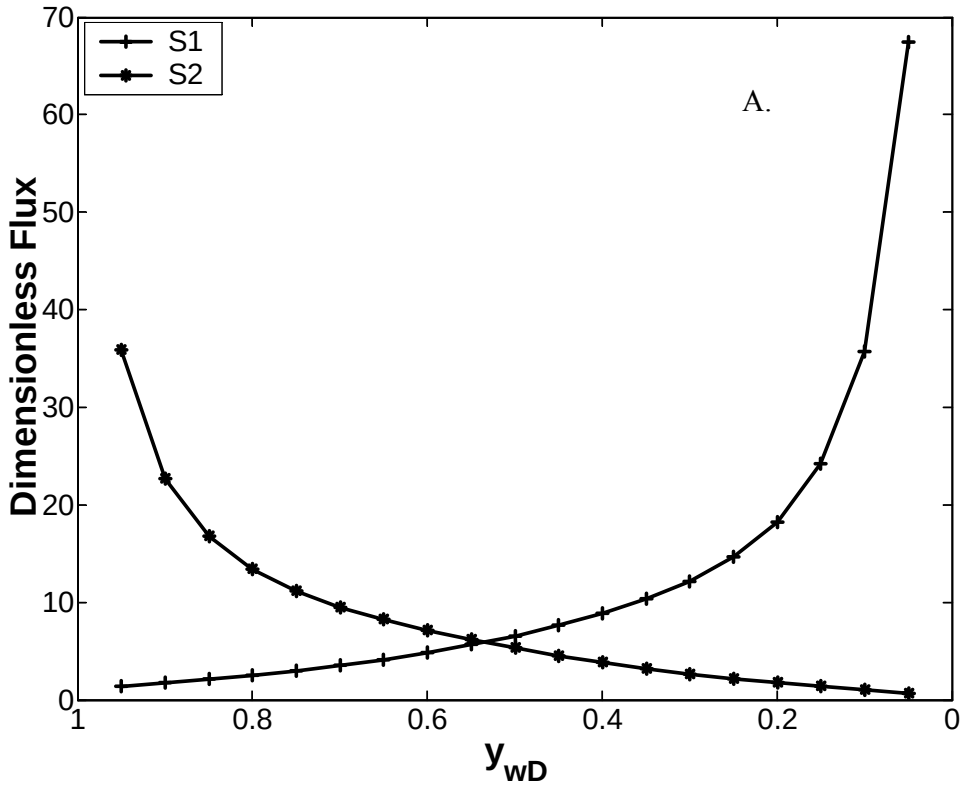

Figure 3.7 Thickness control of water competition between two surface water bodies.

A: $B_1 / B_2 = 0.1$; B: $B_1 / B_2 = 0.01$.

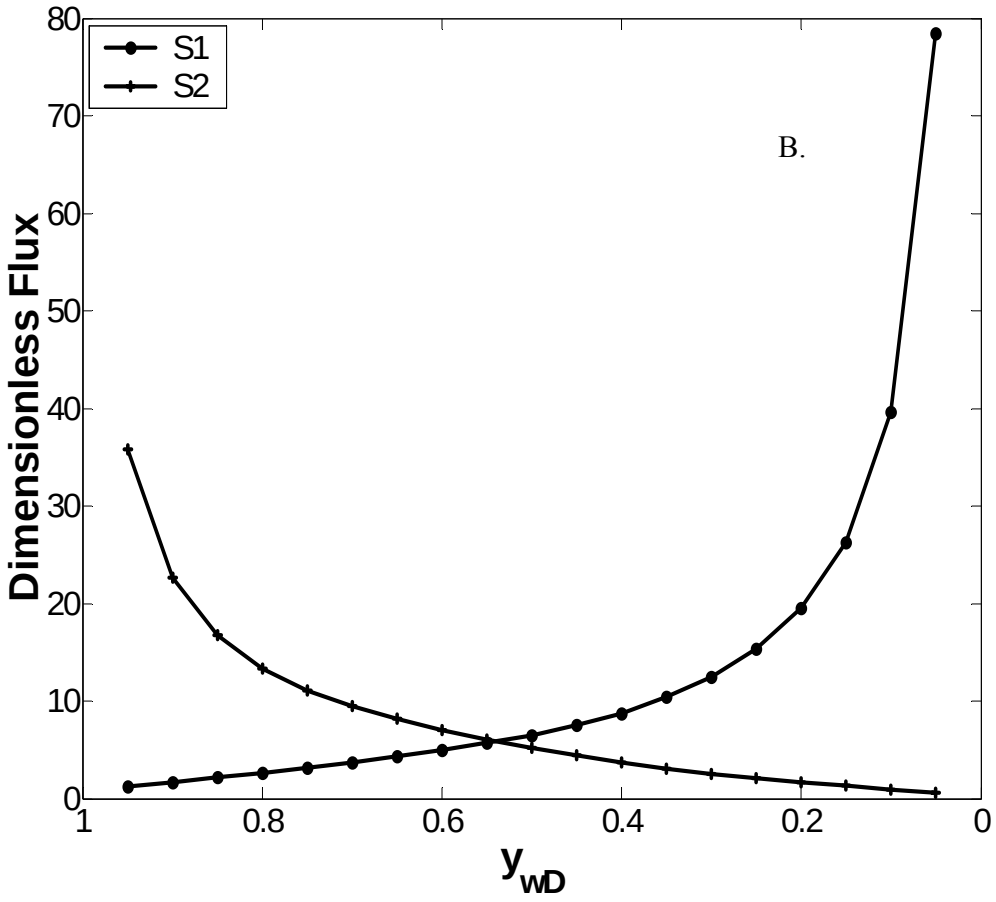

Figure 3.7 Continued

3.3.2.3 Aquitard hydraulic conductivity ratio (K_{y1}/K_{y2})

Figure 3.8A shows the control of aquitard hydraulic conductivity ratio on the stream depletion competition between two streams for K_{y1}/K_{y2} equals 10. When aquitard 1 is more permeable, water is easy to leak through it. As shown in Figure 3.8A, stream 1 is often the major water supplier even the well is relatively far away from that stream. The equal flux point has moved to $y_{wD}=0.72$. Given the same dimensionless distance 0.1 from the streams, the flux from S1 and S2 are 78, and 19, with a ratio of 4.1 which is much greater than what has been observed in sections 3.2.1-3.2.2. Different from Figures discussed in this section, Figure 3.8B shows the control of aquitard hydraulic conductivity ratio on the total fluxes along the aquitard-aquifer boundaries. It is interesting to know that there is a linear relationship between well location and total flux. Stream 1 is the major water supplier even when well is positioned $< y_{wD}=0.95$ which indicates that the hydraulic conductivity difference of the aquitard is the most important factor in affecting flow dynamics.

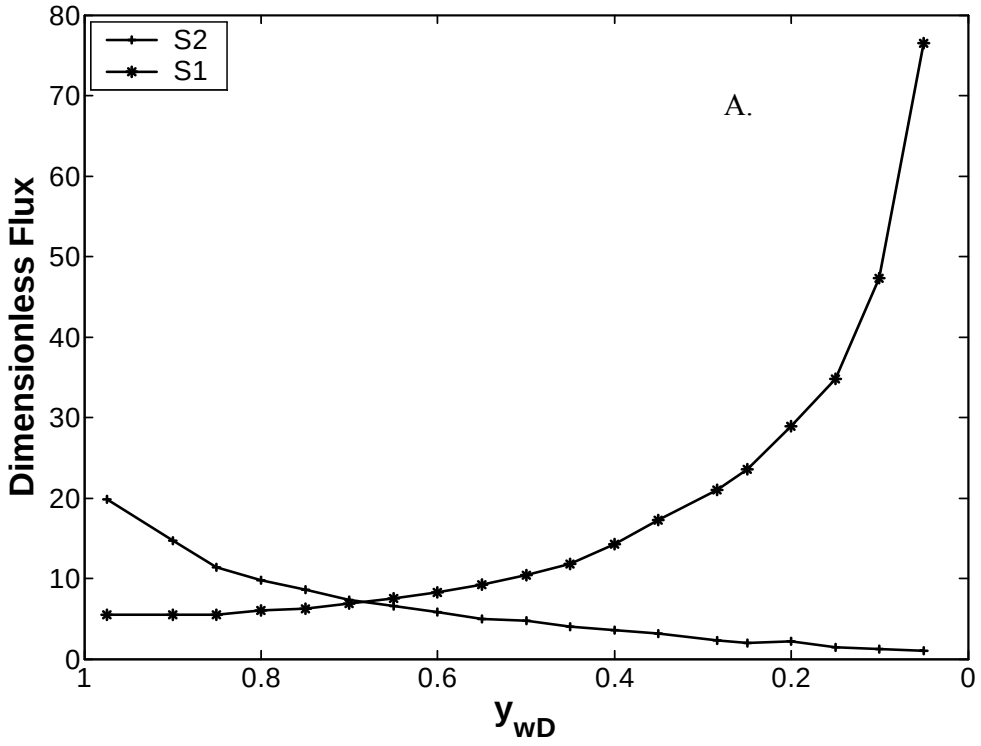

Figure 3.8 Hydraulic conductivity control of water competition between two surface water bodies at $K_{y1} / K_{y2} = 10$. A: fluxes at (x_D, y_D) =(0, 0) and (0, 1) B: total flux along the boundaries of aquitard-aquifer.

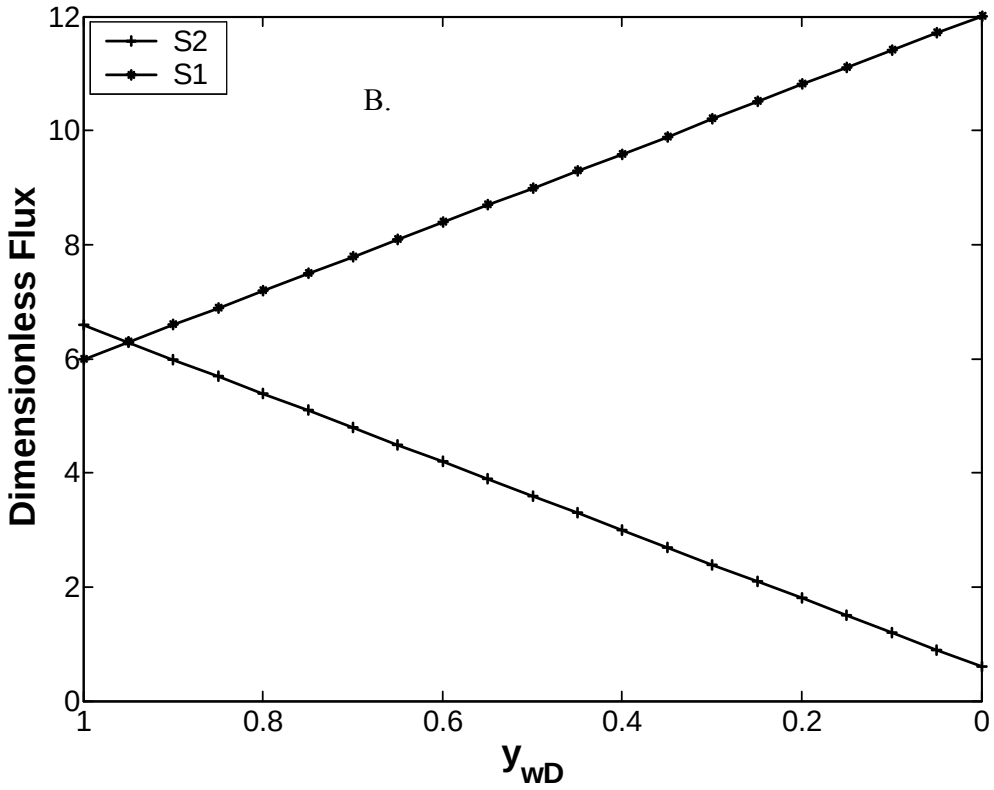

Figure 3.8 Continued

3.4. Summary and Conclusions

A pumping well is sometimes installed between two surface water bodies, such as streams or canals. Previous studies focus on one stream and aquifer system and treat leakage from the surface water body as a volumetric source term in the governing equation of flow in the main aquifer, a hypothesis termed "Hantush's assumption" (Hantush, 1964). In this paper, new analytical and semi-analytical solutions are acquired for the pumping induced dynamic interaction between two surface water bodies and ground water for two different cases. In the first case, the sediment layer separating surface water from ground water is not considered. In the second case, the two low permeable layers are considered. Instead of adopting Hantush's assumption, the solutions are derived based on the mass conservation laws by maintaining continuity of flux and head along the aquitard-aquifer boundaries. Results from these two cases are compared to demonstrate the effects of aquitards. The interconnection of two aquitard properties such as thickness ratio, hydraulic conductivity ratio, and specific storage ratio is tested while well is positioned at difference locations. The results in this paper could provide guidance for well design, water management, and other applications. In general, we draw the following conclusions from this study.

1. The aquitard hydraulic conductivity is the most important factor controlling the stream-aquifer interaction, followed by the aquitard thickness which greatly influences the drawdown at observation points that are close to the aquitards. The thickness of aquitards does not greatly influence the drawdown at observation points that are close to the pumping well.

2. Aquitard storages do not play significant roles when the two streams are relatively far from each other or the well is not very close to the river.
3. Aquitards properties control the competition of stream depletion when a pumping well is positioned between two streams. When the two aquitards are identical, the so called "equal flux point" is located right at the center between the two aquitards. The equal flux point will move off the center when the aquitard thickness ratio and/or the aquitard hydraulic conductivity ratio are different than unity.

CHAPTER IV

SEA WATER UPCONING DUE TO A FINITE HORIZONTAL WELL IN CONFINED AQUIFERS

We have investigated the seawater upconing due to a finite-length pumping horizontal well and derived an analytical solution of sharp fresh/sea interface based on the solution of Dagan and Bear (1968). The results are compared with those of vertical wells. The upconing profile exhibits three stages with time: an early slow increase stage, an intermediate rapid increase stage, and a late steady state stage. The sensitivity of the interface rise to the well length, the well location, the aquifer anisotropy, and the observation point location is analyzed. We have also investigated the critical condition of seawater upconing based on Muskat's (1982) idea by relating fresh/sea water interface upconing to drawdown. The critical condition which includes the critical rise and the critical time at a certain pumping rate depends on the well length, the initial interface location, the well location, and the pumping rate. The critical rise and the critical time are coupled together at any given pumping rate. The critical rise has an inversely linear relationship with the pumping rate and the initial interface location, respectively. The critical rise is more sensitive to a shorter well, while the critical time continuously increases with the well length. In real field applications, installing long wells as shallow as possible is always desirable for sustaining long periods of pumping with significant rates.

4.1. Introduction

Coastal margins are one of the nation's greatest natural resources and economic assets. Due to increasing concentration of human settlements and economic activities in the coastal margins, it is critical to find better technologies of managing the coastal groundwater resources. Coastal aquifers always have saline water underneath the freshwater. This phenomenon substantially limits the groundwater pumping rates using traditional vertical wells because of the upconing of the fresh/sea water interfaces and the potential of seawater intrusion (Henry, 1959, 1964; Bear and Dagan, 1964, Dagan and Bear, 1968; Muskat, 1982; Voss, 1984; Bear et al., 1999. Cheng et al., 2000). A horizontal well often has a much longer screen length than a vertical well, thus can intercept a significant amount of freshwater flow in a shallow coastal aquifer; meanwhile, a horizontal well distributes its pumping rate over a much longer screen length than a vertical well, thus generates much less upconing of the fresh/sea water interface and has less chance to be invaded by the underneath saline water. Therefore, a horizontal well might be a better means for coastal aquifer development.

Horizontal wells have been widely used in the petroleum industry in the past two decades (Goode and Thambynayagam, 1987; Daviau et al., 1988; Ozkan et al., 1989a,b, 1991; Kuchuk et al., 1991; Penmatcha et al., 1997). They have been applied to environmental geology and hydrogeology since the pioneering work of collecting wells (Hantush and Papadopulos, 1962; Morgan, 1992; Tarshish, 1992; Cleveland, 1994; Murdoch, 1994; Falta, 1995; Sawyer and Lieuallen-Dulam, 1998; Zhan, 1999; Zhan and

Cao, 2000; Streward, 2001; Zhan et al., 2001; Park and Zhan, 2002, 2003; Zhan and Zlotnik, 2002; Chen et al., 2003; Zhan and Park, 2003).

The analyses of upconing phenomenon have been classified into two groups depending on the assumptions made regarding the interface of freshwater and seawater. One is sharp interface model, the other is transition zone model. The sharp interface model considers freshwater and seawater as immiscible fluids, ignores the mixing zone of these two fluids (e.g., Henry, 1959, 1964; Bear and Dagan, 1964, Dagan and Bear, 1968; Schmorak and Mercado, 1969; Sahni, 1973; Haubold, 1975; Strack, 1976, 1995; Taylor and Person, 1998). This model is valid if mixing zone between the two fluids is relatively small compared with the thickness of the aquifer. The transition zone model considers the two fluids as miscible fluids, and a mixing zone exists at the boundary where these two fluids are in contact (e.g. Frind, 1982; Volker and Rushton, 1982; Voss and Souza, 1987; Diersch, 1988; Galeati et al., 1992). The basis of the most initial works of freshwater and saline water studies, especially the sharp interface model is Ghyben- Herzerg model. Following the Ghyben-Herzerg model, extensive studies have been carried out (e.g., Glover, 1959; Strack, 1976, 1984, 1995; Mercer et al., 1980; Liu et al, 1981; Haitjema, 1991; Cheng, et al., 2000; Bakker, 2003).

Two methods are widely used among previous sharp-interface studies. The first method is developed by Muskat (1982) based on the Ghyben-Herzerg model, and the second method is devised by Dagan and Bear (1968), hereinafter called DB model] based the small perturbation of the free interface. Muskat's model is capable of

calculating the critical rise of the interface while the DB model can find the interface profile.

Most of studies related to seawater intrusion refer to vertical wells (e.g, Dagan and Bear, 1968; Schmorak and Mercado, 1969; Sahni, 1973; Haubold, 1975; Chandler and Mcwhorter, 1975; Reilly and Goodman, 1985, 1987). Only a few investigations are about the upconing under infinitely-long horizontal wells (Zhang and Hocking, 1996, 1997; Zhang et al. 1997; Butler and Jiang, 1996). Zhang and Hocking (1996, 1997) used boundary integral equation method to find the interface for different pumping rates of point sinks, and used hodograph method to obtain the shape of the interface for an infinitely long line-sink to solve the critical rate problem. Butler and Jiang (1996) considered the effect of gravity to study the movement of the water-oil interface toward a horizontal well.

To the knowledge of the authors, seawater upconing under a finite-length horizontal well during transient flow condition has not been studied yet. This article has two primary purposes. The first is to investigate the upconing profile under a finite-length horizontal well at different times of pumping. The second is to derive the critical pumping time and the critical rise at any given pumping rate. The results are compared with previous vertical well solutions. The sensitivity of upconing to the well length, the initial interface, and the well location has been investigated. This research is particularly useful for guiding the coastal aquifer development.

4.2. Seawater Upconing Profile under a Horizontal-Well in a Thick Aquifer

4.2.1 Analytical formulation

The coordinate system is set up in such a way that the origin is at the lower boundary of the aquifer, the *x*- and *y*- axes are alone the horizontal directions and the *z*-axis is along the upward vertical direction. The horizontal well is positioned along the *x*-axis with its center at (0, 0, z_w), where z_w is the distance from the horizontal well to the lower aquifer boundary(see Figure 4.1). The length of the well is L. z_0 is the distance from the pre-pumping initial horizontal interface to the lower boundary, and d is the distance from the horizontal well to the initial interface. The upper and lower aquifer boundaries are impermeable. In consistent with previous studies of Dagan and Bear (1968), we adopt the following assumptions in this investigation: (1) the medium is homogeneous, horizontally isotropic but vertically anisotropic; (2) the fresh/sea water mixing zone has a negligible width (the so-called sharp interface); (3) the regional flow is not considered; (4) the upper and lower aquifer boundaries are far from the well's intake point and the fresh/sea water interface (the so-called thick aquifer in Dagan and Bear's paper). The sharp interface treatment is a mathematical simplification of the problem since the focus of this article is to obtain some analytical solutions of the problem to gain physical insights.

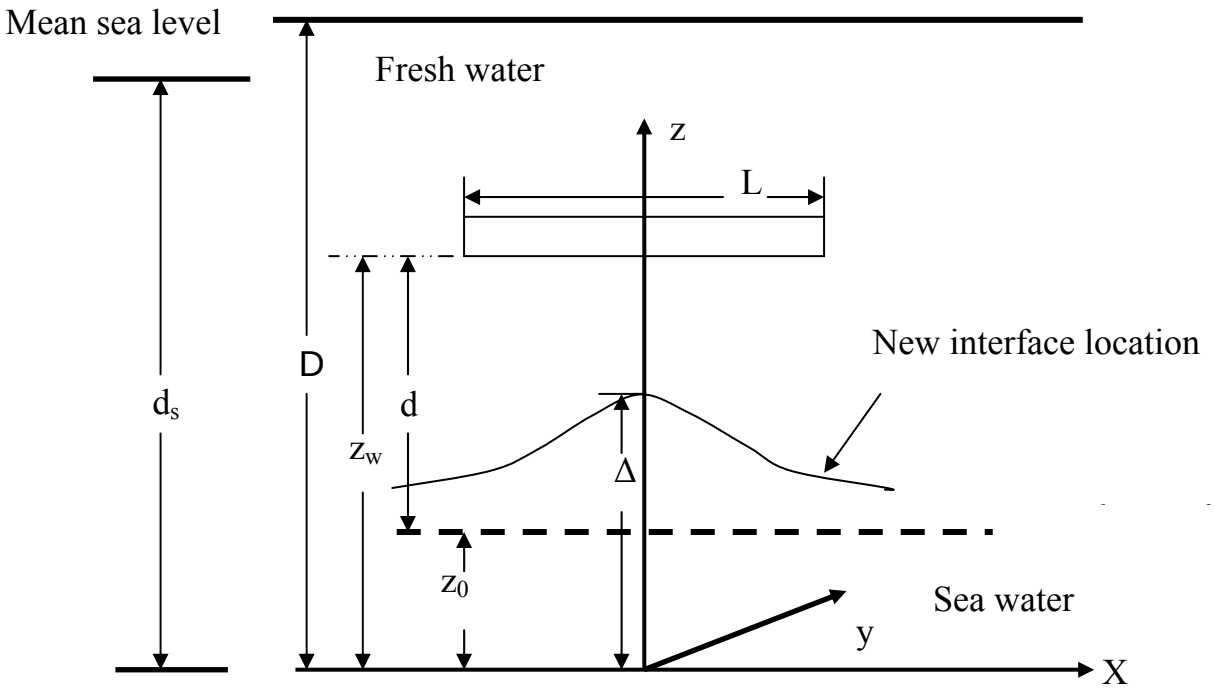

Figure 4.1 A schematic cross-section diagram of a pumping finite-length horizontal well above a fresh/sea water interface in a confined aquifer.

Dagan and Bear (1968), the so-called DB model, has derived an equation describing the upconing of the interface as a function of time and distance from a pumping point in a thick aquifer. Expressed in the notation of this study, the DB model gives:

$$Z(r,t) = \frac{Q}{2\pi(\Delta\gamma/\gamma)K_x d}\left[\frac{1}{(1+R'^2)^{\frac{1}{2}}} - \frac{1}{[(1+\gamma')^2 + R'^2]^{\frac{1}{2}}}\right], \tag{4.31}$$

where R' and γ' are respectively the dimensionless distance and the time given by:

$$R' = \frac{r}{d}\left(\frac{K_z}{K_x}\right)^{\frac{1}{2}}, \tag{4.32}$$

$$\gamma' = \frac{(\Delta\gamma/\gamma)K_z}{2nd}t, \tag{4.33}$$

where Z is the rise of interface above the initial position, Q is the pumping rate of the well, γ is the specific density of freshwater, $\Delta\gamma/\gamma$ is the dimensionless density difference between the two fluids, d is the distance between the well's intake point and the initial interface, r is the radial distance from the well, n is the aquifer porosity, K_x and K_z are the horizontal and vertical hydraulic conductivities, respectively, and t is the pumping time.

We must emphasize that it is assumed that the aquifer is so thick that the upper and lower boundaries will not affect the pumping in using Eq. (4.1). This assumption is the precondition to achieve a possible stable profile of upconing when time becomes very large. If the aquifer thickness is limited, the aquifer boundaries will greatly affect the rise of the upconing and it will not be possible to achieve a stable upconing profile, even

with a small pumping rate. That is because drawdown at a point near the sink will continuously increase with time and steady-state flow is not possible near a sink point in a finite-thickness confined aquifer. If the thick aquifer assumption cannot be satisfied, Eq. (4.1) is at most an approximation of calculating the rise of upconing before reaching the critical condition. A rigorous theoretical investigation considering the finite-thickness aquifer could be challenging. In this part, we will keep using the thick aquifer assumption in order to use Eq. (4.1).

The DB model deals with transient flow and will serve as the starting point of this study. The interface upconing due to a pumping horizontal well can be derived by an integration of the point-sink solution along the horizontal well axis. For any point at the initial interface (x, y), the rise of interface is

$$Z(r,t) = \frac{1}{L}\int_{-L/2}^{L/2} \frac{Q}{2\pi(\Delta\gamma/\gamma)K_x d}\left[\frac{1}{(1+R'^2)^{\frac{1}{2}}} - \frac{1}{[(1+\gamma')^2+R'^2]^{\frac{1}{2}}}\right]dx' \ , \qquad (4.34)$$

where $r = \sqrt{(x-x')^2 + y^2}$ in Eq.(4.2) for the calculation of R'. The integration can be carried out straightforwardly and the result is:

$$Z(x,y,t)=\frac{Q}{2\pi(\frac{\Delta\gamma}{\gamma})L\sqrt{K_z K_x}}\left\{-\ln\left|\frac{Kz\,(L/2+x)}{Kxd^{\,2}}+\frac{\sqrt{\frac{Kz}{Kx}}}{d}\sqrt{(1+r')^2+\frac{\left[(x+L/2)^2+y^2\right]\frac{Kz}{Kx}}{d^2}}\right|\right.$$
$$+\ln\left|\frac{Kz\,(x-L/2)}{Kxd^{\,2}}+\frac{\sqrt{\frac{Kz}{Kx}}}{d}\sqrt{(1+r')^2+\frac{\left[(x-L/2)^2+y^2\right]\frac{Kz}{Kx}}{d^2}}\right|$$
$$+\ln\left|\frac{Kz\,(L/2+x)}{Kxd^{\,2}}+\frac{\sqrt{\frac{Kz}{Kx}}}{d}\sqrt{\frac{Kz\,(x+L/2)^2}{K_x d^2}+1+\frac{y^2}{d^2}\frac{Kz}{Kx}}\right|$$
$$\left.-\ln\left|\frac{Kz\,(x-L/2)}{Kxd^{\,2}}+\frac{\sqrt{\frac{Kz}{Kx}}}{d}\sqrt{\frac{Kz\,(x-L/2)^2}{K_x d^2}+1+\frac{y^2}{d^2}\frac{Kz}{Kx}}\right|\right\} \tag{4.35}$$

4.2.2 Comparison of upconing profiles of vertical and horizontal wells in a thick aquifer

Eq. (4.5) is employed to analyze the upconing profile under a pumping horizontal well. Figure 2.2A is a three dimensional view of the upconing profile after pumping the horizontal well for t=10^5s=1.16 days. The following parameters were used in this Figure: d=10m, L=40m, K_x=K_z= 0.0001m/s, n=0.1, and Q= 0.01m^3/sec. A three-dimensional upconing profile due to a vertical pumping well is plotted in Figure 4.2B based on Eq. (4.1). We should point out that this vertical well only withdraws water from a point that is at the same vertical location as the horizontal well. For the sake of comparison, we use exactly the same aquifer parameters, initial interface, and pumping rate as those used in Figure 4.2A. As expected, Figure 4.2A shows a symmetric profile in respect to the y-axis, and the largest upconing is at point x=y=0. At time t=10^5s=1.16 days, the maximal rise of interface is 3.31m under a pumping horizontal well. In contrast, the highest rise of

interface under a vertical well is 7.07m, which is more than twice of that of the horizontal well. This is understandable because the horizontal well distributes its pumping stress over a great lateral length, but a vertical well concentrates its pumping stress over a small localized volume. In fact, hydrogeologists have recognized the importance of using a series of laterally distributed small-rate vertical wells instead of a single large-rate vertical well to pump coastal aquifers to prevent seawater upconing a long time ago (Hantush, 1964;Dagan and Bear, 1968;Sahni, 1973). The study here moves one step further by replacing the series of vertical wells by a single horizontal well to reduce the seawater upconing. Figure 4.3A shows the rise of interface versus time under both vertical and horizontal wells at point $x=y=0$ in a semi-log paper. It is interesting to observe a three stage interface rise with time. At early time, the interface rise is small and the rate of rise is slow; from time between10^3 to 6×10^7 seconds, there is a rapid interface rising; when time gets further longer, the interface almost reaches a steady-state condition.

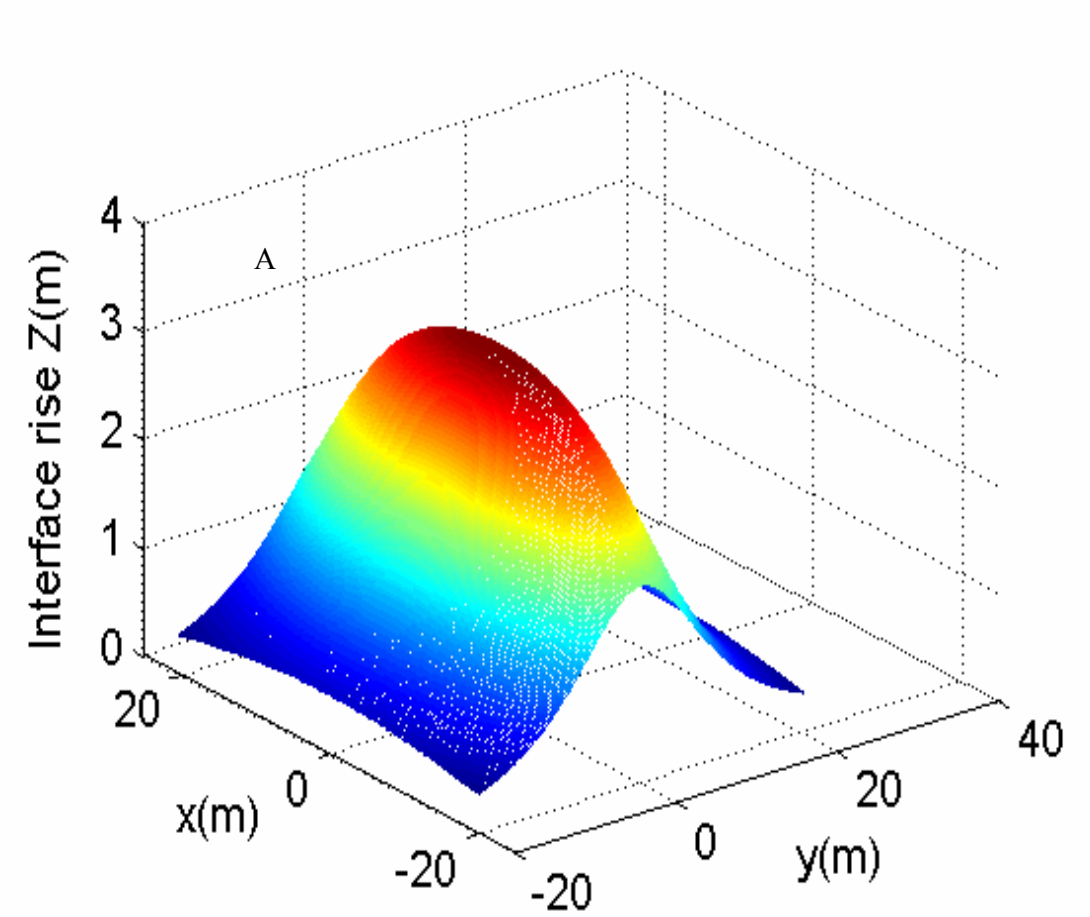

Figure 4.2 Three dimensional upconing profiles at x=y=0, L= 40m, d=10m, at 1.16 days. A) horizontal-well B) vertical-well.

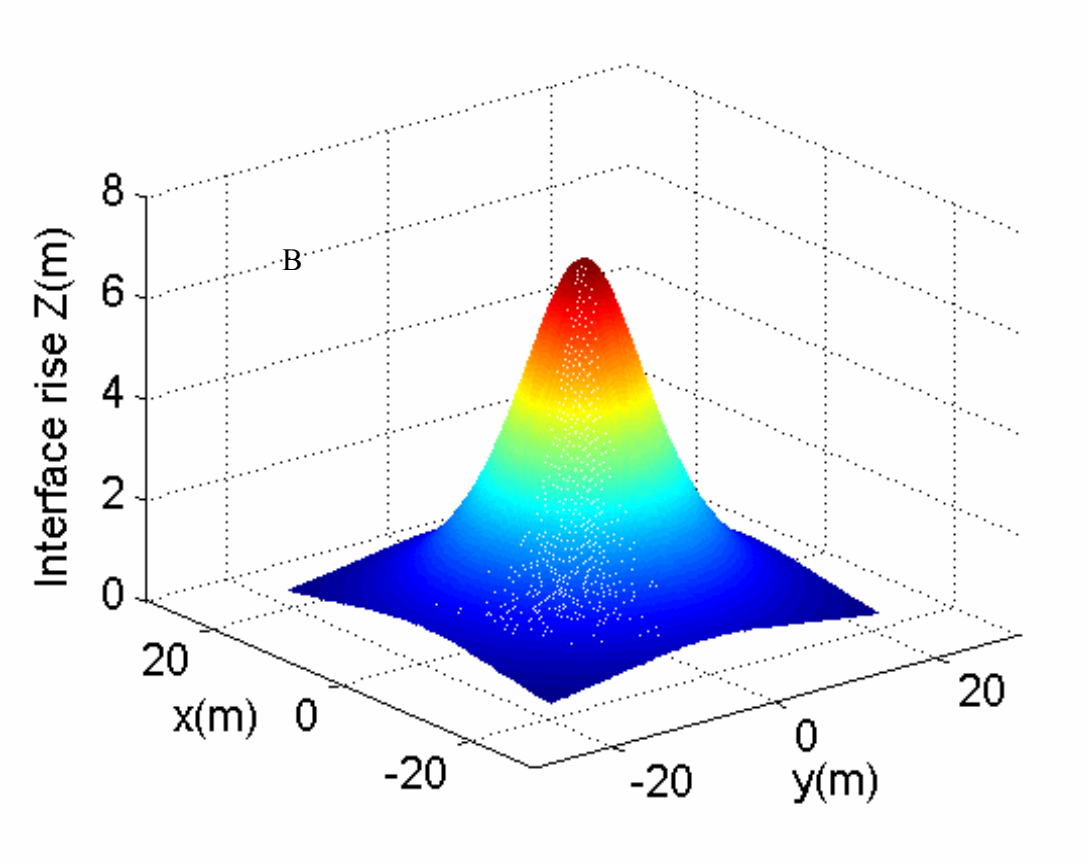

Figure 4.2 continued

The three stage interface rise can be explained in the following. When the pumping starts, it takes some time (often quite short) for the pumping effect to reach the fresh/sea water interface, depending on the pumping rate and the distance to the interface, among other hydraulic properties. During this early stage, the fresh/sea water interface will not be affected. When the pumping effect propagates to the fresh/sea water interface, the interface will start to rise, first rapidly, then gradually slow down until reach a steady-state, this is the second stage. When the time is long enough, stead-state is reached, that is the third stage.

Another interesting result shown in Figure 4.3B is that the ratio of interface rise under a vertical versus horizontal well is almost constant at the early time (before 10^3 seconds), while this ratio decreases during 3×10^4 to 2×10^7 seconds, and it is constant at 1.39 after 2×10^7 seconds. The ratio of 1.39 at the large time can be validated by comparing the steady-state simplification of Eqs. (4.1) and (4.5). When time goes to infinity, the second term in Eq. (4.1) goes to zero; whereas the first and second terms in Eq. (4.5) cancel each other. Given the parameters of L=40m and d=10m, it can be easily proven that the ratio of rises calculated by Eq. (4.1) and (4.5) is approximately 1.39 after a few steps of mathematical manipulations.

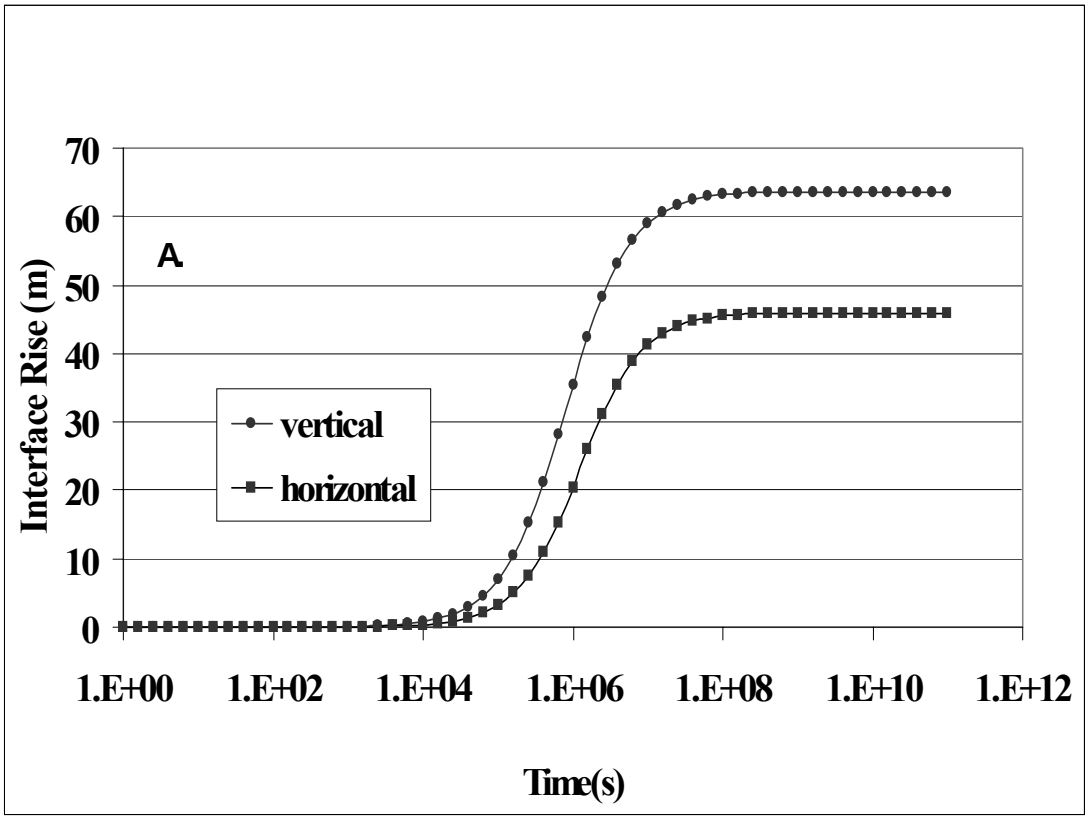

Figure 4.3 A) The interface rises versus time for horizontal and vertical wells; B) The ratio of the interface rise of a vertical well over that of a horizontal well.

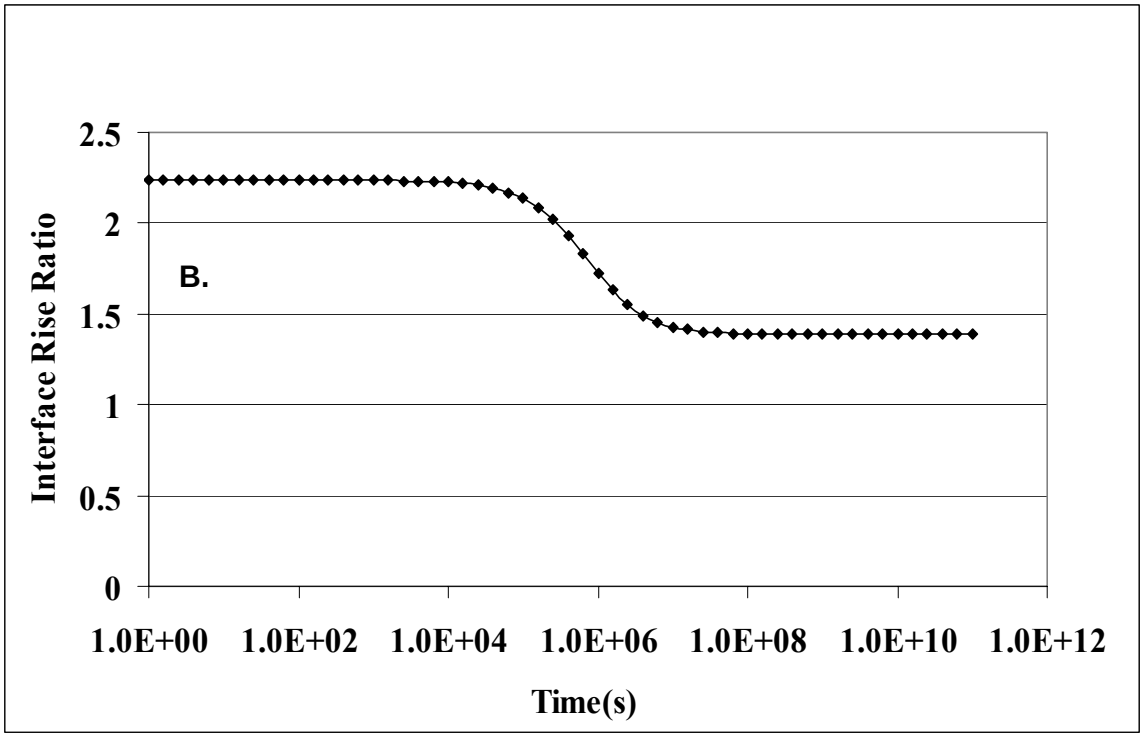

Figure 4.3 Continued

4.2.3 Physical analysis of interface rise under a horizontal well

As shown in Eq. (4.5), the interface rise under a pumping horizontal well is controlled by several parameters including the observation location, the well location, the well length and the aquifer anisotropy. It is important to find out the response of upconing to the variation of those parameters. The same parameters as that in section 2.2 were also used here.

4.2.3.1 Well location

Figures 4.4A and 4.4B show the interface rises at time t=10^5s as functions of well locations for three observation points at the interface with x=y=0, x=y=20m, x=y=30m, where x=y=0 is the point directly below the center of the horizontal well. This figure shows a few interesting aspects. First, for the point directly below the center of the well, the interface rise is somewhat inversely proportional to d, reflected by the rapid decrease when the well is close to the interface, and then the asymptotic approach to zero when the well is away from the interface. This result is directly reflected in Eq. (4.4) which shows that Z is approximately inversely proportional to d if excluding the negligible contribution of γ'. The relationship of the well location and the interface rise can be described by a regression function $Z = 61.199 \times d^{-1.3201}$ with a correlation coefficient R= 0.992.

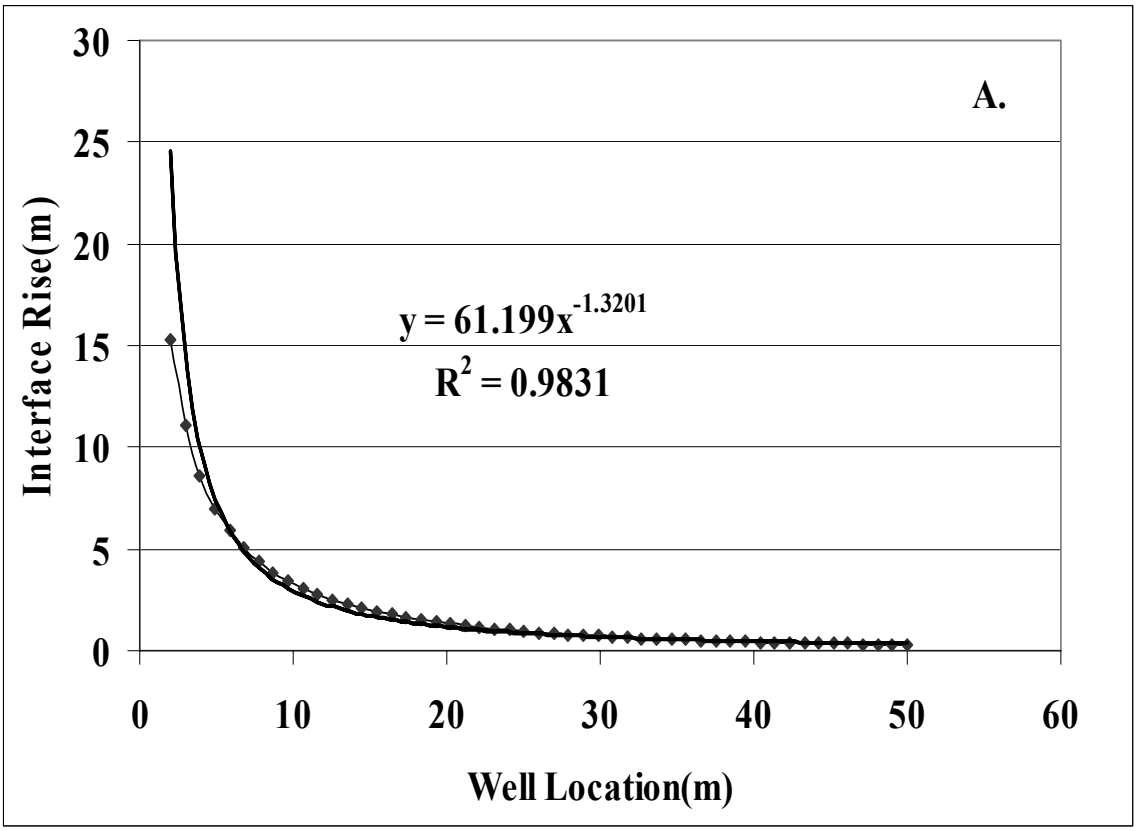

Figure 4.4 A) Effect of the well location on the interface rise at an observation point directly below the well center (x=y=0m); B) Effect of the well location on the interface rise at two off-center observation points x=y=20m, and 30m.

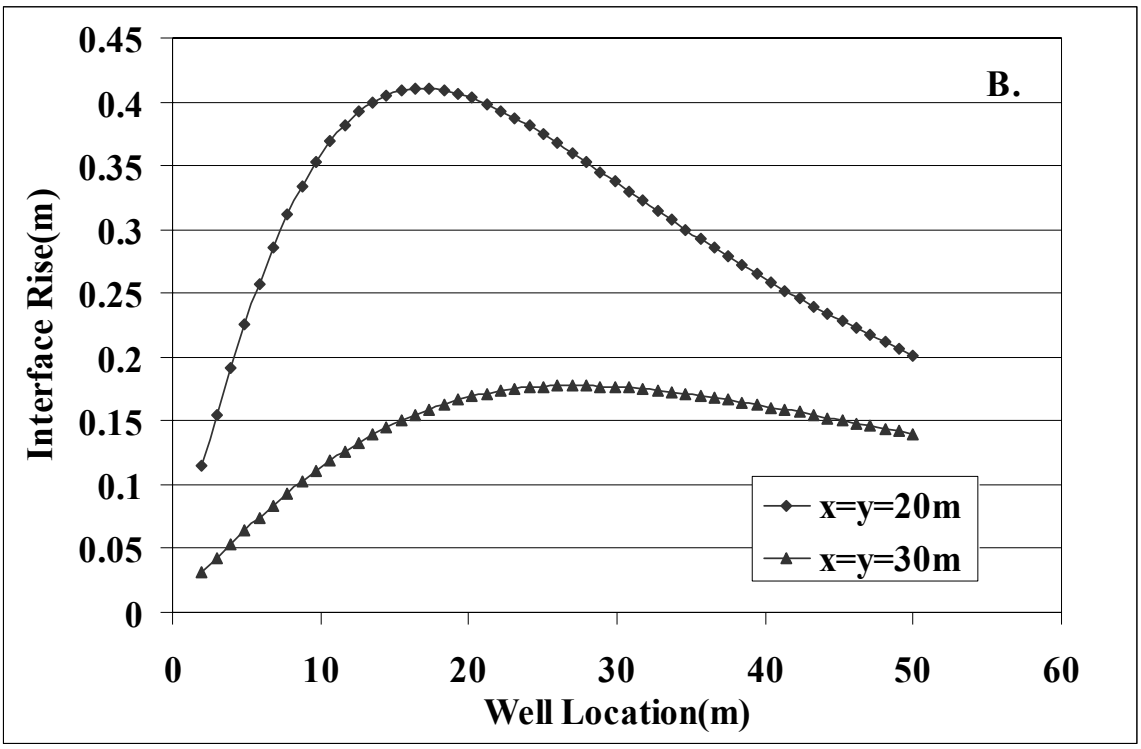

Figure 4.4 Continued

Second, for an observation point at the interface that is not directly below the well center, the interface rise depends on the interplay of the well location *d*, denoted as factor 1, and the horizontal distance between the observation point and the well center, denoted as factor 2. When the horizontal well is close to the interface (small value of *d*), its influence upon the upconing mostly concentrates on a local area below the well. When *d* increases, the interface rise tends to decrease. However, the influence area of the pumping also augments and reaches far, causing the increase of interface rises at points not directly below the well center. For example, at an off-center point of $x=y=20$m, when *d* is sufficiently small, the factor 1 dominates over the factor 2, thus one observes smaller interface rise at small *d* in Figure 4.4B; When *d* reaches a moderate value, the factor 2 dominates over the factor 1, thus one observes a maximal rise; when *d* further increases, the factor 1 dominates again, and the interface rise decreases. As a result, one observes a parabolic type of profile in Figure 4.4B.

If the observational point is further away, for instance, at $x=y=30$m, the well has to be further away from the initial interface to generate a large enough influence area to let the interface rise reaches its maximum at $d=26.96$m (see Figure 4.4B). One also observes that the curve of interface rise over the well location *d* becomes flatter when the horizontal distance from the observational point to the well center becomes greater.

The maximal upconing is reached when the distance from the well to the initial interface is slightly smaller than the horizontal distance from the observation point to the well (Figure 4.4B).

4.2.3.2 Well length

Figures 4.5A and 4.5B show the relationship of interface rise with the well length at different monitoring points at the interface. For a point directly below the well center, x=y=0, the function of the interface rise Z, versus the well length L, can be approximated by a regression function $Z = 122.92 \times L^{-0.9685}$ with a correlation coefficient R=0.999. The interface rise decreases rapidly when the well length increases, and it gradually approaches zero when well is infinitely long. This is because the pumping rate has been distributed over a larger horizontal distance for a longer well, thus the pumping strength per unit screen length becomes weaker, causing a smaller interface rise right below the well. Although Figure 4.4A and Figure 4.5A show some similar trend, the rate of change in Figure 4.4A is faster than that in Figure 4.5A, indicating that the interface rise is more sensitive to the well location than to the well length for the point below the well center.

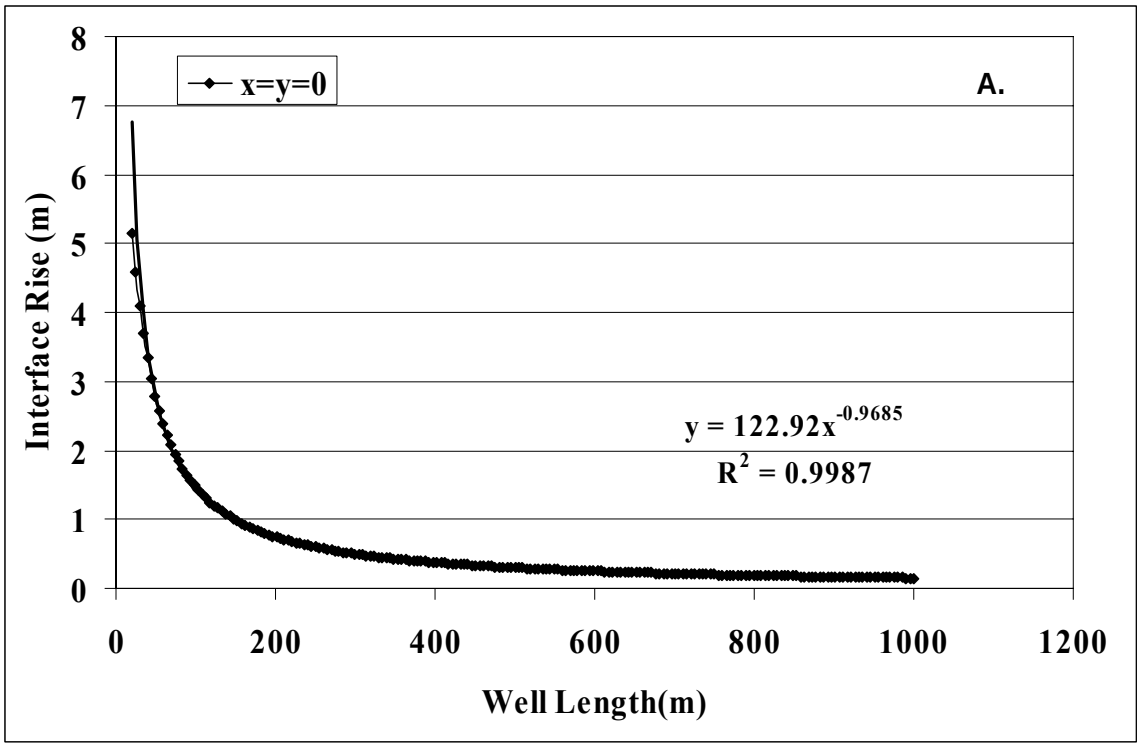

Figure 4.5 A) Effect of the well length on the interface rise at an observation point directly below the well center (x=y=0m); B) Effect of the well length on the interface rise at two off-center observation points at x=y=20m, and 40m.

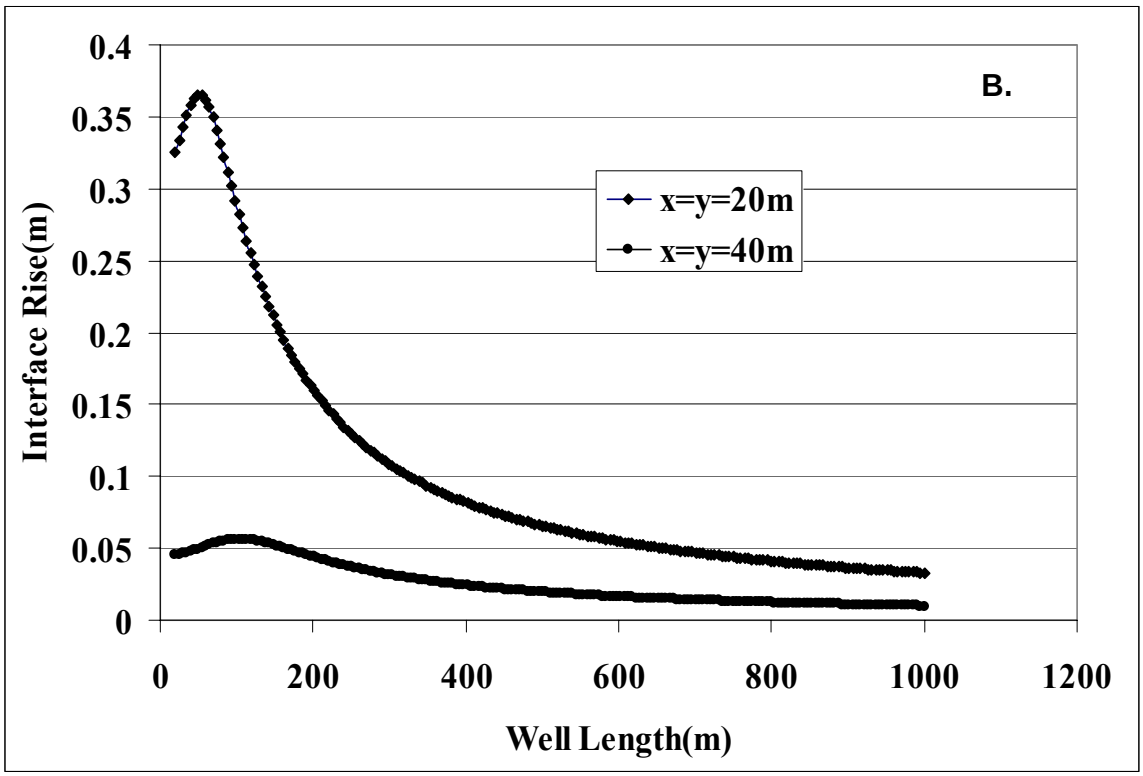

Figure 4.5 Continued

For observational points that are not directly below the well center, such as those at x=y=20m and 40m, the interface rises depend on the interplay of two controlling factors in a fashion similar to that discussed in section 4.2.3.1: the pumping strength (reflected by the pumping rate per unit length), and the influence area of the well. The interface rise reaches its maximum at a certain length of the well, as indicated in Figure 4.5B.

4.2.3.3 Aquifer anisotropy

Figure 4.6 shows the dependency of the interface rise as a function of the anisotropy ratio (K_z/K_x) for a point directly below the well. From an isotropic case of K_z/K_x=1 down to an anisotropic case of K_z/K_x=0.3, the interface rise almost linearly decreases from 3.31 to 1.56. However, when the anisotropic ratio further decreases, the decrease of interface rise becomes slightly steeper, until reaches zero when K_z/K_x=0.

4.3. Analysis of Critical Condition of Seawater Upconing

The study described above is based on the work of Dagan and Bear (1968). Although Dagan and Bear (1968) claimed that the interface will be stable for upconed heights that do not exceed one third of the distance between the well bottom and the initial interface, they did not directly solve the critical rise problem rigorously. In addition, Dagan and Bear (1968) is for an infinitely thick aquifer and it might not be suitable for dealing with a finite-thickness aquifer. In this section, we directly solve the critical rise problem using Muskat's (1982) idea based on the Ghyben-Herzerg model. The limitation of this method is analyzed in the discussion.

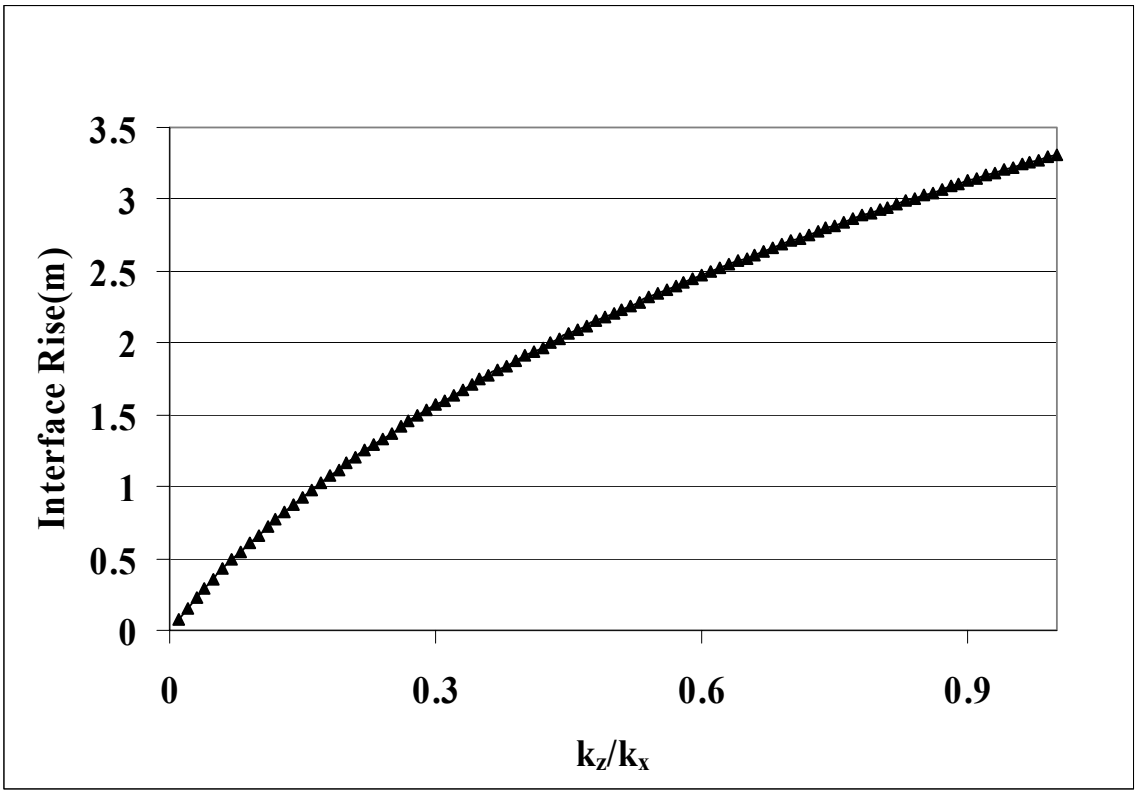

Figure 4.6 Effect of the aquifer anisotropy on the interface rise.

4.3.1 Critical condition

It is well-known that a stable interface profile is only possible under a certain critical condition beyond which seawater will flow into the well (Bear and Dagan, 1964; Schmorak and Mercado, 1969; Sahni, 1973; Haubold, 1975; Muskat, 1982; Reilly and Goodman, 1985, 1987; Wirojanagud and Charbeneau, 1985; Motz, 1992; Bower and Motz, 1999). The critical condition includes the critical pumping rate, the critical pumping time, and the critical rise. In a transient flow problem, these three parameters are interdependent on each other. The critical pumping rate refers to the maximal pumping rate without any seawater extraction at a certain time. The critical rise is the maximal interface rise to maintain a stable interface profile, and the critical time refers to the time when the critical rise is reached at a given pumping rate. It is of great importance to study the critical condition for managing coastal aquifers.

The critical rise is often expressed in terms of the ratio of the interface rise over the distance between the well and the initial interface (d). The critical rise due to a pumping vertical well has been studied by several investigators such as Bear and Dagan (1964), Schmorak and Mercado (1969), Sahni (1973), Haubold (1975), Muskat (1982, pp 481-496), Wirojanagud and Charbeneau (1985), Motz (1992), and Bower and Motz (1999). To the best knowledge of the authors, the previous studies of the critical rise are for vertical wells, and often focus on steady-state problems (Sahni, 1973; Haubold, 1975; Bower and Motz, 1999). The primary focus of this section is to investigate the transient critical rise problem under a pumping horizontal well.

4.3.2 Physical model

Muskat (1982) proposed an idea to acquire the critical rise for a two-fluid flow system. That idea states that: at the critical condition, both the pressure and the pressure gradient across the fresh/sea water interface are continuous. This idea has been employed in the following studies such as Glover (1959), Sahni (1973), Haubold (1975), Motz (1992), and Bower and Motz (1999). In this work, we will use this idea to study the horizontal well problem.

The assumptions used here are identical to those used in section 2.1 except that the aquifer thickness is not necessarily infinite. In addition, Muskat (1982) assumed a small perturbation of the interface variation that did not change the hydraulic head distribution of freshwater zone. Bear et al. (1968) pointed out that the Muskat's model was valid for less than 20% rise of the cone from the initial position of the interface to the bottom of a vertical pumping well. Haubold (1975) applied an empirical factor 1.33 to extend the Muskat's model from 20% to 50% of distance from the initial position of the interface to the bottom of a vertical well. Given the same pumping rate, a short-screen vertical well generally has a much steeper interface rise profile near the well bottom than a long-screen horizontal well, as can be seen from Figures 4.2A and 4.2B. Therefore, the small perturbation assumption used by Muskat often results in less error with the use of a horizontal well, as compared to the use of a vertical well, given the same pumping rate. Nevertheless, when the interface rise is more than 50% of distance from the initial position of the interface to the well, greater error will be introduced with the use of such an assumption.

Continuity of pressure at the interface before pumping results in (Figure 4.1),

$$(h_0 - z_0)\gamma_f = (d_s - z_0)\gamma_S \tag{4.36}$$

where γ_f and γ_s are the specific weights of seawater and freshwater, respectively; h_0 is the initial hydraulic head in the aquifer; d_s is the depth of mean sea level to the lower aquifer boundary; and z_0 is the initial fresh/sea water interface location in relative to the lower aquifer boundary.

4.3.2.1 *Equal pressure*

After the start of pumping, the hydraulic head in the aquifer is $h = h_0$-s, where s is the drawdown. Denoting Δ as the distance from the new interface to the lower aquifer boundary, the pressure balance at the interface becomes

$$(d_s - \Delta)\gamma_s = (h - \Delta)\gamma_f = (h_0 - s(z,t) - \Delta)\gamma_f . \tag{4.37}$$

It can be obtained from Eqs. (4.6) and (4.7) that

$$\Delta = \frac{s}{\delta - 1} + z_0 \tag{4.38}$$

where $\delta = \gamma_s / \gamma_f$ is the ratio of specific weight of seawater over that of freshwater.

4.3.2.2 *Equal pressure gradient*

At any vertical location z in the freshwater zone, the pressure after certain time of pumping, p_f, is

$$p_f = (h_0 - s - z)\gamma_f \tag{4.39}$$

If the point is located in the seawater zone, one has

$$p_s = (d_s - z)\gamma_s \tag{4.40}$$

Therefore, their pressure gradients are,

$$\frac{\partial p_f}{\partial z} = -\left(1 + \frac{\partial s}{\partial z}\right)\gamma_f \tag{4.41}$$

and

$$\frac{\partial p_s}{\partial z} = -\gamma_s . \tag{4.42}$$

At the critical condition, the pressure gradients at the interface are continuous. This leads to

$$\left.\frac{\partial s}{\partial z}\right|_{z=\Delta^c} = \delta - 1 , \tag{4.43}$$

where Δ^c refers to the distance from the interface to the lower aquifer boundary at the critical condition.

4.3.3 Application to confined aquifers

We consider a problem of transient flow to a horizontal pumping well (Figure 4.1). Because the interface rise is largest at location x=y=0, thus this point is chosen to analyze the critical rises under different circumstances. From Eqs. (4.8) and (4.13) and with the knowledge of drawdown in the aquifer, one can obtain the critical position of the interface, Δ^c, and the corresponding critical time, t^c. Eqs. (4.8) and (4.13) are written into the following dimensionless formats:

$$\Delta_D^c = \alpha s_D\left(t_D^c, \Delta_D^c\right) + z_{0D} , \tag{4.44}$$

$$\frac{\partial s_D}{\partial z_D}\left(\Delta_D^c, t_D^c\right) = \frac{1}{\alpha}, \tag{4.45}$$

with the definition of the dimensionless terms: $\Delta_D^c = \Delta^c / D$, $t_D^c = \left(k_z / S_s D^2\right) t^c$, $\alpha = \dfrac{Q}{2\pi K_x D^2 (\delta - 1)}$, $s_D = (2\pi k_x D / Q) s$, $z_{0D} = z_0 / D$, where D is the aquifer thickness.

For a confined aquifer, the drawdown at the interface below the center of a pumping horizontal well ($x = y = 0$) was given by Zhan et al. (2001):

$$s_D(z_D, t_D) = \frac{\sqrt{\pi}}{L_D} \int_0^{t_D} erf\left[\frac{(L_D/2)}{2\sqrt{\tau}}\right] \left[1 + 2\sum_{n=1}^{\infty} \cos(n\pi z_D)\cos(n\pi z_{WD})\exp\left(-n^2\pi^2\tau\right)\right] \frac{d\tau}{\sqrt{\tau}}, \tag{4.46}$$

where $t_D = \dfrac{K_z}{S_s D^2} t$, $L_D = \dfrac{L}{D}\sqrt{\dfrac{K_z}{K_x}}$, $x_D = \dfrac{x}{D}\sqrt{\dfrac{K_z}{K_x}}$, $y_D = \dfrac{y}{D}\sqrt{\dfrac{K_z}{K_x}}$, $z_D = \dfrac{z}{D}$, $z_{wD} = \dfrac{z_w}{D}$.

Eqs. (4.14) and (4.15) can be solved simultaneously for Δ_D^c and t_D^c. To do this, letting $z_D = \Delta_D$ in Eq. (4.16), where $\Delta_D = \Delta / D$, and substituting Eq. (4.16) into (4.14), results in the critical rise Δ_D^c and the critical time t_D^c simultaneously.

4.3.4 Discussion of the critical condition

The critical condition is affected by several parameters such as the pumping rate, the well location, the initial interface location, and the well length. The dependency of the critical condition on those parameters is discussed below. The following default parameters are used in this discussion: horizontal well is located at the center of the aquifer (z_{wD} =0.5), the dimensionless well length L_D=10, and the dimensionless initial fresh/sea water interface z_{0D} is 0.1.

4.3.4.1 *Pumping rate*

The effect of pumping rate is studied by changing the dimensionless pumping rate α from 1 to 3.0. Figures 4.7A and 4.7B show the effect of pumping rate on the critical rise and the critical pumping time, respectively. Several observations are notable from these Figures.

Under the transient flow condition in a confined aquifer, drawdown near the horizontal well will continuously increase with time, which will result in a continuously rising fresh/sea water interface until to a certain time (so-called critical time in our terminology) according to Eqs. (4.14) and (4.15). Thus, a stable interface is only possible within that critical time. Beyond the critical time, the interface becomes unstable and seawater intrudes the well. Therefore, a steady-state critical rise is not possible in a finite thickness confined aquifer. Under an assumption that the aquifer is infinitely thick, the critical time goes to infinity, and the steady-state critical time is achieved. Bear and Dagan (1964) have discussed such an infinitely thick aquifer under a pumping vertical well and have given estimations of the critical rises up to 0.5.

Under the transient flow condition, both the critical rise and the critical time decrease with pumping rate (see Figures 4.7A and 4.7B), but with different fashions. There is almost a perfect linear relationship between the critical rise and the pumping rate. The function of the critical rise defined as $F^c = (\Delta_D^c - z_{0D})/(z_{wD} - z_{0D})$, versus the dimensionless pumping rate, α , can be approximated by a linear regression function $F^c = -0.1683 \times \alpha + 0.9015$ with a correlation coefficient R=0.994.

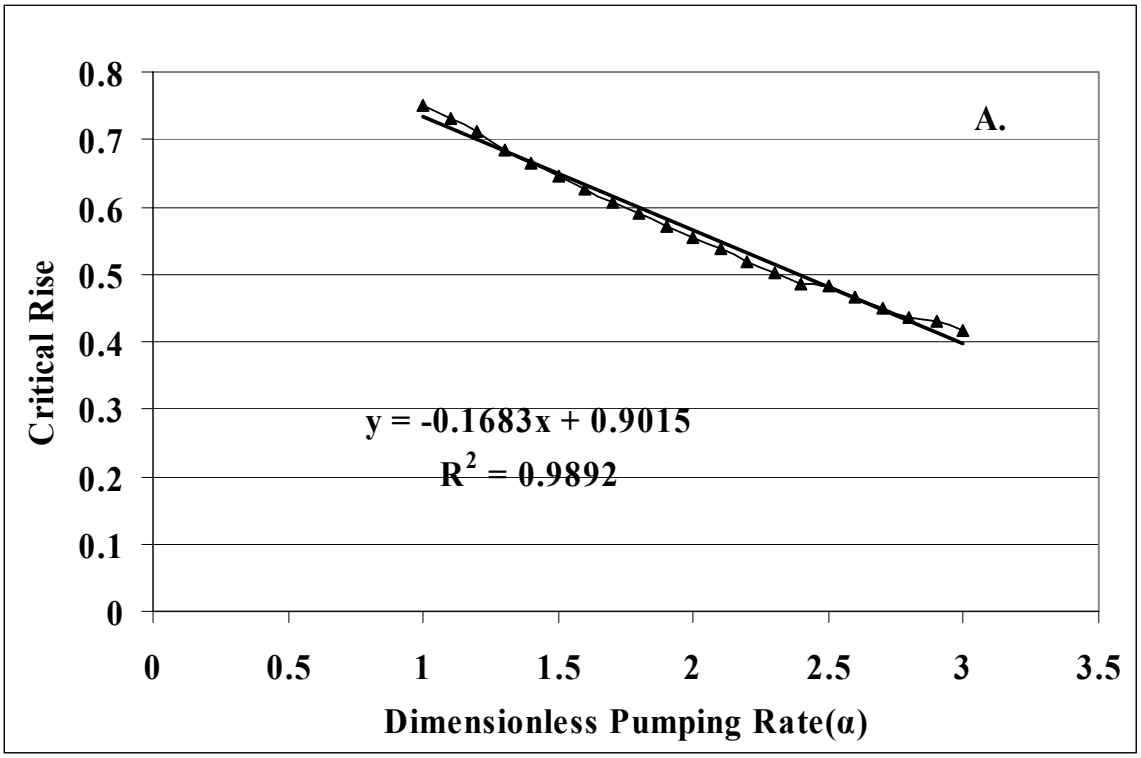

Figure 4.7 A) Effect of the dimensionless pumping rate on the critical rise; B) Effect of the dimensionless pumping rate on the critical time.

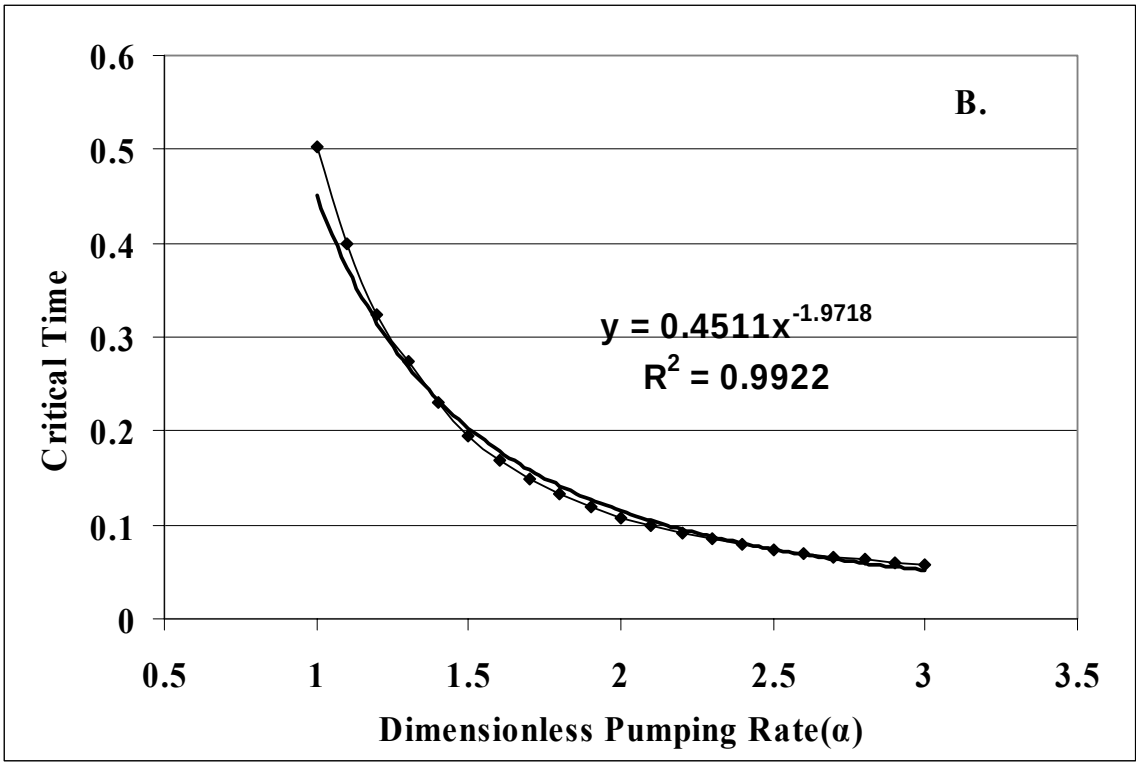

Figure 4.7 Continued

The relationship of t_D^c versus α is nonlinear which can be closely approximated by a regression function of $t_D^c = 0.4511 \times \alpha^{-1.9718}$ with a correlation coefficient R=0.996. The approximate linear relationship of F^c - α in Figure 4.7A indicates that $s_D\left(t_D^c, \Delta_D^c\right)$ is insensitive to the change of Δ_D^c in Eq. (4.14). The nonlinear relationship of Figure 4.7B shows that the critical time is more sensitive to the change of α when α is smaller than 2.2.

4.3.4.2 *Well location*

Figures 4.8A and 4.8B show F^c and t_D^c as functions of z_{wD}, respectively. Both F^c and t_D^c increase with z_{wD} but respond with different trends. When z_{wD} varies from 0.2 to 0.45, the critical time is relatively insensitive to the well location change. When z_{wD} varies from 0.5 to 0.9, t_D^c versus z_{wD} fits into an approximately linear function. F^c changes from 0.66 to 0.84 when z_{wD} varies from 0.25 to 0.9. Figures 4.8A and 4.8B clearly show that the closer the well to the initial interface location, the smaller of the critical rise, and the shorter of the critical pumping time. The critical rise is more sensitive to the change of well location when the well is closer to the initial interface.

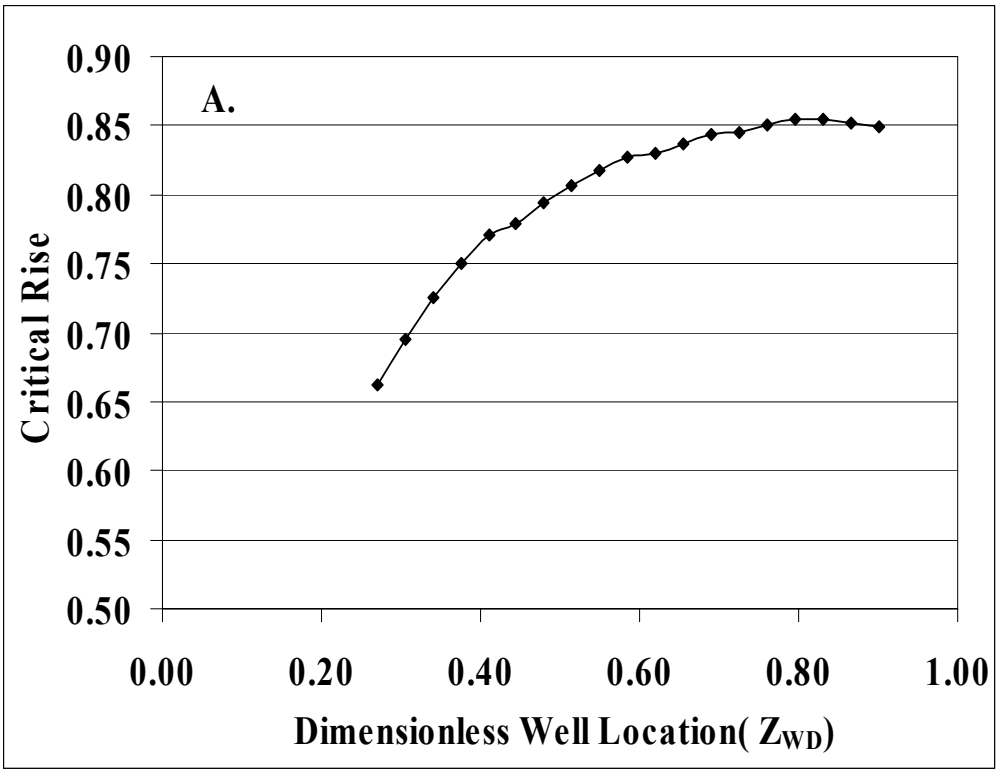

Figure 4.8 A) Effect of the well location on the critical rise; B) Effect of the well location on the critical time.

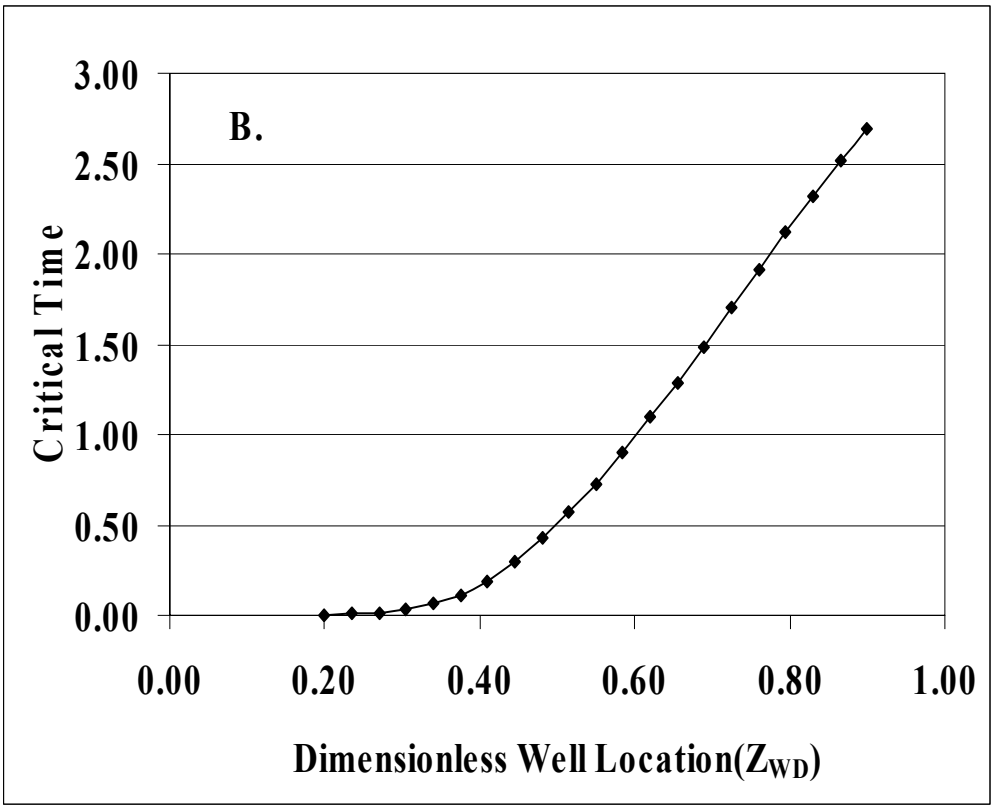

Figure 4.8 Continued.

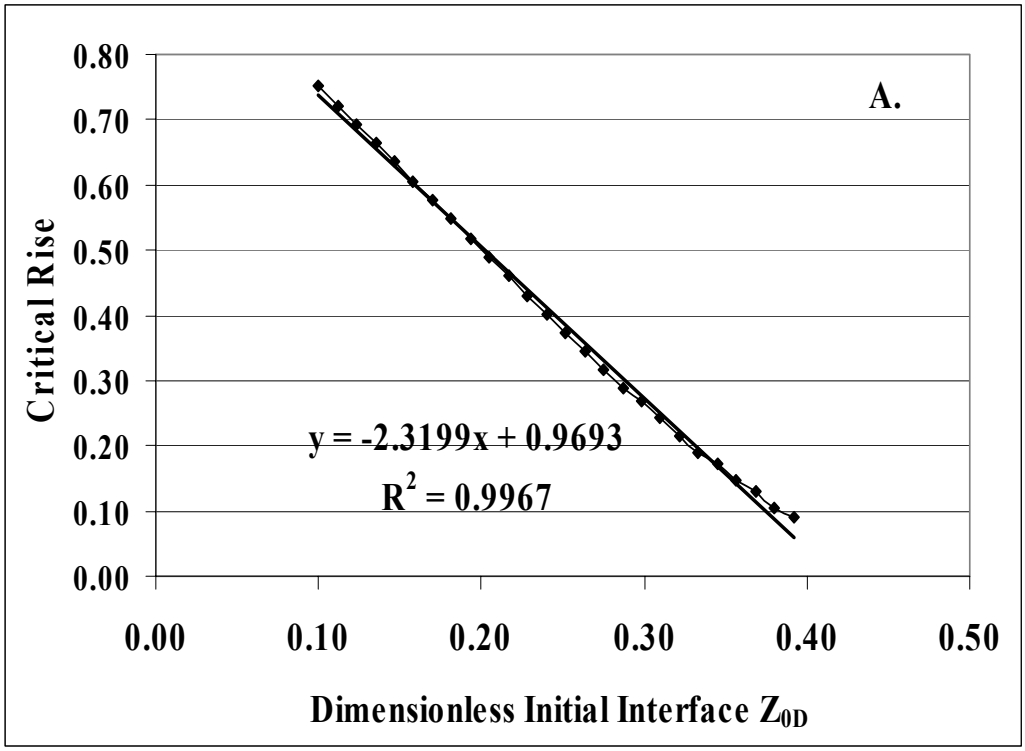

Figure 4.9 A) Effect of the initial interface on the critical rise; B) Effect of the initial interface on the critical time.

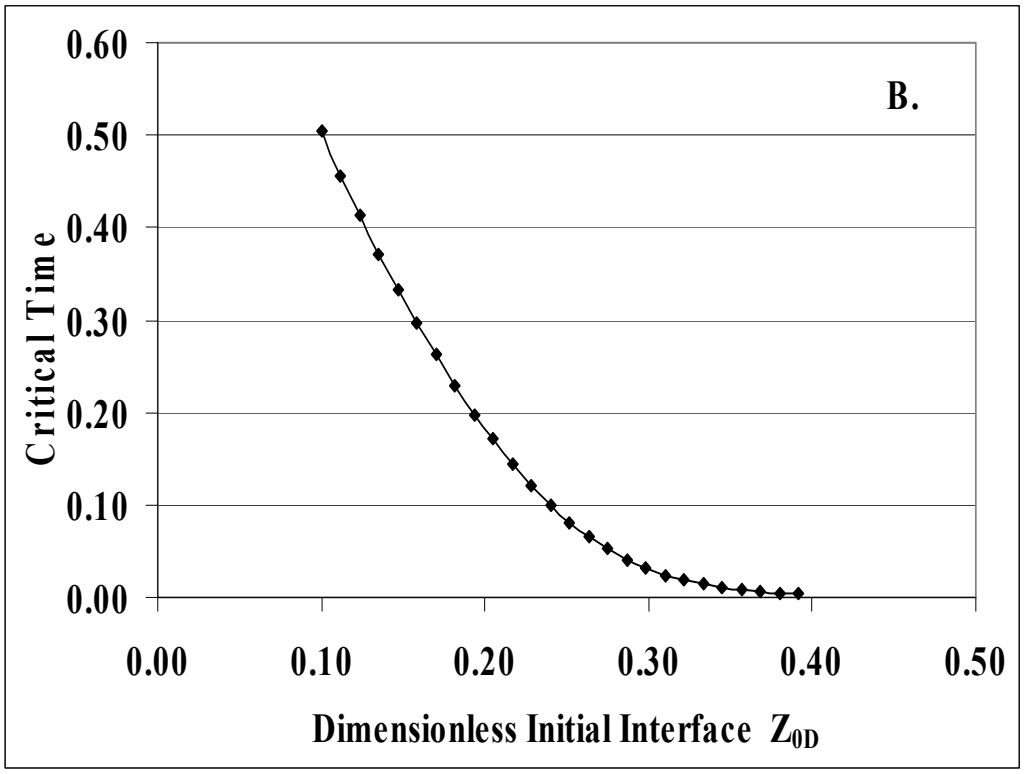

Figure 4.9 Continued

4.3.4.3 *Initial fresh/sea water interface*

Figures 4.9A and 4.9B show the effect of initial interface location. The critical rise is linearly dependent on the initial interface location, and this linear relationship can be approximated by a regression function F^c = -2.3199×z_{0D} + 0.9693 with a correlation coefficient R= 0.998. The critical time also decreases with z_{0D} when the initial interface is farther from the lower aquifer boundary. The case of z_{0D}=0.1 corresponds to F^c=0.79 and t_D^c=0.5, respectively.

When z_{0D} is at 0.3-0.4 which implies that the initial interface is very close to horizontal well (z_{wD}=0.5), the system will reach the critical condition shortly after pumping (t_D^c=0.003) with a small critical rise of 0.09.

4.3.4.4 *Well length*

To know the effect of well length on the critical rise and the critical time, and to choose an optimized well length to prevent seawater intrusion, the critical rise and the critical time are calculated as well length L_D varies over a wide range from 1 to 180. Figure 4.10A shows that the critical rise is very sensitive to the well length when L_D is relatively short. When L_D changes from 1 to 20, the critical rise increases substantially from 0.288 to 0.858. When L_D is longer than 20, the critical rise becomes less sensitive to the well length and its value changes only slightly while well length gets longer. For example, when the well length changes from 50 to 100, the corresponding critical rise only increases 0.015. When L_D is larger than 50, the critical rise is nearly unity, implying that the interface is close to the horizontal well, but the interface profile could still remain stable. This conclusion has important practical application for preventing

seawater intrusion. It means that when the horizontal well is sufficiently long (L_D >50), one can maintain a stable interface profile even when the interface is close to the well. For practice of using horizontal well for water supply in coastal aquifers, this indicates that one can use a long horizontal well to withdraw significant amount of freshwater before the seawater intrudes the well. Such a scenario is hardly seen when using vertical wells in which the critical rises are unlikely above 0.3-0.6 (Muskat, 1982; Bear and Dagan, 1964; Schmorak and Mercado, 1969; Wirojangud and Charbeneau, 1985).

There is an almost perfect correlation between the well length and the critical time shown in Figure 10B, $t_D^c = 0.0049 \times L_D^{2.1546}$ with a correlation coefficient R=0.996. When well gets longer, it takes longer time to reach the critical condition.

This also implies that longer wells would be preferred for practice for pumping freshwater in coastal aquifers.

4.4. Discussion

Several issues of this study deserve further discussion:

1. The three dimensional upconing profile under a pumping horizontal well is acquired based on Dagan and Bear's model (1968) of an infinite thick aquifer, therefore, the conclusion might not be applicable to thin coastal aquifers. This resulting profile is only valid if the interface rise is below one third of the distance from the well to the initial interface (Saeed et al., 2002).

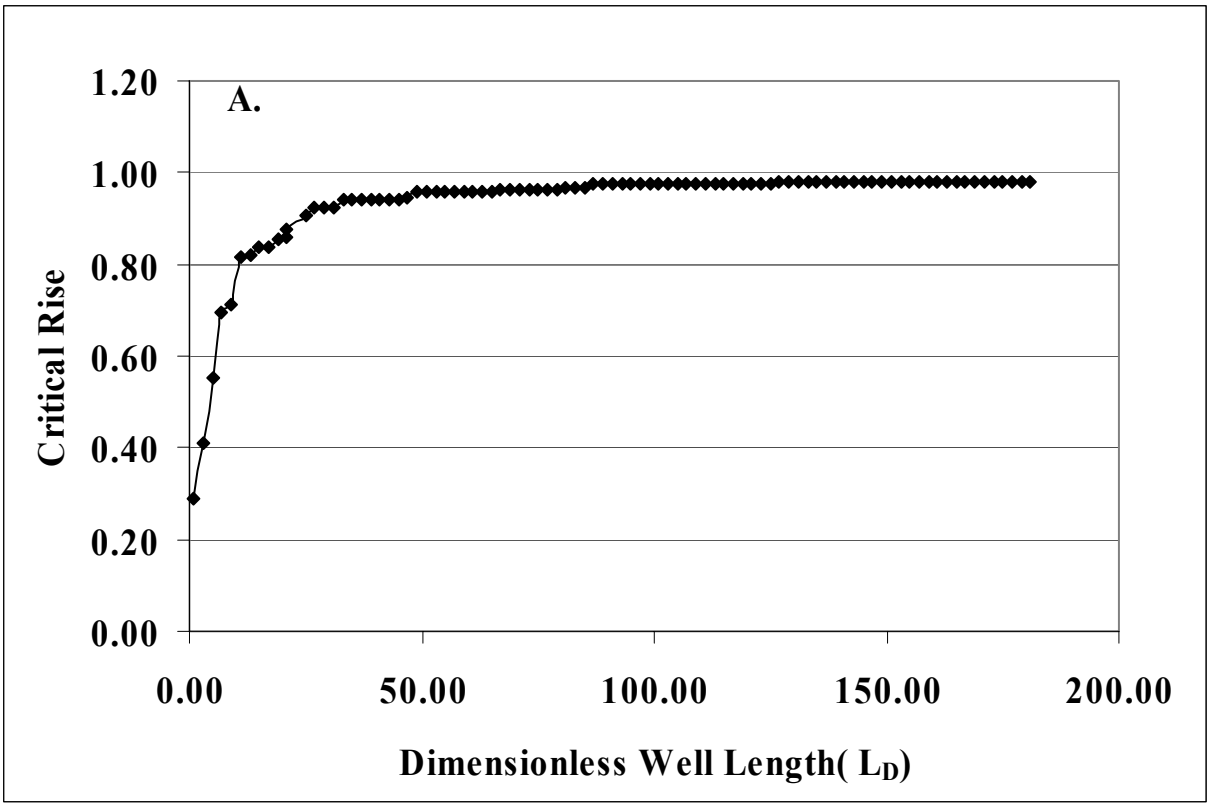

Figure 4.10 A) Effect of the well length on the critical rise; B) Effect of the well length on the critical time

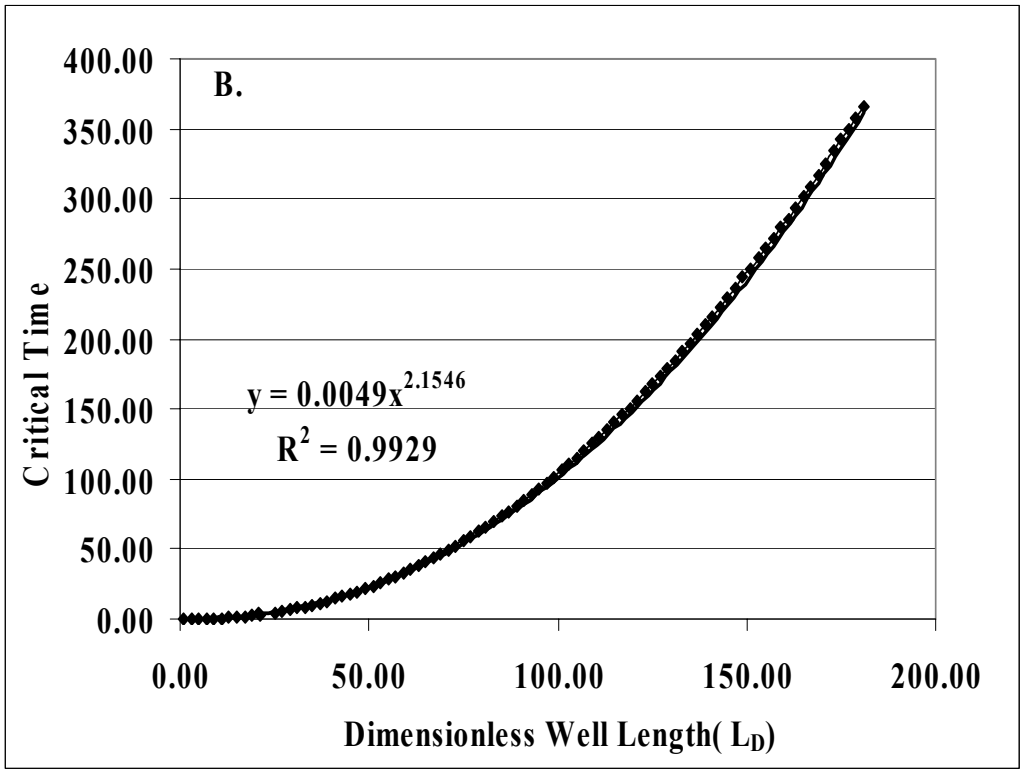

Figure 4.10 Continued

2. Previous studies of critical condition using vertical wells often claimed that the critical rise was around 0.48 (Muskat, 1982), or 0.5 (Bear and Dagan, 1964), or 0.35 (Wirojanagud and Charbeneau, 1985). A maximum permitted pumping rate without seawater intrusion was then given by considering the critical rise (Domenico and Schwartz, 1998). However, the critical condition for a horizontal well pumping case in a confined aquifer is a dynamic process. One needs to consider aquifer and well properties, instead of simply giving a maximal pumping rate based on a critical rise value. This study showed that the critical rise and the critical time are coupled together at any given pumping rate in a transient flow problem. If the pumping rate is determined *a priori*, the critical rise will be reached at a certain critical time beyond which the interface profile becomes unstable. If the pumping period goes to infinity in a confined aquifer, the critical condition will inevitably be reached eventually, no matter how small the pumping rate is. A longer pumping time can be achieved at the expense of smaller pumping rate, while a larger pumping rate is only possible when pumping time is short to maintain a stable profile.

3. The critical condition depends on the well location, the well length, the pumping rate, and the initial fresh/sea water initial interface, as analyzed above. How to balance the effects of these parameters and economic consideration is a challenge for the water management when a horizontal well is applied to a coastal aquifer. As shown in Figures 4.7A and 4.9A, the critical rise has an inverse linear relationship with the pumping rate and the initial interface, respectively. However, the slope in Figure 4.9A is greater than that in Figure 4.7A, indicating that the critical rise is more sensitive to the distance

between the well and the initial interface than the pumping rate. If the initial fresh/sea water interface is low (close to the lower aquifer boundary), the interface could rise up to a position close to the well while is still stable. If the initial interface is high (far from the lower aquifer boundary), the critical rise tends to be small. Therefore, a long horizontal well is preferred to keep a sufficiently long critical time. In summary, a horizontal well with a longer well screen length with further distance from the initial interface is always desirable.

4. The critical condition was investigated based on Muskat's (1982) model which assumed that the seawater was stagnant. Neglecting the dynamic process of response in the seawater zone could result in unrealistically large interface rise. For instance, the Ghyben- Herzerg relationship used by Muskat (1982) deals with static condition which showed that one foot drop of freshwater would cause approximately 40 feet of rising of seawater. The realistic interface rise under transient, dynamic motion of both freshwater and seawater should be smaller than that predicted by the Ghyben- Herzerg relationship. It is generally accepted that the calculated critical condition tends to be accurate when the interface rise is less than 20% of the distance between the well and the initial interface (Saeed et al., 2002). The primary purpose of this study is for gaining the physical insights of interface upconing under a pumping horizontal well. We are aware that the calculated critical time is short in a thin confined aquifer because of the usage of the Ghyben- Herzerg relationship. Therefore, it is not recommended to use the calculated critical time for precise prediction in real field applications. On the other hand, we are also aware that the pressure gradient (Eq. (4.13)) is almost independent of time after a

short period of pumping, which is consistent with previous studies by Rosa and Carvalho (1989) and Zhan and Cao (2000, pp 838). In fact, Zhan and Cao (2000, pp 838) have illustrated this issue in details and shown that the first spatial derivative of drawdown due to a pumping horizontal well in a confined aquifer is independent of time after entering the so-called pseudoradial flow stage. Therefore, the calculated critical rise, which is derived on the basis of continuity of pressure and pressure gradient, is likely to be more reliable than the calculated critical time in this study.

4.5. Conclusions

An analytical solution of three dimensional seawater upconing due to a finite-length horizontal well is derived by integrating the point sink solution of Dagan and Bear (1968) along the horizontal well screen. This study assumes a sharp interface between the freshwater and the seawater, neglecting the transition zone between these two fluids. The resulting upconing profile is compared with that of a vertical well using the same aquifer parameters. The upconing profile exhibits three stages with time: an early slow increase stage, an intermediate rapid increase stage, and a late steady state stage. Given the same pumping rate and the distance from the well bottom to the initial interface, the interface rise at a fixed observation point is much smaller due to a horizontal well than to a vertical well.

The sensitivity of the interface rise to the well location, the well length, and the aquifer anisotropy has been thoroughly discussed. In general, the interface rise is very sensitive to the well location when the well is close to the initial interface for a point right below the well center. For an off- center point, the interface rise depends on the

interplay of the well location and the horizontal distance from the observation point to the well. The maximal upconing is reached when the distance from the well to the initial interface is slightly smaller than the horizontal distance from the observation point to the well. The interface rise is less sensitive to the well length than the well location. For a point right below the well center, the interface rise decreases when increasing the well length. If the well is not very long (see Figure 4.5A), the interface rise is sensitive to the well length. Similar to the influence of the well location, the interface rise also depends on the interplay of the well length and the horizontal distance from the observation point to the well.

The critical rise and the critical time are studied by relating the interface rise to the drawdown and by employing Muskat's (1982) idea: pressure and pressure gradient are continuous across the sea/fresh water interface. They are coupled together at any given pumping rate in a transient flow problem. The critical rise depends on the initial interface location, the pumping rate, the well location, and the well length. The critical rise has an inversely linear relationship with pumping rate and the initial interface location, respectively. However, the critical rise is more sensitive to the distance between the well and the initial interface than the pumping rate. The critical pumping time decreases with the increasing pumping rate. The closer the well to the initial interface, the shorter of the critical time is. The critical condition is also controlled by the well screen length. The critical rise is sensitive to the well length when it is not long ($L_D < 50$ in Figure 4.10A), and less sensitive when well gets longer ($L_D > 50$ in Figure 4.10A), while the critical time continuously increases when well length gets longer. In

real field applications, installing long wells as shallow as possible is always desirable for sustaining long periods of pumping with significant rates.

The limitations of this study are originated from the assumptions used in Dagan and Bear's (1968) model in investigating the interface profile and the Muskat's (1982) model in studying the critical condition.

CHAPTER V

SUMMARY AND FUTURE WORKS

5.1 Summary

In this dissertation, we developed a series of conceptual, physical, and mathematical models of aquitard control of stream-aquifer interaction. The new conceptual model is applied to two cases: the first case is flow to a horizontal well in an aquitard-aquifer system; the second case is the pumping induced interaction between two streams and aquifer. We also investigated the three dimensional profile of fresh-sea water interface due to a pumping horizontal well at various hydrological conditions and well configurations. Meanwhile, we also examined the critical conditions: critical time, critical rise and critical pumping rate.

In Chapter II, we have provided new solutions of flow to a horizontal well in an aquitard-aquifer system based on the mass conservation law. Flow in the aquitard and aquifer is treated as two flow systems that are connected via the continuity of flux and head at the aquitard-aquifer boundary. We do not adopt the Hantush's assumption that was commonly used in previous studies, including Zhan and Park (2003). The leakage induced by the pumping horizontal well under different aquitard hydraulic conditions and a variety of well configurations is analyzed. The flux and the drawdown calculated in this paper are compared with that of Zhan and Park (2003) and the validity of the Hantush's assumption is tested for both transient and steady-state flow conditions. The leakage induced by the pumping horizontal well depends on several parameters such as the aquitard thickness, the vertical hydraulic conductivity of the aquitard, the aquitard

storage, the well location, and the well length. In general, we find that the Hantush's assumption does not offer correct prediction of flux and drawdown during the transient flow condition, particularly at the early time. For steady-state flow, the Hantush's assumption works reasonably well under realistic conditions of aquitard thickness and hydraulic conductivity as long as the aquitard thickness is not too thin (aquitard-aquifer ratio less than 0.001). This assumption also works reasonably well under realistic horizontal well lengths and well locations as long as the well is not too close to the aquitard-aquifer boundary.

In Chapter III, a pumping well is sometimes installed between two surface water bodies, such as streams or canals. Previous studies focus on one stream and aquifer system and treat leakage from the surface water body as a volumetric source term in the governing equation of flow in the main aquifer, a hypothesis termed "Hantush's assumption" (Hantush, 1964). In this chapter, new analytical and semi-analytical solutions are acquired for the pumping induced dynamic interaction between two surface water bodies and ground water for two different cases. In the first case, the sediment layer separating surface water from ground water is not considered. In the second case, the two low permeable layers are considered. Instead of adopting Hantush's assumption, the solutions are derived based on the mass conservation laws by maintaining continuity of flux and head along the aquitard-aquifer boundaries. Results from these two cases are compared to demonstrate the effects of aquitards. The interconnection of two aquitard properties such as thickness ratio, hydraulic conductivity ratio, and specific storage ratio is tested while well is positioned at difference locations. The results in this chapter

could provide guidance for well design, water management, and other applications. We find that the aquitard hydraulic conductivity is the most important factor controlling the stream-aquifer interaction, followed by the aquitard thickness which greatly influences the drawdown at observation points that are close to the aquitards. Aquitards properties control the competition of stream depletion when a pumping well is positioned between two streams. When the two aquitards are identical, the so called "equal flux point" is located right at the center between the two aquitards. The equal flux point will move off the center when the aquitard thickness ratio and/or the aquitard hydraulic conductivity ratio are different than unity.

In Chapter IV, an analytical solution of three dimensional seawater upconing due to a finite-length horizontal well is derived by integrating the point sink solution of Dagan and Bear (1968) along the horizontal well screen. This study assumes a sharp interface between the freshwater and the seawater, neglecting the transition zone between these two fluids. The resulting upconing profile is compared with that of a vertical well using the same aquifer parameters. Given the same pumping rate and the distance from the well bottom to the initial interface, the interface rise at a fixed observation point is much smaller due to a horizontal well than to a vertical well.

The critical rise and the critical time are studied by relating the interface rise to the drawdown and by employing Muskat's (1982) idea: pressure and pressure gradient are continuous across the sea/fresh water interface. They are coupled together at any given pumping rate in a transient flow problem. The critical rise depends on the initial interface location, the pumping rate, the well location, and the well length. The critical

rise has an inversely linear relationship with pumping rate and the initial interface location, respectively. However, the critical rise is more sensitive to the distance between the well and the initial interface than the pumping rate. The critical pumping time decreases with the increasing pumping rate. The closer the well to the initial interface, the shorter of the critical time is. In real field applications, installing long wells as shallow as possible is always desirable for sustaining long periods of pumping with significant rates.

The limitations of this study are originated from the assumptions used in Dagan and Bear's (1968) model in investigating the interface profile and the Muskat's (1982) model in studying the critical condition.

Finally, the results in this dissertation could be applied to groundwater development both for inland and coastal aquifers.

5.2 Future Works

In Chapter II, we only investigated a case that aquifer is bounded by an upper aquitard and bottom bedrock. In fact, aquifer could be bounded by upper and lower aquitards by different ways. It will be very interesting to examine aquitard control of flow in different combination of aquitard, aquifer, water table and bedrock for any types of wells, such as partially penetrating wells, horizontal wells, and slanted wells. This study will provide a general method for aquitard control in aquitard-aquifer-aquitard system for arbitrary orientation of wells.

In Chapter III, we investigated a dynamic interaction among two fully penetrating streams due to a fully penetrating well. Regional flow and hydrograph is not considered

in this study. It will be interesting to consider some more realistic cases for stream-aquifer interaction studies, for example, partial penetrating streams and variation of streamflow. In future, a more general model for arbitrary orientation well pumping induced interaction among groundwater and two partial penetrating streams will be addressed.

In Chapter IV, sea water intrusion is studied only for a confined aquifer. However, costal aquifers are often shallow and unconfined aquifer. It will be very meaningful to investigate the three dimensional profile of cone and its critical condition for a water table aquifer as well as the effect of regional flow and fresh water recharge.

In this study, we only investigated on aquitard effect on flow. The model we derived in this study could be extended to the effect of aquitard on solute transport on aquitard-aquifer system and subsidence study.

REFERENCES

Abramowitz, M., Stegun, I.A., 1972. Handbook of Mathematical Functions, Dover, Mineola, NY.

Bakker, M. ,2003. A Dupuit formulation for modeling seawater intrusion in regional aquifer systems, Water Resour. Res., 39(5), doi:10.1029/2002WR001710.

Barends, F.B.J, Brouwer, F.J.J., Schroder, F.H., 1995. Land subsidence: by fluid withdrawal, by solid extraction; theory and modeling, environmental effects and remedial measures. In: Proceedings of the Fifth International Symposium on Land Subsidence, 16 – 20 October 1995, The Hague, Netherlands. Kluwer Academic Pub., Dordrecht.

Barlow, P.M., Moench, A.F.,1998. Analytical solutions and computer programs for hydraulic interaction of stream-aquifer systems. U.S. Geological Survey Open-File Report 98-415 A, PP 85.

Barlow, P.M. Desimone, L.A., Moench, A.F., 2000. Aquifer response to stream-stage and recharge variations. II. Convolution method and applications. J. Hydrol. 230, 211-229.

Bear, J., 1979. Hydraulics of Ground Water. McGraw-Hill, New York.

Bear, J., Dagan, G., 1964. Some exact solutions of interface problems by means of the hodograph method, J. Geophys. Res. 69(2), 1563-1572.

Bear, J., Zaslavasky, D., Irmay, S.,1968. Physical Principles of Water Percolation and Seepage, UNESCO, Paris.

Bear, J., Cheng, A. H.-D., Sorek ,S., Ouazar, D., Herrera, I.,1999. Seawater Intrusion in Coastal Aquifers: Concepts, Methods and Practices, Kluwer Academy, Norwell, MA.

Bower, J.W., Motz, L. H., Durden, D.W. ,1999. Analytical solution for determining the critical condition of saltwater upconing in a leaky artesian aquifer, J. Hydrol., 221, 43-54.

Bruen. M., Osman, Y.Z., 2004. Sensitivity of stream-aauifer seepage to spatial variability of the saturated hydraulic conductivity of the aquifer. J. Hydrol. 293, 289-302.

Butler, J.J., Zlotnik, V.A., Tsou, M.S., 2001. Drawdown and stream depletion produced by pumping in the vicinity of a finite width stream of shallow penetration. Ground Water 39(5), 651-659.

Butler, R.M., Jiang ,Q. , 1996. Effect of gravity on movement of water-oil interface for bottom water driving upwards to a horizontal well, Journal of Canadian Petroleum Technology, 35(*7*), 47-56.

Chandler, R.L., McWhorter, D.B.,1975. Upconing of the salt-water-fresh-water interface beneath a pumping well, Ground Water*,* 13(4), 354-359.

Chen, X., 2003. Analysis of pumping-induced stream-aquifer interactions for gaining streams. J. Hydrol. 275, 1-11.

Chen, X., Chen, X., 2003a. Stream water infiltration, bank storage, and storage zone changes due to stream-stage fluctuations. J. Hydrol. 280, 246-264.

Chen, X., Chen, X., 2003b. Sensitivity analysis and determination of streambed leakance and aquifer hydraulic properties. J. Hydrol. 284, 270-284.

Chen, C., Wan, J., Zhan, H., 2003. Theoretical and experimental studies of coupled seepage-pipe flow to a horizontal well. J. Hydrol. 281, 163-175.

Cheng, A.H.-D., Halhal, D., Naji ,A., Ouazar, D., 2000. Pumping optimization in saltwater-intruded coastal aquifers, Water Resour. Res., 36(8), 2155-2165.

Cleveland, T. G., 1994. Recovery performance for vertical and horizontal wells using semianalytical simulation. Ground Water 32(1), 103-107.

Daviau, F., Mouronval, G., Bourdarot, G., Curutchet, P. , 1988. Pressure analysis for horizontal –wells. SPE Formation Eval. 3(4), 716-724.

De Hoog, F.R., Knight, J.H., Stokes, A.N., 1982. An improved method for numerical inversion of Laplace transforms. SIAM J. Sci. Stat. Comp. 3, 357–366.

Dagan, G., Bear J. , 1968. Solving the problem of interface upconing in a coastal aquifer by the method of small perturbations, J. Hydraul. Res., 6, 15-44.

Daviau, F., Mouronval, G. , Bourdarot, G. , Curutchet ,P. , 1988. Pressure analysis for horizontal –wells, SPE Formation Eval. 3(4), 716-724.

de Hoog, F.R., Knight, J.H., Stokes, A.N., 1982. An improved method for numerical inversion of Laplace transforms. SIAM J. Sci. Stat. Comp. 3, 357–366.

Diersch, H. J. , 1988. Finite element modeling of recirculating density driven saltwater intrusion processes in groundwater, Adv. Water Resour., 11, 25-43.

Domenico, P. A., Schwartz, F. W., 1998, Physical and Chemical Hydrogeology, 2nd ed., John Wiley & Sons, New York.

Falta, R. W., 1995. Analytical solutions for gas-flow due to gas injection and extraction from horizontal wells. Ground Water 33(2), 235-246.

Fox, G. A., Durnford, D.S., 2003. Unsaturated hyporheic zone flow in stream/aquifer conjunctive systems. Adv. Water Resour. 26, 989-1000.

Frind, E. O.,1982, Simulation of long –term transient density-dependent transport in ground water, Adv. Water Resour., 5, 89-97.

Galeati, G., Gambolati, G., Neuman, S.P. ,1992. Coupled and partially coupled Eulerian-Lagrangian model of freshwater-saltwater mixing, Water Resour. Res., 28(1), 149-165.

Glover, R.E., Balmer, C.G., 1954. River depletion resulting from pumping a well near a river. Eos. Trans. Am. Geophys. Union. 35, 468-470.

Glover, R. E. ,1959. The pattern of fresh- water flow in a coastal aquifer, J. Geophys. Res., 64(4), 457-459.

Goode, P. A., Thambynayagam, R.K.M. ,1987. Pressure drawdown and buildup analysis of horizontal wells in anisotropic media, SPE Formation Eval., 2(4), 683-697.

Haitjema, H.M. ,1991. An analytic element model for transient axi-symmetric interface flow, J. Hydrol., 129, 215-244.

Hantush, M. S., Papadopulos, I. S., 1962. Flow of ground water to collector wells, J. Hydraulic. Div. Proc. Am. Soc. Civ. Eng. HY5, 221-244.

Hantush, M. S., 1964. Hydraulic of wells. In: Chow, V.T. (Ed.). Advances in Hydroscience, 281-442, Academic Press, New York.

Hantush, M.S., 1965. Wells near streams with semipervious beds. J. of Geophys. Res. 70, 2829-2838.

Haubold, R.G. , 1975. Approximation for steady interface beneath a well pumping fresh water overlying salt water. Ground Water, 13(3), 254-259.

Henry, H. R. ,1959. Salt intrusion into freshwater aquifers, J. Geophys. Res., 64, 1911-1919.

Henry, H. R. ,1964. Effects of dispersion on salt encroachment in coastal aquifers, U.S. Geol. Survey Water-Supply Paper 1613-C C71-C84.

Hollenbeck, K.J., 1998. INVLAP.M, A MATLAB function for numerical inversion of Laplace transforms by the de Hoog algorithm, http://www.isva.dtu.dk/staff/karl/invlap.htm.

Hunt, B., 1999. Unsteady stream depletion from ground water pumping. Ground Water 37(1), 98-102.

Hunt, B. 2003. Unsteady stream depletion when pumping from semi-confined aquifer. ASCE J. Hydrol. Engineering. 8(1), 12-19.

Hussein, M. Schwartz, F.W., 2003. Modeling of low and contaminant transport in coupled stream-aquifer systems. J. Contaminant Hydrol. 65, 41-64.

Jenkins, C.T.,1968. Techniques for computing rate and volume of stream depletion by wells. Ground Water 6(2), 37-46.

Kollet, S.J., Zlotnik, V.A., 2003. Stream depletion predications using pumping test data from a heterogeneous stream-aquifer system (a case study from the Great Plains, USA), J. Hydrol. 281, 96-114.

Kollet, S.J., 2005. Comment on “sensitivity analysis and determination of streambed leakance and aquifer hydraulic properties” by Xunhong Chen and Xi Chen, J of Hydrology, 2003, vol284, 270-284. J. Hydrol. 303, 328-330.

Kuchuk, F. J., Goode, P. A. , Wilkinson, D. J. , Thambynayagam, R. K. M. ,1991. Pressure transient behavior of horizontal wells with and without gas cap or aquifer, SPE Formation Eval., 6, 86-94.

Lal, A.M.W., 2001. Modification of canal flow due to stream-aquifer interaction. J. Hydraulic Engineer. 127(7), 567-576.

Lin, Y., Medina Jr, M.A., 2003. Incorporating transient storage in conjunctive stream-auifer modeling. Adv. Water Resour. 26, 1001-1019.

Liu, P. L.-F., Cheng, A. H.-D. , Liggett, J.A. , Lee, J. H. ,1981. Boundary integral equation solutions of moving interface between two fluids in porous media, Water Resour. Res., 17, 1445-1452.

Mercer, J.W., Larson, S. P. , Faust ,C. R. ,1980. Simulation of salt water interface motion, Ground Water, 18, 374-385.

Moench, A.F. , Barlow, P.M., 2000. Aquifer response to stream-stage and charge variations. I. Analytical step-response functions, J. Hydrol. 230, 192-210.

Motz, L. H. ,1992. Salt-water upconing in an aquifer overlain by a leaky confining bed, Ground Water, 30(2), 192-198.

Morgan, J. H., 1992. Horizontal drilling applications of petroleum technologies for environmental purposes, Ground Water Monit. Rev., 12(3), 98-102.

Murdoch, L. C., 1994. Transient analyses of an interceptor trench, Water Rescour. Res., 30(11), 3023-3031.

Muskat, M., 1982. The Flow of Homogeneous Fluids through Porous Media, International Human Resources Development Corporation, Boston.

Neuman, S. P., Witherspoon, P. A., 1969a. Theory of flow in a confined two-aquifer system. Water Resour. Res. 5(4), 803-816.

Neuman, S. P., Witherspoon, P. A., 1969b. Application of current theories of flow in leaky aquifers. Water Resour. Res. 5(4), 817-829.

Ozkan, E., Raghavan, R. ,Joshi ,S. D. , 1989. Horizontal –well pressure analysis, SPE Formation Eval., 4, 567-575.

Ozkan, E., Raghavan ,R. , 1991a. New solutions for well-test analysis problems: part 1-analytical considerations. SPE Formation Eval., 6(3), 359-368.

Ozkan, E., Raghavan ,R. , 1991b, New solutions for well-test analysis problems: part 2-computational considerations and applications. SPE Formation Eval., 6(3), 369-378.

Park, E., Zhan, H., 2002. Hydraulics of a finite-diameter horizontal well with wellbore storage and skin effect in leaky aquifers, Adv. Water Resour. 25(4), 389-400.

Park, E., Zhan, H., 2003. Hydraulics of horizontal well in fractured shallow aquifer systems, J. Hydrol. 281, 151-162.

Penmatcha, V. R., Arbabi , S. , Aziz, K. ,1997. Effect of pressure drop in horizontal wells and optimum well length. In: Proceedings of the 1997 SPE Production Operation Symposium, 9-11, March. Soc. Pet. Eng. Oklahoma City, Oklahoma.

Press, W. H., Flannery, B. P., Teukolsky, S. A., Vetterling, W. T., 1989. Numerical Recipes, the Art of Scientific Computing (FORTRAN Version), Cambridge Univ. Press, New York.

Reilly, T. E., A. S. Goodman (1985), Quantitative analysis of saltwater-freshwater relationships in groundwater systems- a historical perspective, J. Hydrol. 80, 125-160.

Reilly, T. E., Goodman, A. S. , 1987. Analysis of saltwater upcoming beneath a pumping well, J. Hydrol. 89, 169-204.

Rosa, A.J., Carvalho,R.de S.,1989. A mathematical model for pressure evaluation in an infinite-conductivity horizontal well. SPE Formation Eval. 4(4), 559-566, 1989.

Saeed, M., Bruen, M. , Asghar ,M.N. , 2002. A review of modeling approaches to simulate saline-upconing under skimming wells, Nordic Hydrology, 33(2-3), 165-188.

Sahni, B. M.,1973. Physics of brine coning beneath skimming wells, Ground Water, 11(1), 19-24.

Sawyer, C.S., Lieuallen-Dulam, K. K.,1998. Productivity comparison of horizontal and vertical ground water remediation well scenarios, Ground Water, 36(1), 98-103.

Schmorak, S., Mercado, A.,1969. Upconing of fresh water-sea water interface below pumping wells, field study, Water Resour. Res., 5(6), 1290-1311.

Stehfest, H., 1970. Numerical inversion of Laplace transforms. Commun. ACM 13(1), 47-49.

Strack, O. D. L. ,1976. A single-potential solution for regional interface problems in coastal aquifers, Water Resour. Res., 12(6), 1165-1174.

Strack, O.D.L., 1984. Three-dimensional streamlines in Dupuit-Forchheimer models, Water Resour. Res., 20(7), 812-822.

Strack, O. D. L., 1995. A Dupuit –Forchheimer model for three –dimensional flow with variable density, Water Resour. Res., 31(12), 3007-3017.

Streward, D. R., Jin ,W. ,2001.Gaining and losing sections of horizontal wells, Water Resour. Res., 37(11), 2677-2685.

Talbot, A., 1979. The accurate numerical inversion of the Laplace transforms. J. Inst. Math. Its Appl. 23, 97-120.

Tarshish, M., 1992. Combined mathematical model of flow in an aquifer-horizontal well system, Ground Water 30(6), 931-935.

Taylor, J. Z., Person ,M. ,1998. Capture zone delineations on island aquifer systems, Ground Water, 36(5), 722-730.

Theis, C.V.,1941. The effect of a well on the flow of a nearby stream. Eos Trans., Am. Geophys. Union 22, 734-738.

Volker, R., Rushton ,K. , 1982. An assessment of the importance of some parameters for sea-water intrusion in aquifers and comparison of dispersive and sharp-interface modeling approaches, J. Hydrol., 56, 239-250.

Voss, C. I., 1984. SUTRA: A finite element simulation model for saturated-unsaturated, fluid-density-dependent ground-water flow with energy transport or chemically-

reactive singles-species solute transport, U.S. Geol. Surv. Water Resour. Invest., 84-4369.

Voss, C. I., Souza, W. R. , 1987. Variable density flow and solute transport simulation of regional aquifers containing a narrow freshwater-saltwater transition zone, Water Resour. Res., 23(10), 1851-1866.

Wirojanagud, P., Charbeneau, R. J., 1985. Saltwater upconing in unconfined aquifers. J. Hydraulic Engineering. 111(3), 417-434.

Woessner, W. W., 2000, Stream and fluvial plain ground-water interactions: re-scaling hydrogeologic thought. Ground Water, 38 (3), p. 423-429.

Zhan, H., 1999. Analytical study of capture time to a horizontal well, J. Hydrol. 217, 46-54.

Zhan, H., Cao, J., 2000. Analytical and semi-analytical solutions of horizontal well capture times under no-flow and constant –head boundaries, Adv. Water Resour. 23(8), 835-848.

Zhan H., Wang, L.V., Park, E., 2001. On the horizontal-well pumping tests in anisotropic confined aquifer, J. Hydrol. 252, 37-50.

Zhan, H., Zlotnik, V.A., 2002. Ground water flow to horizontal and slanted wells in unconfined aquifers, Water Resour.Res.38(7), 1108.

Zhan, H., Park, E., 2003. Hydraulics of horizontal wells in leaky aquifers, J. Hydrol.281, 133-150.

Zhang, H., Hocking, G. C., 1996. Withdrawal of layered fluid through a line sink in a porous medium, J. Aust. Math. Soc. B 38, 240-254.

Zhang, H., Hocking, G. C. , 1997. Axisymmetric flow in an oil reservoir of finite depth caused by a point sink above an oil-water interface, J. Eng., Math., 32(4), 365-376.

Zhang, H., Hocking, G. C., and Barry,D. A., 1997. An analytical solution for critical withdrawal of layered fluid through a line sink in a porous medium, J. Aust. Math. Soc. B 39, 271-279.

Zlotnik, V.A., Huang, H., 1999. Effect of shallow penetration and streambed sediments on aquifer response to stream stage fluctuations (analytical model). Ground Water 37(4), 599-605.

APPENDIX A

As seen from the detailed derivation of Zhan and Park (2003), and also shown in Zhan et al. (2001) and Zhan and Zlotnik (2002), the solution to Eq. (2.17) is

$$H_n = \frac{4}{pf(\omega_n)}\cos(\omega_n z_{wD}) K_0\left|\sqrt{\omega_n{}^2 + p} r_D\right| , \tag{A1}$$

where K_0 is the second-kind, zero-order, modified Bessel function, and

$$f(\omega_n) = 1 + \frac{\sin(2\omega_n)}{2\omega_n},\ r_D = \left(x_D{}^2 + y_D{}^2\right)^{1/2}. \tag{A2}$$

Based on the governing Eq. (2.12) and boundary condition (2.14), the solution in the aquitard is:

$$\overline{s'_D} = F(x_D, y_D, p)\sinh\left[\sqrt{\alpha p}(1 + B_D - z_D)\right], \tag{A3}$$

where F is a function that only depends on the horizontal coordinates and will be determined later via the continuity of head at the aquitard-aquifer boundary. Hantush (1964) also proposed a similar solution in his discussion of aquitard flow.

Based on the continuity of head at z_D=1 (Eq. (2.15)), one obtains

$$F(x_D, y_D, p) = \frac{\overline{s_D}(z_D = 1)}{\sinh(\sqrt{\alpha p} B_D)}. \tag{A4}$$

Substituting Eq. (A4) into (A3) results in:

$$\overline{s'_D} = \overline{s_D}(z_D = 1)\frac{\sinh(\sqrt{\alpha p}(1 + B_D - z_D))}{\sinh(\sqrt{\alpha p} B_D)}. \tag{A5}$$

Substituting Eqs. (2.20) and (A5) into the continuity of flux at z_D=1 (Eq. (2.16)) results in:

$$\beta\omega_n \tan(\omega_n) = \sqrt{\alpha p}\coth(\sqrt{\alpha p}B_D)\,. \tag{A6}$$

ω_n is determined by Eq. (A6) for any given p.

APPENDIX B

Recall the identity

$$L^{-1}\left[\frac{1}{\sqrt{p}}e^{-k\sqrt{p}}\right]=\frac{1}{\sqrt{\pi t}}\exp(-\frac{k^2}{4t}), \tag{B1}$$

and let $a=(n\pi)^2$, then Eq.(3.12) becomes:

$$\overline{s_D}(p)=4\pi\sum_{n=1}^{\infty}\sin(n\pi y_D)\sin(n\pi y_{wD})\frac{1}{p}\frac{1}{\sqrt{a+p}}\exp(-\sqrt{a+p}\,|x_D|). \tag{B2}$$

Recall the following identity

$$L^{-1}\left[\frac{1}{\sqrt{p+a}}e^{-k\sqrt{p+a}}\right]=\frac{1}{\sqrt{\pi t}}e^{-at}\exp(-\frac{k^2}{4t}), \tag{B3}$$

then

$$A=L^{-1}\left[\frac{1}{p}\frac{1}{\sqrt{a+p}}e^{-k\sqrt{a+p}}\right]=\int_0^t\frac{1}{\sqrt{\pi\tau}}\exp(-\frac{k^2}{4\tau}-a\tau)d\tau. \tag{B4}$$

We define:

$$u=\frac{k}{2\sqrt{\tau}}+\sqrt{a\tau},\ v=\frac{k}{2\sqrt{\tau}}-\sqrt{a\tau},\ u_0=\frac{k}{2\sqrt{t}}+\sqrt{at}\text{, and }v_0=\frac{k}{2\sqrt{t}}-\sqrt{at}, \tag{B5}$$

Then Eq. (B4) becomes

$$A=\frac{1}{\sqrt{\pi a}}\left[e^{-k\sqrt{a}}\int_{v_0}^{\infty}e^{-v^2}dv-e^{k\sqrt{a}}\int_{u_0}^{\infty}e^{-u^2}du\right]. \tag{B6}$$

Recall the definition of the complementary error function:

$$\frac{2}{\sqrt{\pi}}\int_{u_0}^{\infty}e^{-u^2}du=erfc(u_0), \tag{B7}$$

Eq. (B6) and be evaluated and Eq. (B2) will become Eq. (3.13).

APPENDIX C

As seen from the detailed derivation of Zhan and Park (2003), and also shown in Zhan et al. (2001) and Zhan and Zlotnik (2002), the solution to Eq. (3.5) is

$$H_n = \frac{4}{pf(\omega_n)}\cos(\omega_n z_{wD}) K_0\left|\sqrt{\omega_n{}^2 + p} r_D\right| , \tag{C1}$$

where K_0 is the second-kind, zero-order, modified Bessel function, and

$$f(\omega_n, \mu_n) = 1 + \frac{1}{2\omega_n}\left[\sin(2\omega_n + 2\mu_n) - \sin(2\mu_n)\right],\ r_D = \left(x_D{}^2 + z_D{}^2\right)^{1/2}. \tag{C2}$$

Based on the governing Eq. (3.30) and the boundary condition Eq.(3.32), the solution in aquitard 1 is:

$$\overline{s_{D1}} = F_1(x_D, y_D, p)\sinh\left[\sqrt{\alpha_1 p}(B_{D1} + y_D)\right], \tag{C3}$$

In the same way, based on the governing Eq.(3.35) and the boundary condition Eq.(3.39), the solution in aquitard 2 is:

$$\overline{s_{D2}} = F_2(x_D, y_D, p)\sinh\left[\sqrt{\alpha_2 p}(1 + B_{D2} - y_D)\right] , \tag{C4}$$

where both F_1 and F_2 only depend on the horizontal coordinates x and y, and they can be determined later via the continuity of head at the aquitard-aquifer boundary. Hantush (1960) has also proposed a similar solution in his discussion of aquitard flow.

Based on the continuity of head at y_D=0 (Eq. (3.33)), one obtains

$$F_1(x_D, y_D, p) = \frac{\overline{s_D}(y_D = 0)}{\sinh(\sqrt{\alpha_1 p} B_{D1})}, \tag{C5}$$

Substituting Eq. (C5) into (C3) results in:

$$\overline{s_{D1}} = \overline{s_D}(y_D = 0) \frac{\sinh(\sqrt{\alpha p}(B_{D1} + y_D))}{\sinh(\sqrt{\alpha p} B_{D1})}. \tag{C6}$$

Based on the continuity of head at y_D=1 (Eq. (3.38)), one obtains

$$F_2(x_D, y_D, p) = \frac{\overline{s_D}(y_D = 1)}{\sinh(\sqrt{\alpha_2 p} B_{D2})} \tag{C7}$$

Substituting Eq.(C7) into Eq.(C4) results in:

$$\overline{s_{D2}} = \overline{s_D}(y_D = 1) \frac{\sinh(\sqrt{\alpha_2 p}(1 + B_{D2} - y_D))}{\sinh(\sqrt{\alpha_2 p} B_{D2})}. \tag{C8}$$

Substituting Eqs. (3.40) and (C6) into the continuity of flux at y_D =0 (Eq. (3.34)) results in:

$$-\beta_1 \omega_n \tan(\mu_n) = \sqrt{\alpha_1 p} \coth(\sqrt{\alpha_1 p} B_{D1}). \tag{C9}$$

Substituting Eqs.(3.40) and (C8) into the continuity of flux at y_D=1 (Eq.(3.39)) results in:

$$\beta_2 \omega_n \tan(\omega_n + \mu_n) = \sqrt{\alpha_2 p} \coth(\sqrt{\alpha_2 p} B_D). \tag{C10}$$

ω_n and μ_n can be determined by solving Eqs. (C9) and (C10) for any given p. We define

$$A = \sqrt{\alpha_2 p} \coth(\sqrt{\alpha_2 p} B_D) / \beta_2, \tag{C11}$$

$$B = \sqrt{\alpha_1 p}\coth(\sqrt{\alpha_1 p}B_D)/\beta_1, \tag{C12}$$

$$\text{then } \tan(\mu_n) = -B/\omega_n, \tag{C13}$$

Putting Eq. (C13) into Eq. (C10), we got

$$(\omega_n^2 - AB)\tan\omega_n - (A+B)\omega_n = 0. \tag{C14}$$

VITA

NAME: Dongmin Sun

ADDRESS: Xueyuan Road, NO.20, P.O.X. 910, Beijing, China, 100083

EDUCATION: B.S. (Petroleum geology), Daqing Petroleum Institute, Anda, China

M.S. (Petroleum Geology), RIPED(Research Institute of Petroleum Exploration &Development), CNPC(China National Petroleum Corporation), Beijing, China

Ph.D. (Geology), Texas A&M University, College Station, USA.

RESEARCH INTEREST:

Environmental application of Horizontal Well in inland and coastal Aquifers

Flow and contaminant transport in fracture media

NAPL dissolution in the subsurface

Stream-aquifer interaction

Experimental and in-situ groundwater and soil remediation techniques

Hydrogeophysics, especially application of GPR

Scaling issue in vadose zone hydrology

GIS application in groundwater and small watershed modeling